To the Graduate Council:

I am submitting herewith a dissertation written by Mohamed Sayed Genidy entitled "On the Reduction of Cure-Induced Stresses in Thermoset Polymer Composites." I have examined the final copy of this dissertation for form and content and recommend that it be accepted in partial fulfillment of the requirements for the degree of Doctor of Philosophy, with a major in Engineering Science.

Madhu S. Madhukar

Madhu S. Madhukar, Major Professor

We have read this dissertation
and recommend its acceptance:

J. F. Fellers

Paul Phillips

Accepted for the Council:

Associate Vice Chancellor and
Dean of The Graduate School

On the Reduction of Cure-Induced Stresses in Thermoset Polymer Composites

A Dissertation

Presented for the

Doctor of Philosophy

Degree

The University of Tennessee, Knoxville

Mohamed Sayed Genidy

August, 1999

DEDICATION

This dissertation is dedicated to my wife Taga,

to my parents overseas, and

to my son Ahmed and daughter Summer.

ACKNOWLEDGMENT

I would like to express my gratitude to Dr. Madhu S. Madhukar for his help, advice, and encouragement since the first day I started my study at the University of Tennessee, Knoxville. He demonstrated complete understanding of graduate student expectations and needs. He made himself available all the times despite his busy schedule. I learned much from him through his innovative approaches to solve research problems.

I also want to thank my graduate committee members; Dr Y. Jack Weitsman, John F. Fellers, and Paul J. Phillips for all their contributions and constructive criticism.

I want to thank Dr John D. Russell at Air Force Research Laboratory, Ohio for his technical consultations and help running materials characterization tests.

This research work was supported in part by United States Air Force, Air Force Research Laboratory, Materials and Manufacturing Directorate under contract number F49620-96-1-0085. Their support is gratefully acknowledged.

I would like also to thank Chad Davis for his help in running tests at Composite Materials Laboratory at the University of Tennessee, Knoxville.

I would like to thank my wife Taga for all the support and understanding. She left no effort in taking care of every aspect of our family life so I have time to study and do research. She stayed beside me all the way in the time she missed her family overseas the most.

ABSTRACT

This work concerns the study of the effect of cure cycles on the development of cure induced stresses in thermoset polymer composites. The study includes experimental testing as well as theoretical modeling. The experimental part included modifying a newly developed test method to monitor the development of cure induced stresses in thermoset polymer composites. Test results were shown to be highly reproducible and gave a clear understanding of the mechanisms of stresses development as well as cancellation. Good qualitative agreement between test results and the independently measured polymer volume change data was seen. The test method was further modified with a closed loop feedback control system to modify the cure cycles to reduce cure induced stresses. Several composite material systems were studied. Test results show that the modified cure cycles reduce residual stresses in composite laminates compared to the cure cycles recommended by materials manufacturers while maintaining the same glass transition temperature. It was shown that the modified cure cycles may also enhance the matrix-dominated mechanical properties, maintain better dimensional stability, and reduce cure time. The theoretical part of the study included the development of a mechanical optimization model and a computer program, OPTICURE, to study the effect of changing the cure cycle on the development of residual stresses in composite laminates. The model and the program were used to generate cure cycles that reduce residual stresses in thermoset polymer composites and hence enhance the dimensional stability and mechanical properties. Findings of the theoretical modeling were found to agree well with those of the experimental study.

TABLE OF CONTENTS

1. Introduction and Literature Review 1

    1-1 Introduction 1

    1-2 Experimental Studies 2

    1-3 Theoretical Studies 9

    1-4 Problem Statement 15

2. Experimental Methods 17

    2-1 Introduction 17

    2-2 Cure Induced Stress Test (CIST) 18

        2-2-1 Test Setup 23

        2-2-2 Typical Results 26

        2-2-3 Parameters of CIST 29

    2-3 Modification of Cure Cycles Using Trial and Error Method 42

    2-4 Modification of Cure Cycles Using Closed Loop Feedback Control System (CLFS) 48

        2-4-1 Optimization Procedure 50

        2-4-2 Optimization Parameters 50

        2-4-3 Typical Results 53

    2-5 Summary 56

3. Effect of Cure Cycle on Cure Induced Stresses 57

3-1 Introduction 57

3-2 Standard Cure Cycles 58

3-2-1 3501-6 and 934 Epoxies 58

3-2-2 974-3 Toughened Epoxy 61

3-2-3 5250-4 BMI 63

3-2-4 X343-59 and LTM-45 ELD Low Cure Temperature Epoxies 63

3-3 Modified Cure Cycles 71

3-3-1 3501-6 and 934 Epoxies 71

3-3-2 977-3 Toughened Epoxy 76

3-3-3 5250-4 BMI 78

3-3-4 X343-59 and LTM-45 ELD Low Cure Temperature Epoxies 82

3-3-5 Applications 88

3-4 Effect of Post Cure and Cool Down Rates 92

3-5 Classification of Cure Cycles 95

3-5-1 3501-6 Epoxy 98

3-5-2 974-3 Toughened Epoxy 100

3-5-3 Applications 102

3-6 Effect of Modified Cure Cycles on Mechanical Properties 104

3-7 Summary and Conclusion 106

4. Cure Cycle Optimization Model and Computer Program 107

4-1 Introduction 107

4-2 Sub-Models 110

4-2-1 Temperature Distribution 110

4-2-2 Cure Kinetics 113

4-2-3 Resin Flow Model 114

4-2-4 Gelation 115

4-2-5 Volume Change Model 117

4-2-6 Viscosity Model 124

4-2-7 Calculation of Stresses 126

4-2-7-1 Elastic Analysis 126

4-2-7-2 Viscoelastic Analysis 129

4-2-7-3 Materials Properties 131

4-3 Computer Program 133

4-4 Results 135

4-4-1 Effect of Gelation Temperature 136

4-4-2 Effect of Heating Rate Beyond Gelation 142

4-5 Summary and Conclusion 146

Bibliography 148

Vita 159

LIST OF FIGURES

Figure 1.1	Cure cycle modification to reduce residual stresses.	7
Figure 1.2	Another method for cure cycle modification to reduce residual stresses.	8
Figure 1.3	Comparison between test results and model predictions.	11
Figure 2.1	Mechanism of cure induced stress test.	19
Figure 2.2	Details of the PVT apparatus.	20
Figure 2.3	Variation in polymer volume during standard cure cycle.	22
Figure 2.4	Schematic diagram of single fiber test.	24
Figure 2.5	Cure induced stress test.	25
Figure 2.6	Variation in the fiber tension during the standard cure cycle of 3501-6 epoxy.	28
Figure 2.7	Fiber tension during the standard cure cycle for a single fiber coated with a thin layer of 3501-6 epoxy.	28
Figure 2.8	Fiber tension change during a typical two dwell cure cycle.	30
Figure 2.9	Effect of temperature change on the fiber tension (no polymer).	32
Figure 2.10	Effect of embedded fiber length on the variation in the fiber tension during cure.	34
Figure 2.11	Effect of initial fiber tension on the variation in the fiber tension during cure.	34
Figure 2.12	Effect of changing cure cycle on the fiber tension in AS4/Epon 828 single fiber composites.	35
Figure 2.13	Schematic of the model used to calculate fiber stress during cure.	37
Figure 2.14	Fiber stresses during a typical two dwell cure cycle.	39
Figure 2.15	Cure induced stresses produced fiber fracture in a pretensioned fiber.	41
Figure 2.16	Variation in fiber stresses during a modified cure cycle.	41
Figure 2.17	Fiber tension during an intermediate cure cycle obtained using trial and error modification method.	44

Figure 2.18	Fiber tension during a modified cure cycle of 3501-6 epoxy obtained using trial and error modification method.	44
Figure 2.19	Volume changes during the modified cure cycle of 3501-6 shown in Figure 2.18.	45
Figure 2.20	Variation in fiber tension during another modified cure cycle of 3501-6 epoxy.	47
Figure 2.21	Flow chart of the Closed Loop Feedback System (CLFS) used to obtain cure cycle with reduced cure induced stresses.	51
Figure 2.22	Fiber tension data during a cure cycle modified using CLFS.	54
Figure 2.23	Volume change data during a cure cycle modified using CLFS.	54
Figure 3.1	Variation in the fiber tension during the standard cure cycle of 3501-6 epoxy.	59
Figure 3.2	Volume change of 934 epoxy during the standard cure cycle.	60
Figure 3.3	Variation in the fiber tension during the standard cure cycle of 934 epoxy.	60
Figure 3.4	Volume change of 977-3 epoxy during the standard cure cycle	62
Figure 3.5	Fiber tension data during the standard cure cycle of 977-3 epoxy resin.	62
Figure 3.6	Volume change data of 5250-4 BMI during the standard cure cycle.	64
Figure 3.7	Variation in the fiber tension during standard cure cycle of 5250-4 BMI.	64
Figure 3.8	Volume change of X343-59 during the standard low temperature cure cycle.	66
Figure 3.9	Variation in the fiber tension during the standard low temperature cure cycle of X343-59 epoxy.	66
Figure 3.10	Volume change of X343-59 during an autoclave type cure cycle.	68
Figure 3.11	Variation in the fiber tension during an autoclave type cure cycle of X343-59 epoxy.	68

Figure 3.12 Volume change of LTM-45 ELD epoxy during the standard low temperature cure cycle. 70
Figure 3.13 Variation in the fiber tension during the standard low temperature cure cycle of LTM-ELD epoxy. 70
Figure 3.14 Volume change of LTM-45 ELD during an autoclave type cure cycle. 72
Figure 3.15 Variation in the fiber tension during an autoclave type cure cycle of LTM-45 ELD epoxy. 72
Figure 3.16 A modified cure cycle for S2/3501-6 glass/epoxy system. 73
Figure 3.17 A modified cure cycle for AS4/934 graphite/epoxy. 75
Figure 3.18 Another modified cure cycle for AS4/934 graphite/epoxy. 77
Figure 3.19 A modified cure cycle for AS4/977-3 graphite/epoxy. 77
Figure 3.20 Another modified cure cycle for AS4/977-3 graphite/epoxy. 79
Figure 3.21 A modified cure cycle for AS4/5250-4 graphite/BMI. 80
Figure 3.22 Volume change data of 5250-4 BMI during the modified cure cycle shown in Figure 3.21. 80
Figure 3.23 Another modified cure cycle for 5250-4 BMI with higher initial temperature. 81
Figure 3.24 Variation in the fiber tension during a modified low temperature cure cycle for AS4/X343-59 graphite/epoxy. 85
Figure 3.25 Variation in the fiber tension during another modified low temperature cure cycle for AS4/X343-59 graphite/epoxy. 85
Figure 3.26 Variation in the fiber tension during a modified autoclave type cure cycle for AS4/X343-59 graphite/epoxy. 87
Figure 3.27 Volume change of X343-59 during the modified cure cycle shown in Figure 3.26. 87
Figure 3.28 Variation in the fiber tension during a modified low temperature cure cycle for LTM-45 ELD. 89
Figure 3.29 Volume change during the modified cure cycle shown in Figure 3.28. 89

Figure 3.30	Curvature of unsymmetric AS4/3501-6 graphite/epoxy laminates cure with different cure cycles.	91
Figure 3.31	Effect of cooldown rate on residual stresses in AS4/5250-4 graphite/BMI single fiber composites.	93
Figure 3.32	Schematic showing the effect of the cure cycle selection on the contribution of cure volume changes to fiber stresses.	96
Figure 3.33	Different types of cure cycles for AS4/3501-6 graphite/epoxy.	99
Figure 3.34	Different types of cure cycles for AS4/974-3 graphite/epoxy.	101
Figure 3.35	Curvature of unsymmetric IM7/977-3 graphite/epoxy laminates cured using different cure cycles.	103
Figure 3.36	Effect of cure cycle modification on mechanical properties of IM7/977-3 graphite/epoxy composites.	105
Figure 4.1	Flow diagram of OPTICURE.	109
Figure 4.2	Diagrammatic flow chart of OPTICURE.	111
Figure 4.3	Degree of cure and viscosity during a cure cycle of 3501-6 epoxy.	116
Figure 4.4	Degree of cure, glass transition temperature, and volume changes during a cure cycle of 3501-6 epoxy.	120
Figure 4.5	Variation in cure shrinkage and thermal expansion during cure.	121
Figure 4.6	Predicted versus measured volume changes beyond gelation.	123
Figure 4.7	Comparison between measured and predicted cure volume changes for linear increase in temperature.	125
Figure 4.8	Geometry of $[90^\circ_n/0^\circ_n]$ unsymmetric laminate considered in the mechanical model.	127
Figure 4.9	Relationship between gelation temperature and gelation time.	137
Figure 4.10	Relationship between cure cycle time and gelation temperature.	137
Figure 4.11	Moment due to cure volume changes at different gelation temperatures.	139
Figure 4.12	Moment due to cure volume changes and cooldown shrinkage at different gelation temperatures.	141

Figure 4.13 Typical cure volume changes beyond gelation. 143
Figure 4.14 Effect of heating rate beyond gelation on polymer volume changes. 144
Figure 4.15 Moment due to cure volume changes at different heating rates. 144

CHAPTER 1

INTRODUCTION AND LITERATURE REVIEW

1-1 INTRODUCTION

The inhomogeneous structure of thermoset polymer composites causes cure shrinkage and thermal volume changes during processing to produce residual stresses. These stresses may be high enough in epoxy polymer composites to cause microdamages such as ply cracking and delamination which may affect their mechanical properties and durability (1-3). In addition, these stresses result in geometrical distortion of composite parts which increases as the part size increases. This goes against the current trend in aerospace and other industries to develop large integrated structures to reduce the expensive cost of assembling small parts. Part assembly and fit up are known as the major cost item of producing tight-tolerance parts as those used in stealth technology.

Residual stresses in polymers and polymer composites have been the subject of many previous studies. These stresses develop during cure process as well as during cooldown after cure is complete. Contradictory findings and assumptions have been found regarding the contribution of cure shrinkage to the residual stresses. Also, little work was done to modify the cure cycles to reduce residual stresses. In Sections 1-2 and 1-3, a brief discussion of key experimental and theoretical studies done up to date is given. The problem statement of the current study is given in Section 1-4.

1-2 EXPERIMENTAL STUDIES

Several experimental methods have been used to measure residual stresses in polymers and polymer composites. This includes double beam method [4-6], photoelasticity [7-10], confinement tubes with different geometry [11-18], fiber optics [19], piezoresistivity [20], peel-ply [21], unsymmetric laminates [21-23], single fiber stress test [24], and others [25]. Double beam method is simple and can be used to study the development of stresses in thin polymer films but not in composites or polymers under constraints. Using this method, Dannenberg studied the development of residual stresses in Epon 828 and 1002 epoxies cured with different agents [4]. It was shown that residual stresses increase with curing temperature and depend on the curing agent. Also, it was shown that stresses start to develop significantly when temperature drops below glass transition temperature. Using similar test setup, Wang and Yu studied residual stresses in diglycidyl ether of bisphenol A [5]. They used different cure cycles and showed that lowering cure temperatures may reduce stresses build up. However, longer cure time is needed at lower cure temperatures. Using a film coat on ac quartz beam, Feger and his coworkers studied the development of residual stresses in PMDA-ODA polyamic acide polyimide films [6]. They showed that the removal of solvent and changes in moisture content cause stresses to develop in the polyimide films. Results indicate that the polyimide films maintained about 25% of total stresses in the vicinity of glass transition temperatures and disappeared only after heating to higher temperatures.

Pawlak and Galeski [7] used three-dimensional photoelasticity to study residual stresses in polymer matrix with spherical inclusions. It was shown that residual stresses increase

significantly as the space between inclusion decreases. Similar conclusions were shown by Theocaris and Paipetis [8]. Asamoah and Wood used photoelasticity to study residual stresses in fiber reinforced epoxies [9]. They showed that stresses in resin increases significantly as fiber spacing decreases. A tri-con of matrix material is created between fibers which is subjected to high level of constraining by the fibers. The authors used elastic finite element analysis to confirm their conclusions qualitatively. Cunningham and his coworkers studied residual stresses in resin materials between fibers in fiber reinforced composites inside a rigid outer shell [10]. The constrained resin was shown to undergo significant residual stresses.

Shimbo and his coworkers measured the effect of modifying epoxide resin with a spiro ortho-ester on residual stresses [11]. They measured stresses by measuring strains in a ring surrounded by the curing polymer. It was found that the modified resin has a lower glass transition temperature and hence less build up of residual stresses. In another paper, they modified the polymer to reduce the polymer stiffness while maintaining the same glass transition temperature [12]. Reducing stiffness causes residual stresses to decrease as expected. In both cases, reduction of stresses is accompanied by scarifying desirable properties. In a later study, Shimbo and his coworkers studied the mechanism of stresses development in epoxide resins [13]. It was shown that contribution of cure shrinkage to final residual stresses increases significantly when the cure is carried below glass transition temperature.

Lee and Schile attempted to simulate the development of stresses in fiber reinforced epoxy composites. They arranged glass rods inside a curing polymer and measured strains in the rods during cure and cooldown [14]. Also, they conducted an elastic finite

element analysis of the same problem. They studied different epoxy/hardener systems used in composites. The results show that the glass rods constraint the polymer volume changes. Residual stresses due to thermal shrinkage during cooldown assuming elastic analysis were smaller than measured values. The difference was attributed to cure shrinkage. Different systems of epoxy-hardener produced different relative values of stresses due to cure shrinkage to cooldown thermal shrinkage. Plepys and his coworkers studied the effect of degree of confinement of the polymer during cure on the development of residual stresses used in Epon 828 epoxy cured with different curing systems [15,16]. Test data show that when one-dimensional constraints exists, the contribution of cure shrinkage to the final residual stresses is much smaller than that of thermal shrinkage. When three-dimensional constraints were considered, stresses due to cure shrinkage were significantly high and of comparable values to that of thermal stresses during cooldown. Similar findings were shown by Korothov and his coworkers [17,18]. According to the principles of mechanics, the behavior of polymer approaches pure elastic behavior under three-dimensional confinement. In this case, stress relaxation of stresses due to cure shrinkage may be ignored and cure shrinkage, which is usually of large value, will contribute significantly to residual stresses. Interestingly, Plepys showed that for certain cure schedules, stresses due to cure volume changes (thermal expansion during heating and cure shrinkage) after the cure is complete may be in the opposite direction of stresses due to cure shrinkage and hence will reduce final residual stresses.

Lawrence and his coworkers used embedded fiber optics to measure strains in composites due to residual stresses [19]. It was shown that significant strains are

developed during processing of cross ply laminates made of HyE/6049U carbon/epoxy composites. Results indicate that strains start to build up during cure due to chemical shrinkage. These strains may constitute up to 25% of the total mechanical strains and hence residual stresses. Crasto and Kim tried to utilize carbon fiber piezoresistivity to measure residual stresses in composites [20]. It was shown that, as already established, that increasing cure temperature results in increasing fiber stresses as measured by fiber piezoresistivity.

In another study, Crasto and Kim measured stress free temperature in AS4/3501-6 graphite/epoxy as an indication on residual stresses [21]. A definition for the stress free temperature is the temperature at which a freestanding unsymmetric laminate will be flat. The higher the residual stresses, the higher the stress free temperature will be. The unsymmetric laminates were cured at different temperatures and produced different glass transition and stress free temperatures. Test data showed that stress free temperature is higher than both curing temperature and glass transition temperature. The difference between stress free temperature and cure temperature, about 15°C, was attributed to cure shrinkage stresses. Stress free temperature was higher than glass transition temperature with about 8°C. It was expected that above glass transition temperature the softening of the matrix will cause composite to loose stiffness and the laminate will remain flat at higher temperatures. However, when the temperature was raised above stress free temperature the direction of the laminate curvature was reversed indicating that the laminate still maintaining significant stiffness. This can be explained by the fact the behavior of the polymer in composites in the existence of fiber confinement may be different than that of neat polymers.

Some case studies have been conducted to investigate the effect of cure cycle modification on the cure induced residual stresses [22,23]. In these studies, the cure cycles were modified arbitrarily to see the effect on residual stresses. In one study [22], the standard two dwell cure cycle (cure cycle recommended by the prepreg manufacturer) for IM6/CYCOM 3100 graphite/BMI composite was modified by introducing a third dwell temperature. Different locations and duration of the third dwell temperature were investigated (see Figure 1.1). One of the modified cycles reduced the stresses by up to 25% while maintaining the mechanical properties as that of the specimens cured with the standard cure cycle. There were no criteria for choosing the location and duration of the additional dwell temperature. In another study [23], the two dwell cure cycle of 976 epoxy was modified by extending the first dwell temperature. As can be seen from Figure 1.2, such extended cycles can reduce spring back of unsymmetric laminates by more than 25%. While these studies showed that modifying cure cycles can reduce residual stresses in composites, they are not effective because of the trial and error methods involved. These experimental methods to modify the cure cycles to reduce the residual stresses demonstrated the validity of such approach. However, they did not provide definite criteria to modify the cure cycles.

A new test method was developed by Madhukar and his coworkers which is based on curing the polymer around a pretensioned fiber and monitor the change in the fiber tension [24]. After the polymer develops significant stiffness, volumetric changes in the polymer will change fiber tension which is a measure of the residual stresses. They demonstrated that changing the cure cycle of Epon 828 cured with mPDA will change the contribution of cure volume changes to the residual stresses in the fibers.

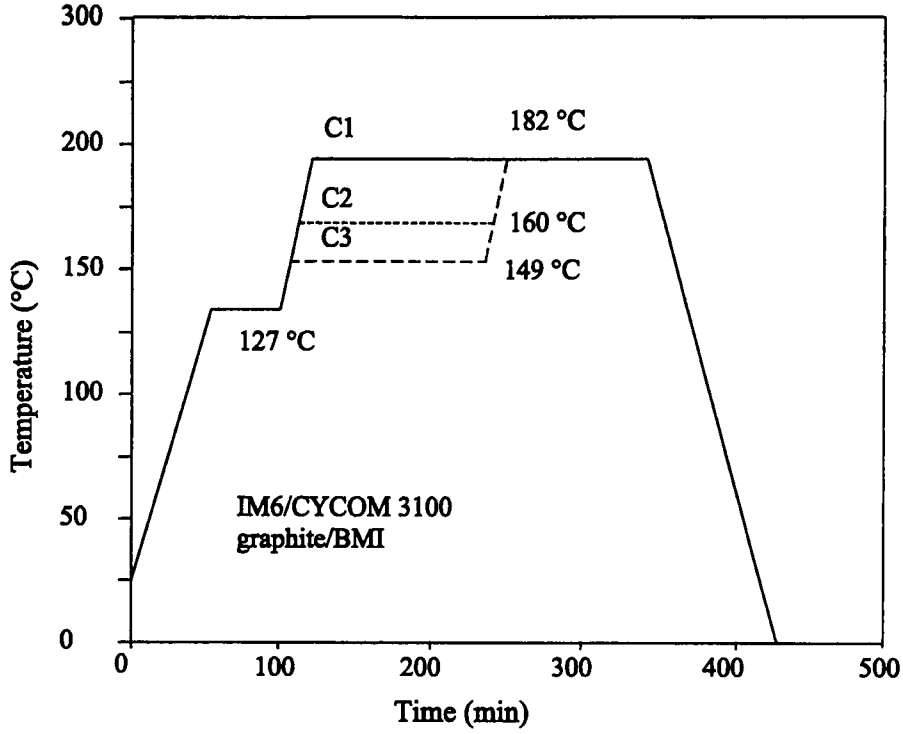

(a) Cure cycles

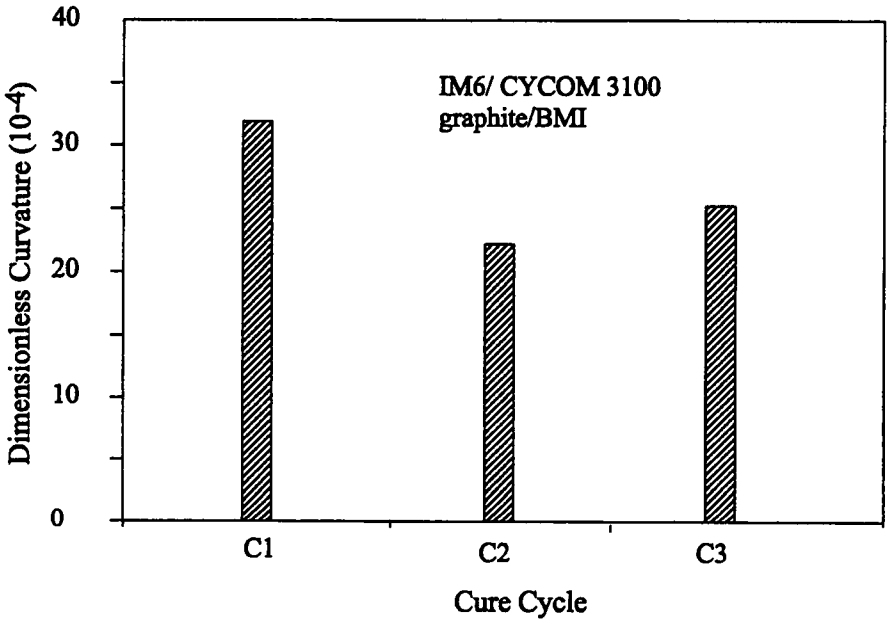

(b) Dimensionless curvature

Figure 1.1 Cure cycle modification to reduce residual stresses.

Adapted from White, S. R. and H. T. Hahn. 1993. "Cure Cycle Optimization for the Prediction of Processing-Induced Residual Stresses in Composite Materials," J. of Composite Materials, 27(14), 1352-1378.

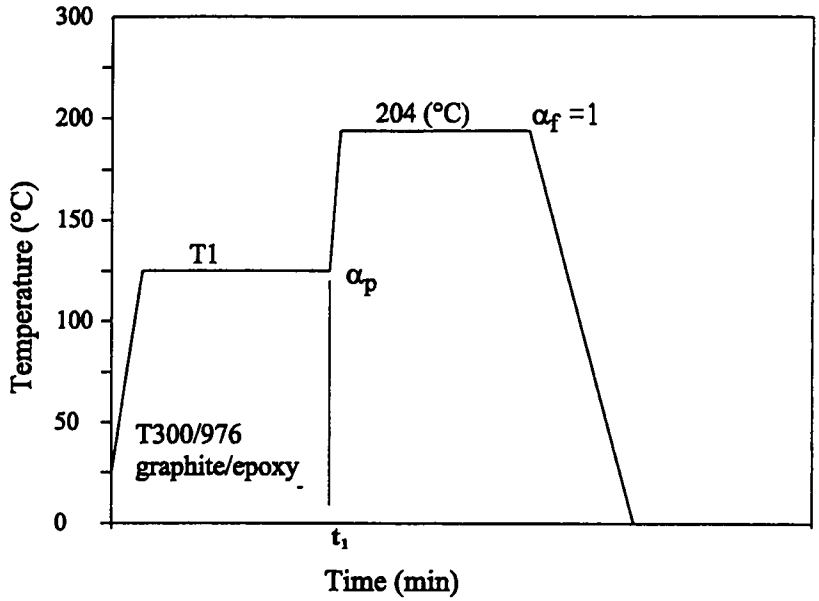

(a) Cure cycles

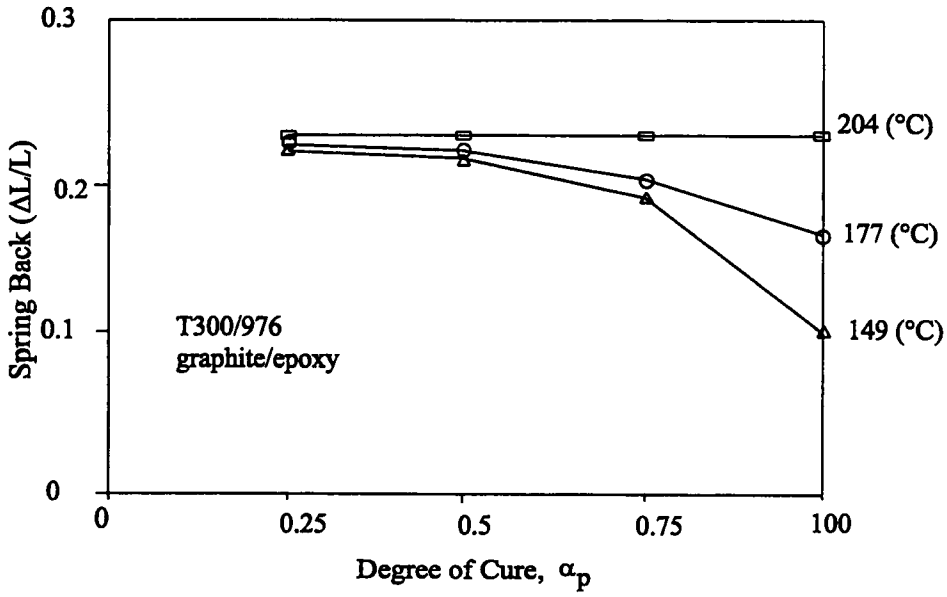

(b) Spring-back

Figure 1.2 Another method for cure cycle modification to reduce residual stresses

Adapted from Sarrazin, H., B. Kim, S-H. Ahn, and G. S. Springer. 1995. "Effect of Processing Temperature and Layup on Springback," J. of Composite Materials, 29(10), 1278-1294.

1-3 THEORETICAL STUDIES

In earlier studies, stresses developed due to thermal shrinkage during cooldown were evaluated using linear elastic analysis [26]. Stresses due to cure shrinkage were neglected assuming that it will be relaxed during cure. In another study, the effect of swelling due to moisture absorption was shown to reduce residual stresses [27]. The author indicated that residual stresses may exceed 50% of the transverse tensile strength. Based on the elastic analysis, he concluded that stress free temperature is lower than the curing temperature. Excluding the effect of moisture which depend on environmental conditions considered, this conclusion can not be generalized in the view of experimental data discussed above. In a later study by the author, the effects of residual stresses on ply cracking and warping in unsymmetric laminates were discussed [1]. It was shown experimentally that stress free temperature can be higher than curing temperature and the cooldown rate apparently has no effect on residual stresses. Also, data shows that changing gelation temperature may reduce residual stresses.

In a later study, White and Hahn studied the development of residual stresses during the curing process [28]. It was shown that transversal stiffness and strength, which are matrix dominated, develop only after the polymer degree of cure exceeds 0.83 in IM6/CYCOM 3100 graphite/BMI composites. Also, it was shown that the postcure causes increase in the residual stresses which was attributed to the shrinkage due to the additional cure and the loss of moisture or volatiles.

Other models were developed to estimate stresses development during curing process [29-35]. Modeling of the mechanical properties as a function of degree of cure and

temperature have been the most difficult because of the interdependency and viscoelasticity involved. Assumptions involved in modeling the mechanical properties development in the composite directly affect the validity of the predicted stresses. A model to evaluate residual stresses in polymer composites predicted that chemical shrinkage contributes less than 5% to final residual stresses in IM6/CYCOM 3100 graphite/BMI composites during cure [29,30]. The model included viscoelastic analysis to account for stress relaxation. Based on experimental data, they considered that the transverse modulus increases significantly only after certain degree of cure. Test data as shown in Figure 1.3, indicates that the model underestimates the residual stresses due to overestimation of stress relaxation and/or underestimation of mechanical properties or cure shrinkage [22]. This can be recognized considering that for thermosetting polymers, the cure induced stresses by chemical shrinkage may exceed 30% of final stresses [15-19, 25]. This is supported by the fact that changing the cure cycle for this composite system (with the same cure temperature and cooldown rate) affects the final residual stresses significantly which is mainly attributed to the change in the contribution of chemical shrinkage [22].

A model was developed to evaluate cure stresses in thick composites [31-35]. Stress relaxation was not considered and resin modulus was evaluated using a rule of mixture type model. Transverse mechanical properties were assumed to develop starting from degree of cure zero, which contradicts experimental findings [28]. Mechanical properties of the composite were estimated from the properties of matrix and fibers using micromechanics neglecting any interaction. As discussed above, behavior of the resin with high fiber volume fraction as in composites may be significantly different from that

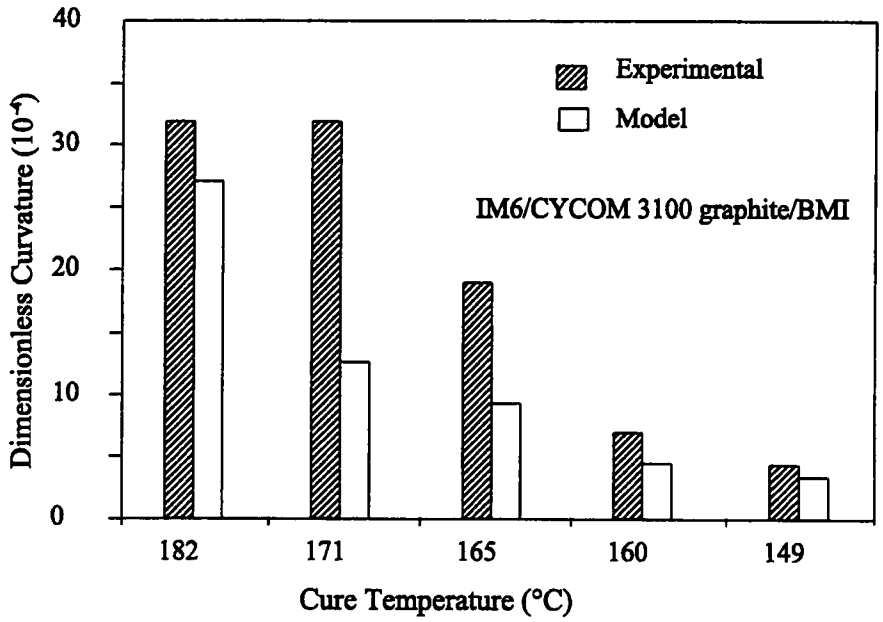

Figure 1.3 Comparison between test results and model predictions

Adapted from White, S. R. and H. T. Hahn. 1993. "Cure Cycle Optimization for the Prediction of Processing-Induced Residual Stresses in Composite Materials," J. of Composite Materials, 27(14), 1352-1378.

of the neat resin. Full cure shrinkage was used to estimate stresses. Experimental results indicate that only part of the cure shrinkage may contribute to residual stresses [4-18,28]. As expected, the model predicts high values of cure stresses. No experimental verification was presented to support the model.

Weitsman developed a rigorous viscoelastic optimization model to maximize stress relaxation during cooldown for a given cooling down time [36,37]. The model predicts about 10% reduction in residual stresses in epoxy-resin composites if optimum cooldown path is applied although this has not yet been supported by experimental data. Harper and Weitsman conducted an experimental and theoretical investigation on the effect of cure shrinkage, moisture, and cooldown path on residual stresses in polymer composites [38-40]. The presence of moisture was shown to enhance viscoelastic behavior. Predictions of stresses due to moisture change were in reasonable agreement with experimental data. Based on their optimal cooldown path for AS4/3502 graphite/epoxy, a 10-15% reduction in residual stresses may be obtained, however, it was not seen experimentally. Using double beam method, Harper showed that cure shrinkage may contribute up to 25% of residual stresses in 3502 epoxy [41].

Several models were developed to evaluate residual stresses in thermoset polymers [42-50]. Levitsky and Shaffer developed an elastic model to evaluate stresses in a solid sphere cast from a thermoset polymer during curing [42-43]. The formulation is rigorous, however results are not directly applicable to composites. Lange and his coworkers studied stresses build up in thermoset films cured below their ultimate glass transition temperatures [44,45]. They used a Maxwell model to simplify viscoelastic analysis. Double beam method was used to verify analysis predictions. It was shown that

contribution of cure changes to final residual stresses depends on the amount of resin shrinkage beyond gelation and density of crosslinking. They indicated that stresses from cure shrinkage vary from 1 to 30 % of the final residual stresses depending on the polymer under consideration and on applied cure cycle. Mallick and Krajcinovic developed a micromechanical model to study stress and strain fields in resin slab [46]. They demonstrated the use of aggregation-percolation models to obtain the constitutive equations of the curing resin. Stresses were shown to develop significantly only after gelation. A similar approach was considered earlier by Adolf and Martin [47-49]. Adolf suggested the use of time-cure superposition to account for nonisothermal cure viscoelasticity. They indicated that changing cure cycle for a given polymer may affect significantly the contribution of cure shrinkage to final residual stresses. Monk and his coworkers developed a viscoelastic model for residual stresses in spun polyimide films [50]. They used fundamentals of chemical reactions and macromolecules to predict macro-properties such as stiffness and strains. Shrinkage due to evaporation was included in the analysis. Given the formulation approach, many parameters were difficult to measure and/or verify. These parameters were estimated by fitting the model predictions with test results obtained using double beam method.

Finite element analysis (FEA) was used to study the development of residual stresses in composites [51-56]. Jain and Mai used linear FEA to study the development of residual stresses in T300/934 graphite/epoxy composite cylinders including the effect of cure shrinkage (which was taken arbitrarily as 1.5%) [51,52]. Measured spring-in values for channel sections were found to change with tooling materials. The predicted results based on the assumed cure shrinkage value appear to agree reasonably with measured

values. Sala and Di Landro used linear FEA and classical laminate theory to study residual stresses in T800/5250-2 graphite/BMI composite system [53]. In their formulation, they considered stress build up form stress free temperature. In that study, stress free temperature was measured experimentally and was found to exceed cure temperature by about $53 \pm 5^{\circ}C$. For a given measured stress free temperature, the elastic solution was shown to overestimate curvature of unsymmetric laminates. In a later study [54], the authors reported that based on the comparison between analytical and experimental results, the transverse modulus of the composite was found to change with time and temperature as an indication of the presence of viscoelasticity.

Wang and Daniel developed a linear viscoelastic model to study residual stresses and warpage in woven-glass/epoxy laminates [55]. In their formulation, they considered a thermorheologically simple model for time-temperature superposition. Chemical shrinkage in addition to thermal expansions were considered in calculating stresses. Because of the woven nature of the fabric, both transverse modulus and longitudinal modulus were found to exhibit time-temperature dependency. The viscoelastic analysis was found to yield satisfactory results when qualitatively compared to experimental data.

Mohan and Grentzer used linear FEA to simulate processing and predict residual stresses development in glass/vinyl ester composites [56]. They applied the method to study stresses development during cure of a composite nozzle. The authors indicated that the contribution of cure shrinkage is significant although it needs more investigation to be quantified.

1-4 PROBLEM STATEMENT

From the above discussion, it can be seen that a substantial amount of research work was done to investigate the development of residual stresses in thermoset polymers and polymer composites. However, contradictory assumptions and conclusions still exist regarding the effect of major parameters on the development of stresses. For example, the extent of cure shrinkage contribution to residual stresses and effect of stress relaxation are not clear yet. In addition, very little work was done to reduce these stresses without scarifying desirable properties or elongating the cure cycle. This necessitates a fundamental understanding for the process of cure stresses development. This fundamental understanding can then be used to study the possibility of reducing residual stresses.

Two approaches will be used in the study. The first approach is mainly experimental using single fiber cure induced stress test (discussed section 1.2) [24]. This new method was developed to monitor fiber stresses during cure in single fiber composites. The method was shown to be simple and effective to study stresses development. In the current study, this method was used to investigate stresses development in single fiber thermoset polymer composites. Different material systems were considered to obtain general understanding. Then, the method was modified as necessary to optimize cure cycles to reduce residual stresses. Experimental tests were conducted to verify that reduction in residual stresses was not compromised with scarifying mechanical properties or other cure requirements (glass transition temperature).

The second approach is theoretical modeling based on the fundamental understanding gained from single fiber test, including cure cycle optimization, other experimental findings from literature, as well as principles of mechanics. The model was used to simulate the cure process and evaluate stresses development during curing and during cooldown. The model was also used to study the relative effect of governing factors on residual stresses.

The thesis is divided into three major parts

1- Experimental methods of single fiber stress test method and feedback control system and their typical applications (Chapter 2).
2- Results of applying the single fiber stress test and feedback control system to different composite systems (Chapter3).
3- Mechanical model formulation and its typical results (Chapter 4).

CHAPTER 2

EXPERIMENTAL METHODS

2-1 INTRODUCTION

A test procedure to study the development of cure induced stresses in thermoset polymer composites was developed at the Composite Materials Laboratory at the University of Tennessee as discussed in Chapter 1 [24]. The method was applied to a simple epoxy system (Epon 828/mPDA system). The test proved to be a simple and effective method to study the development of cure induced stresses. Preliminary results showed how polymer volume changes during cure affect fiber stresses. Also, it was shown that changing the cure cycle changes the stresses developed during cure. However, the early version of the test setup was basic and not suitable to run tests on more complicated polymer systems requiring higher cure temperature and more uniform heating. In addition, test components and procedure were not yet well developed to eliminate the effects of parameters other than polymer volume changes. This includes friction between fiber and test components, degassing technique that takes long time that may advance cure before resin is poured around the fiber, shape of the mold which result in constraining the polymer during shrinkage, and nonuniform temperature along the specimen. For example, results of the early version of the test setup for AS4/3501-6 graphite/epoxy composite were not always consistent.

In the current research work, this test method was modified to resolve the above problems. The modified test setup and the testing procedure produced consistent results for several materials systems. The modified setup and procedure were used to study the effect of the cure cycles on the cure induced stresses. A closed loop feedback control system was also developed to obtain cure cycles that reduce stresses. In this chapter, the modified test method and its typical results are presented and discussed. Feedback control system and its applications are also described.

2-2 CURE INDUCED STRESS TEST (CIST)

Figure 2.1 shows the conceptual mechanism assumed for the development of fiber stresses in CIST due to polymer volume changes. The polymer is cured around a portion of a pretensioned fiber. Once the polymer develops sufficient stiffness, thermal expansion in the polymer (as a result of heating) will result in decreasing fiber tension. On the other hand, shrinkage in the polymer (as a result of crosslinking or cooling down) will result in increasing fiber tension. The change in the fiber tension will decrease with time because of stress relaxation whenever the polymer exhibits viscoelastic behavior. Correspondingly, it can be seen that polymer shrinkage will result in compressive stresses in the fiber portion embedded inside the polymer whereas the expansion will result in tensile stresses.

All volume change data presented here for comparison were obtained at the Air Force Research Laboratory. The volumetric dilatometer used was GNOMIX, Inc. PVT Apparatus (Figure 2.2). More details about the test setup and procedure can be found in

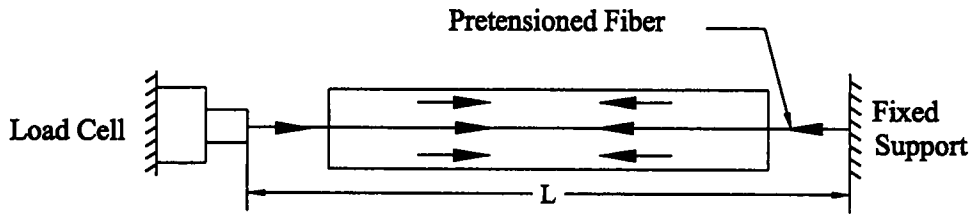

(a) Polymer shrinkage increases the fiber tension.

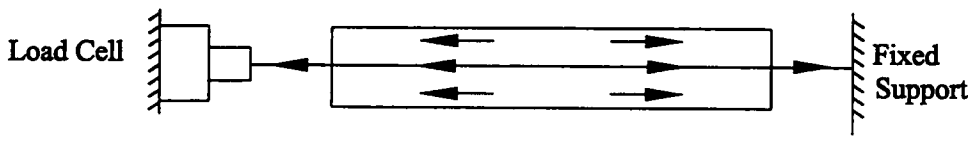

(b) Polymer expansion decreases the fiber tension.

Figure 2.1 Mechanism of cure induced stress test.

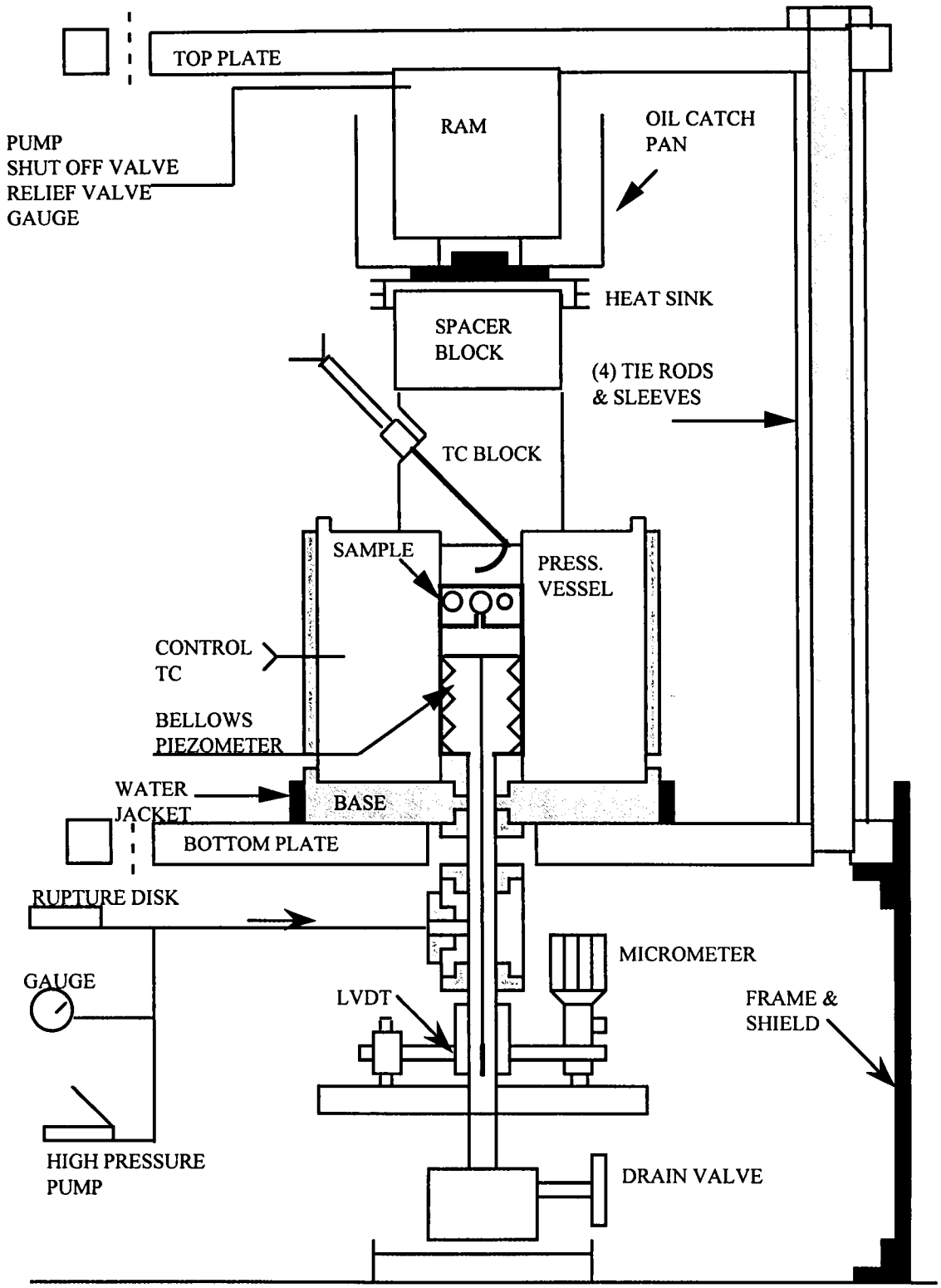

Figure 2.2 Details of the PVT apparatus.

reference [57]. Figure 2.3 shows the volume change data of 3501-6 epoxy during a two dwell cure cycle recommended by resin manufacturer (standard cure cycle). There is expansion during heating from ambient temperature to the first dwell temperature and during heating from the first dwell temperature to the second dwell temperature. On the other hand, there is shrinkage due to crosslinking during the temperature holds and also upon cool down after cure is complete. Hence, there are two types of volume changes occurring during the cure of thermoset composites; first type is the expansion during heating and the other is the shrinkage due to the chemical reaction (crosslinking shrinkage) and during cooling down (thermal shrinkage). Volume changes prior to polymer gelation are not expected to contribute to residual stresses since the melted polymer acts like a fluid with low viscosity and stress relaxation will impede stresses build up. Gelation is defined by the point at which an infinite network of molecules is developed inside the polymer. Beyond gelation, volume changes produce proportional stresses in the fibers and stresses may start to build up.

Through the rest of this thesis, the term *effective* volume will be used to refer to the volume changes that produce stresses in the fibers. *Effective* expansion occurs during any heating beyond the polymer gelation, and *effective* shrinkage results from polymer crosslinking beyond gelation and during cool down. *Effective* expansion will produce tensile stresses in the fiber portion embedded inside the polymer, whereas *effective* shrinkage will produce compressive stresses. This can easily be seen from the test mechanism shown in Figure 2.1. In typical cure cycles, the gelation temperature is close to the maximum cure temperature and hence *effective* expansion (which corresponds to

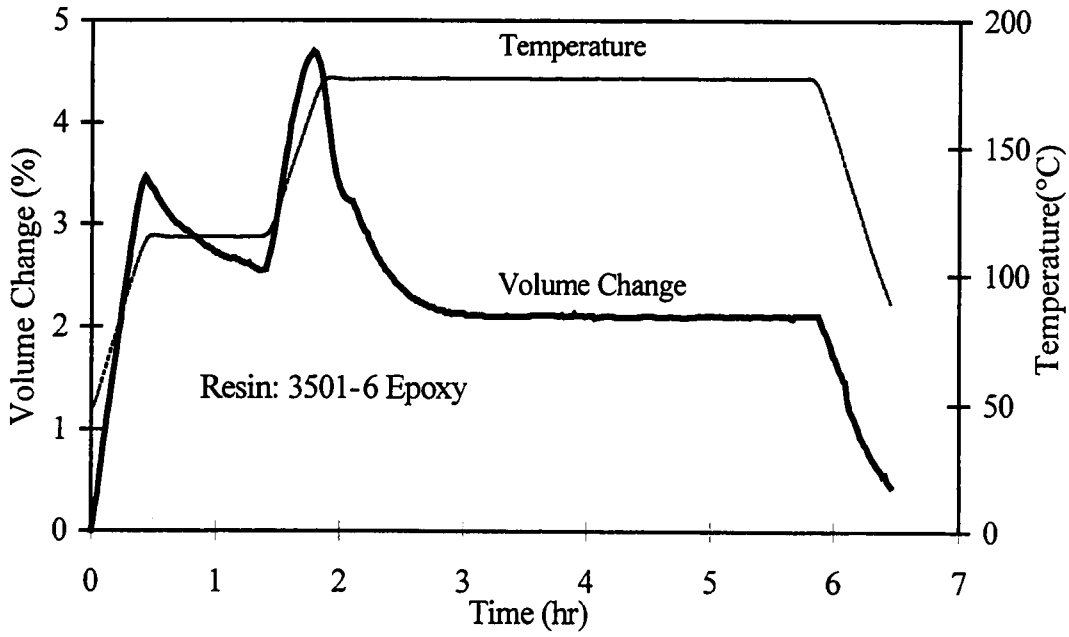

Figure 2.3 Variation in polymer volume during standard cure cycle.

the increase in the temperature from gelation to the maximum cure temperature) is typically small, if any.

2-2-1 Test Setup

Figure 2.4 shows a schematic diagram of CIST. Figure 2.5 shows a photograph of the test setup. The fiber is glued to a rigid support at one end, and the other end is passed through a cavity in a silicone mold and then glued to a load cell (250 gm load capacity and 0.01 gm sensitivity). A ceramic shield is used to form a cure chamber around the mold. The shield has two narrow slots, one at each end to pass the fiber. The sizes of these slots were kept to a minimum to reduce the heat loss at the ends and to avoid significant variation in the temperature inside the cure chamber. The dimensions of the cure chamber are approximately 160 mm long, 70 mm wide, and 76 mm high. A ceramic strip heater (from Research Inc., Model 4184) is placed at the top to apply the time-temperature cycle. A thermocouple is located beside the middle of the silicon mold to monitor temperature. The thermocouple is connected to a data acquisition system. A computer program was written to control the temperature and to collect fiber tension data through the cure cycle. The program was found to produce a heating profile within ±0.25°C of a given input time-temperature cycle. The dimensions of the silicon mold are 76 mm long, 3.5 mm wide, and 2 mm high. The thickness of the base of the silicone mold was kept as small as possible (about 0.3 mm) to minimize the effect of silicone volume changes and constraints applied by mold on the polymer on test results.

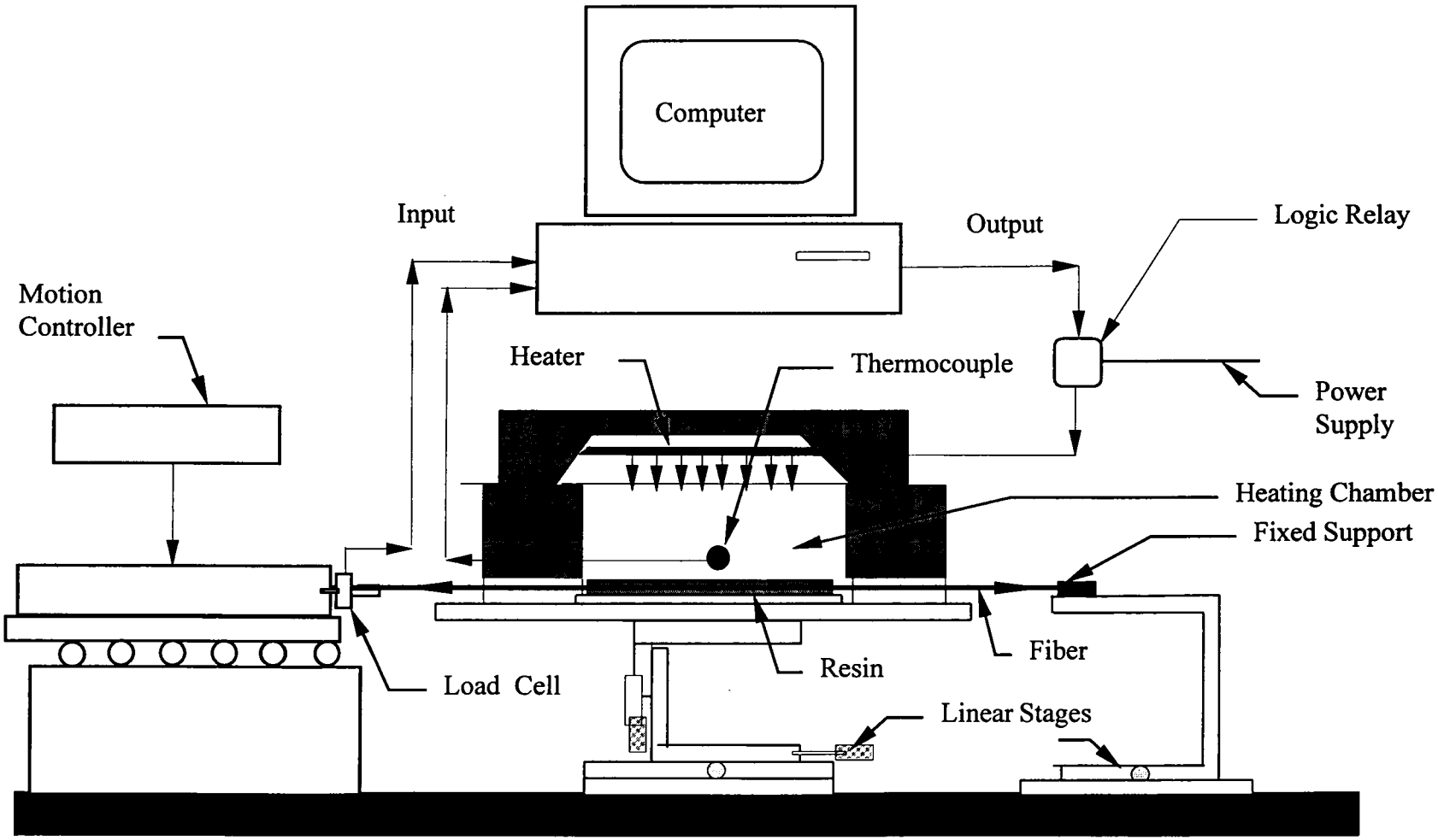

Figure 2.4 Schematic diagram of single fiber test.

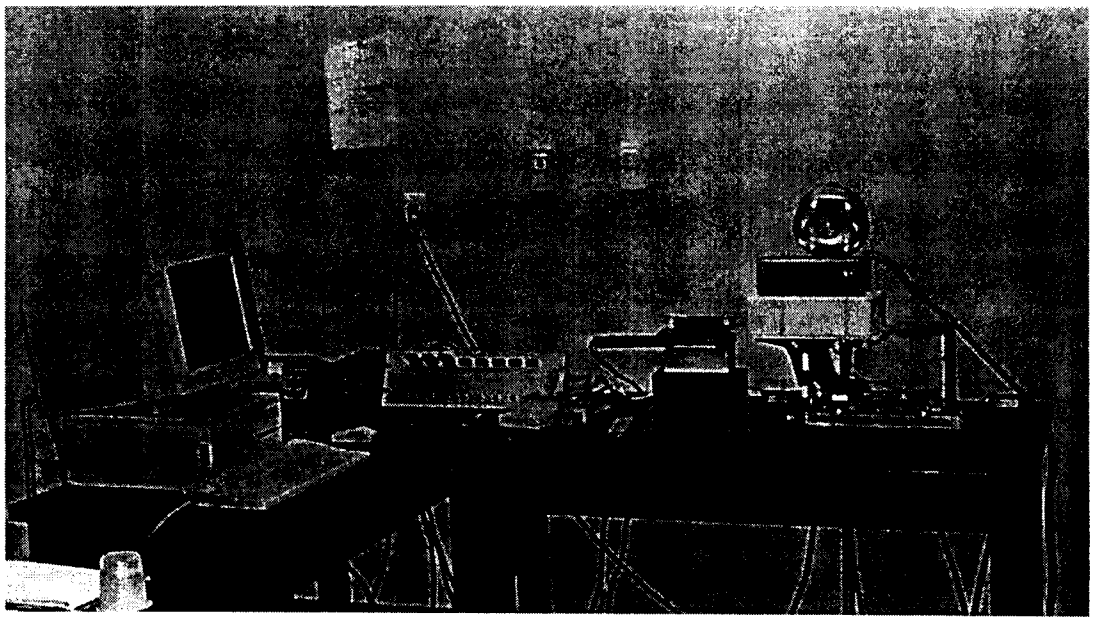

Figure 2.5 Cure induced stress test

After positioning the fiber, the glue is allowed to cure according to the recommendations of its manufacturer. Then, the fiber is pretensioned to about 5 gm. The load cell reading should be stable for at least 5 minutes before pouring the polymer around the fiber to ensure proper fiber fixation and the cure of the glue. About 1 gm of the resin is melted and degassed in a high temperature syringe using a vacuum oven. The degassing temperature is chosen to be the minimum temperature that is high enough to melt the resin and enable degassing while not causing significant cure in the polymer. After degassing, the resin is injected inside the silicon mold around the fiber and the cure cycle is started.

CIST results will be shown as the fiber tension data obtained from the load cell reading. A comparison between fiber tension data and stresses in fiber portion embedded in the resin shows that any increase in the fiber tension more than its initial value (as a result of the resin shrinkage) corresponds to the application of compressive stresses on the fiber portion embedded inside the polymer. On the other hand, any drop in the fiber tension below its initial value (as a result of the resin expansion) corresponds to the application of tensile stresses on the fiber portion embedded inside the polymer. Under no external loads, the matrix in the vicinity of the fiber experiences tensile or compressive stresses when the fiber experience compressive or tensile stresses, respectively.

2-2-2 Typical Results

The material used in this section is AS4/3501-6 graphite/epoxy composite system. The standard cure cycle of 3501-6 consists of: heating the sample from room temperature to

116°C in 30 minutes; holding the temperature at 116°C for 60 minutes; raising the temperature from 116°C to 177°C in 25 minutes; holding the temperature at 177°C for 240 minutes; followed by cool down to room temperature.

Figure 2.6 shows the fiber tension data during such a cycle. The polymer volume change data for this cure cycle is shown in Figure 2.3. A good correlation between fiber tension and volume change can be seen. During the first part of the cure cycle, the fiber tension remains constant because the viscosity of the resin is small. As the resin viscosity increases, the expansion during the heating ramp causes the fiber tension to decrease and the crosslinking shrinkage causes the fiber tension to increase. The crosslinking shrinkage during the second temperature dwell increases the fiber tension. Finally, thermal shrinkage during cool down causes increase in the fiber tension. The drop in the fiber tension during the heating ramp corresponds to the development of tensile stresses in the fiber portion embedded in the polymer. The increase in the fiber tension during the second dwell corresponds to development of compressive stresses in the fiber portion embedded in the polymer. The fiber tension at the end of the cure, just before cool down starts, is higher than the initial fiber tension indicating the development of compressive stresses in the fiber portion embedded in the polymer. These stresses are undesirable because they will be added to compressive stresses developed during cool down and hence increases residual stresses.

In the CIST, the composite system is essentially a single fiber in an infinite polymer. To simulate a more representative fiber volume fraction as in composite laminates, an experiment was performed with fiber coated with a thin layer of resin. Figure 2.7 shows

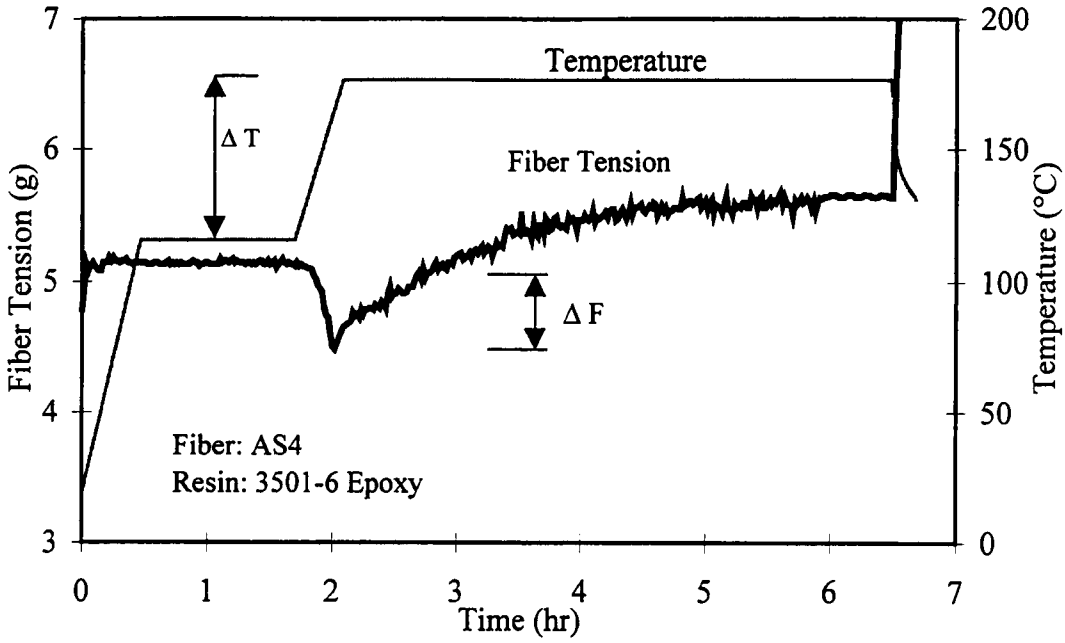

Figure 2.6 Variation in the fiber tension during the standard cure cycle of 3501-6 epoxy.

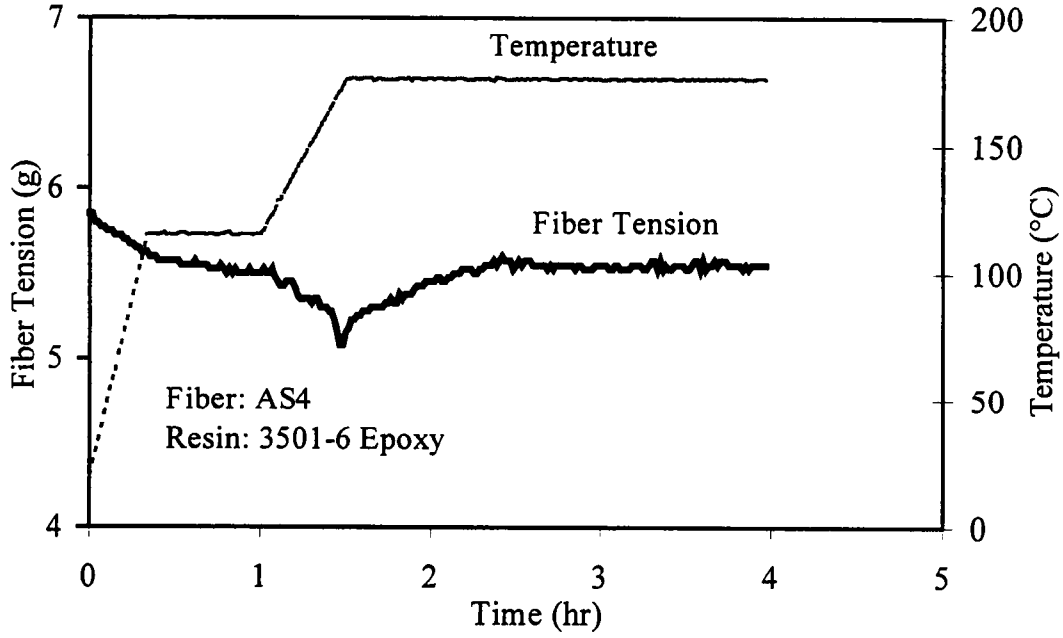

Figure 2.7 Fiber tension during the standard cure cycle for a single fiber coated with a thin layer of 3501-6 epoxy.

variation in the fiber tension when the coated fiber was subjected to the standard cure cycle. The shape of the fiber tension profile is the same as that obtained with the fiber embedded inside a larger volume of polymer (Figure 2.6) but with smaller values. This suggests that the mechanisms that are identified in the single fiber model composites are present in composite laminates as well.

2-2-3 Parameters of CIST

To study the reproducibility of the test results and determine the effect of different parameters including initial fiber tension and fiber embedded length, several CIST experiments were conducted on AS4/EPON 828 graphite/epoxy single fiber composites. This composite system was chosen because it is easy to work with and the duration of the cure cycle is relatively short. The EPON 828 is a diglycidyl ether of bisphenol-A and was cured with 14.5 parts per hundred by weight of meta-phenylene diamine (mPDA). The resin was mixed, degassed under vacuum for 10 minutes, and cured with different cycles. The typical cure cycle used for this resin consists of: heating from ambient temperature to 75°C in 5 minutes then the temperature is held at 75°C for 2 hrs; then it is raised to 125°C and held at 125°C for two hours followed by cool down to ambient temperature.

Figure 2.8 shows typical CIST results for Epon 828/mPDA epoxy. The fiber tension is unchanged for the first 1.5 hours at 75°C. Some increase in the fiber tension occurs during the last 0.5 hour at 75°C. The fiber tension drops rapidly when the temperature is increased from the first dwell at 75°C to the second dwell at 125°C. Then, again there is

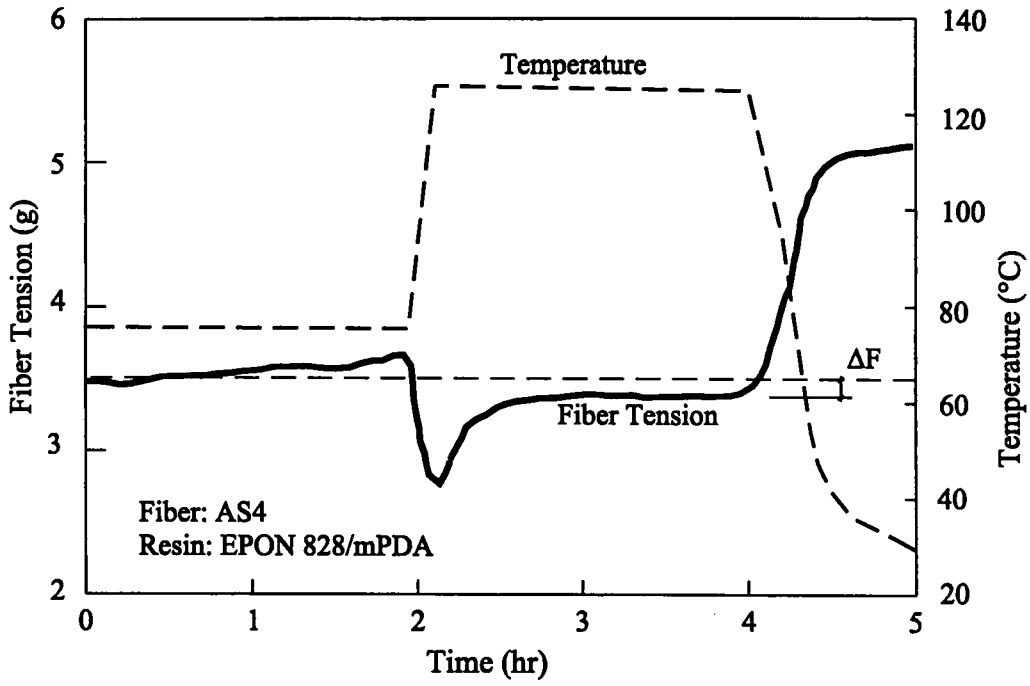

Figure 2.8 Fiber tension change during a typical two dwell cure cycle.

an increase in the fiber tension during the first half-hour at 125°C temperature hold. During cooling to ambient temperature, the fiber tension again increases and stabilizes at the completion of cooling down.

In Figure 2.8, the rapid heating from room temperature to the first dwell temperature just melts the resin without allowing significant resin cure to occur. Thus, it is expected that the resin just flow around the fiber without causing fiber stresses. During the temperature hold at 75°C, the viscosity of the resin increases with the advancement of resin cure. At that stage, volume changes start to be *effective* and the cure shrinkage starts to increase fiber tension. During the temperature ramp between first and second dwell temperatures both thermal expansion and crosslinking shrinkage exists. However, it appears that the rapid heating rate causes thermal expansion to dominate producing net expansion. This expansion causes fiber tension to drop. The chemical shrinkage during second temperature hold causes fiber tension to increase again. Finally, thermal shrinkage during cool down increases the fiber tension.

The changes in the fiber tension shown in Figure 2.8 are primarily due to polymer volume changes because the effect of fiber expansion/shrinkage is relatively small. This can be seen from CIST results shown in Figure 2.9. In that set of tests, the silicon mold cavity was not filled with resin and only the fiber was running through. The cure cycle was applied and the changes in fiber tension were recorded. The test was repeated with different types of fibers. Results show that fiber tension does not change significantly during the cure cycle because of fiber volume changes.

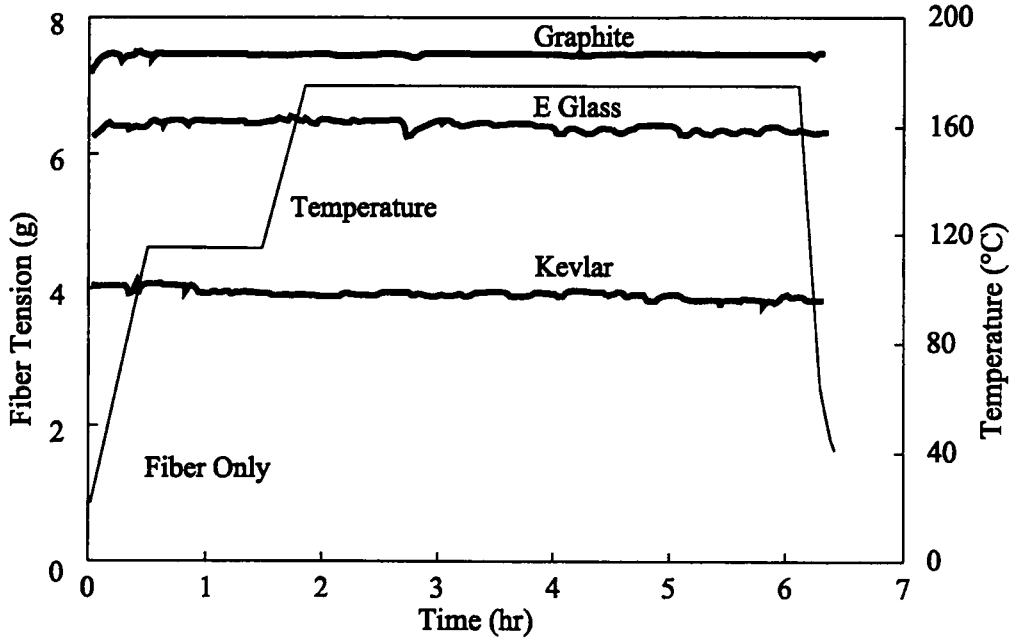

Figure 2.9 Effect of temperature change on the fiber tension (no polymer).

Figure 2.10 shows results of CIST under different values of initial fiber tension. Results indicate that the initial fiber tension has no effect on the changes in the fiber tension during the cure cycle. Figure 2.11 shows the effect of embedded fiber length on the variation in the fiber tension. The tension in the free fiber length is proportional to the deformation at the end embedded in the polymer. This deformation increases as the embedded fiber length increases. Thus the fiber tension in the free length increases as the embedded length increases. This can be seen from CIST results in Figure 2.11. In all cases, test results were highly reproducible.

To further understand the effect of polymer volume change and stress relaxation on the fiber stress, the cure cycle was modified as shown in Figure 2.12. A heating ramp from 65°C to 149°C was divided into 3 equal steps of 16.7°C and one last step of 33.3°C. Similar to the case of typical two dwell cycle, there is no change in the fiber tension during first heating ramp from ambient temperature to the first dwell temperature. The fiber tension remains unchanged until the end of the second temperature ramp suggesting that the polymer has low viscosity and/or insignificant crosslinking shrinkage. The fiber tension starts to increase rapidly during the second temperature hold indicating that the resin now has significant stiffness. The fiber tension drops during the third temperature ramp due to thermal expansion. Beyond this stage, the fiber tension increases during the temperature holds and drops during the following temperature ramps.

A comparison among the change in the fiber tension during different temperature steps in Figure 2.12 shows that after the resin has sufficient stiffness, the rate of the fiber tension increase decays with advancement in the cure cycle. This is expected since the

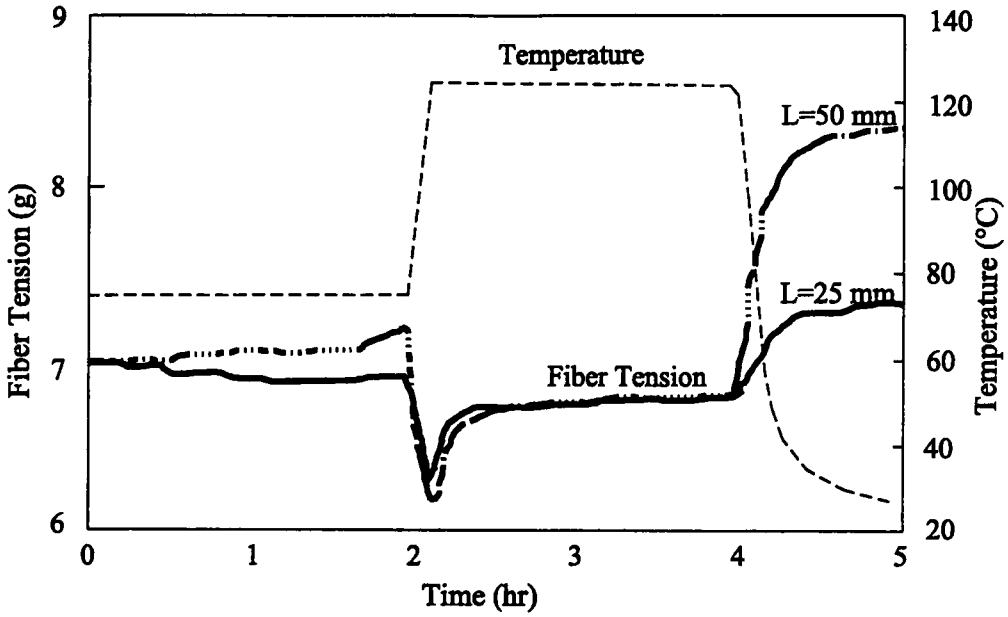

Figure 2.10 Effect of embedded fiber length on the variation in the fiber tension during cure.

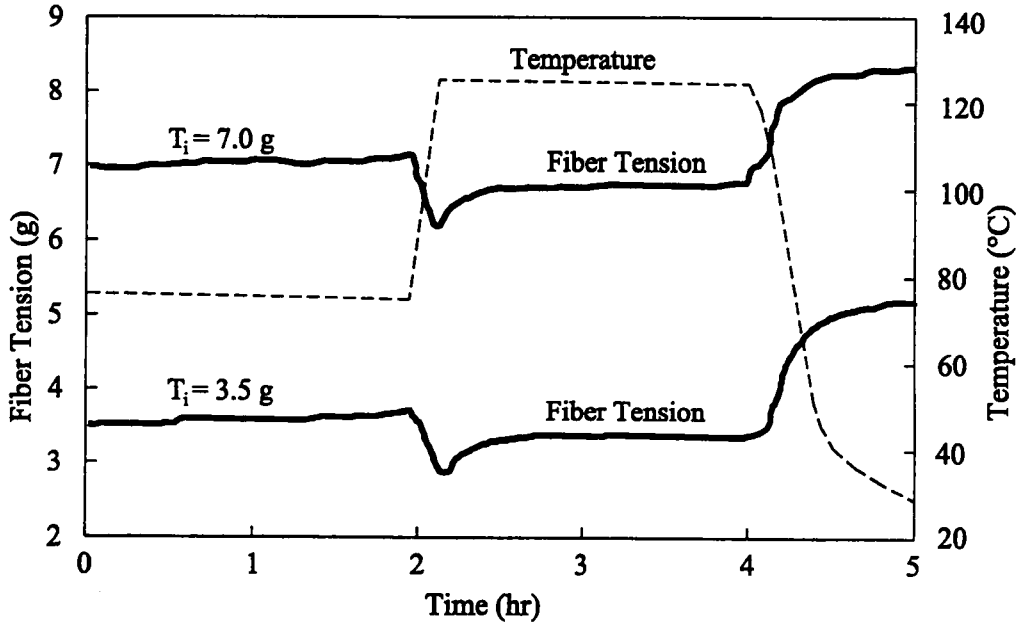

Figure 2.11 Effect of initial fiber tension on the variation in the fiber tension during cure.

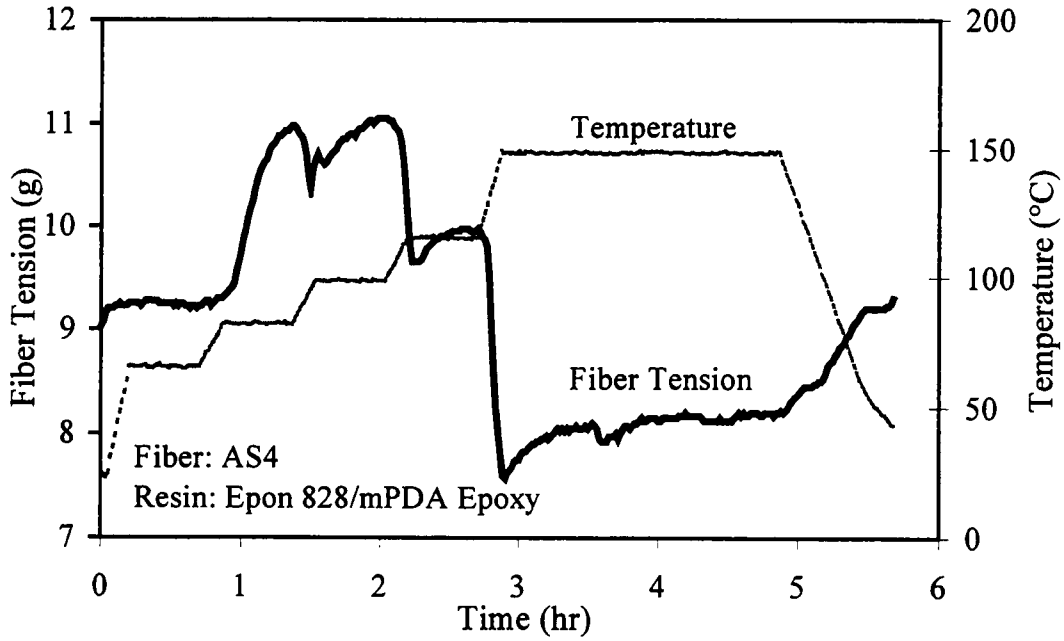

Figure 2.12 Effect of changing cure cycle on fiber tension in AS4/Epon 828 single fiber composites.

rate of the chemical reaction and hence the crosslinking shrinkage decreases after it reaches certain extent. Also, the drop in the fiber tension due to thermal expansion during heating increases with the increase in the polymer cure. This is expected since as the degree of cure increases, the resin attains higher stiffness and exhibits less stress relaxation. The drop in the fiber tension during the last temperature ramp (with 33.3°C temperature increment) is almost twice the drop in the ramp just before it (with 16.7°C increment). This indicates that polymer stiffness and stress relaxation may not change significantly beyond certain extent of cure. Results in Figure 2.12 suggest that when thermal expansion is developed towards the end of the cure cycle it will contribute significantly to fiber stresses.

Average stresses in the embedded part of the fiber during a cure cycle were calculated from simple mechanics of materials. Assuming a uniform fiber stress distribution along the embedded fiber length and perfect bond between the fiber and the matrix, the fiber stresses in the free part of the fiber, $\sigma'_f(t)$ (Figure 2.13), at time t, can be related to the fiber tension as

$$\sigma'_f(t) = \frac{T(t) - T(0)}{A_f} \qquad (1)$$

where $T(t)$ is the fiber tension at any time t, $T(0)$ is the initial fiber tension, and A_f is the cross sectional area of the fiber. The corresponding strain ($\varepsilon'_f(t)$) can be written as

$$\varepsilon'_f(t) = \frac{T(t) - T(0)}{A_f E_f} \qquad (2)$$

where E_f is the Young's modulus of the fiber. The total deformation in the free fiber length ($\Delta'(t)$) is given by:

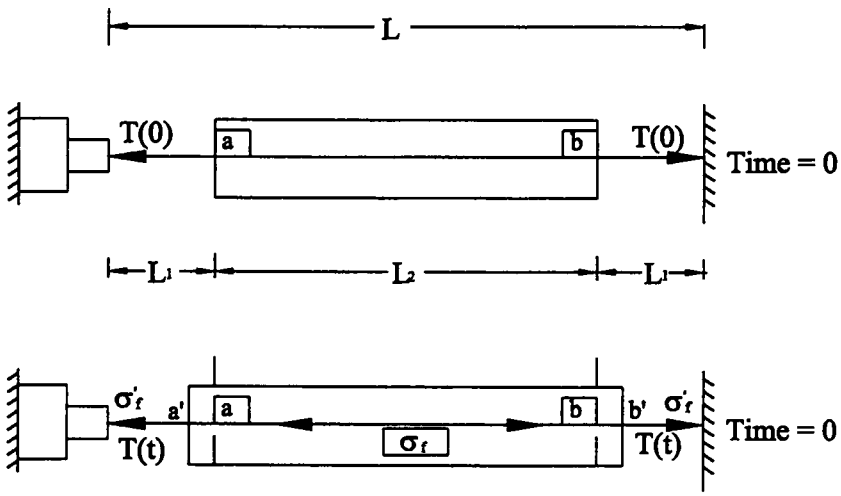

Figure 2.13 Schematic of the model used to calculate fiber stress during cure.

$$\Delta'(t) = \frac{T(t) - T(0)}{A_f E_f} 2 L_1 \qquad (3)$$

where L_1 is as shown in Figure 2.13. Since the fiber length is fixed during the test, the deformation in the embedded part equals that of the free part with a negative sign. Thus, the strain in the embedded length ($\varepsilon_f(t)$) is given as

$$\varepsilon_f(t) = -\frac{T(t) - T(0)}{A_f E_f} \frac{2 L_1}{L_2} \qquad (4)$$

where L_2 is the embedded fiber length as shown in Figure 2.13. Thus, stresses in the embedded fiber length can be written as

$$\sigma_f(t) = -2 \frac{T(t) - T(0)}{A_f} \left(\frac{L_1}{L_2} \right) \qquad (5)$$

The effect of the change in the fiber length due to temperature change was neglected in Equation 5 since the thermal expansion coefficient of fibers is generally very small relative to that of the resin. The fiber stresses calculated from Equation 5 for a single fiber graphite/epoxy composite are plotted in Figure 2.14. The fiber stresses shown in this figure are due to matrix volume changes only, i.e., the fiber stresses resulting from the initial fiber tension *T(0)* are not included. An important observation in Figure 2.14 is that when the temperature is raised from the first dwell to the second dwell, the embedded fiber experiences a tensile stress peak (~1.2 GPa). To verify the results on cure induced fiber stress obtained from Equation 5, independent tests were conducted with different values of *T(0)*. The average tensile strength of AS4 fibers ranged from 2.5 to 3.0 GPa. Thus, if a fiber is prestressed to about 1.4 GPa, the cure induced tensile

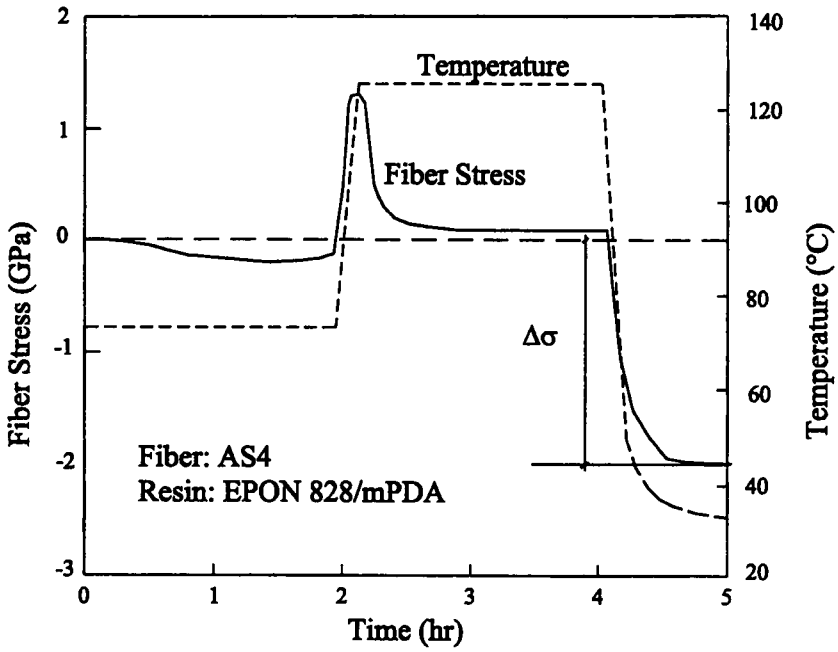

Figure 2.14 Fiber stresses during a typical two dwell cure cycle.

stress (1.2 GPa) superimposed on the fiber prestress value will cause the fiber stress to approach its failure stress. Tests showed that when CIST conducted with the fiber prestressed to ~1.4 GPa, a fiber crack was detected as shown in Figure 2.15. When the fiber was prestressed to less than 1.4 GPa, no fiber crack was detected. These observations suggest that, although the analysis used to calculate the fiber stress during the curing is based on some gross assumptions (such as uniform fiber stress along the entire embedded length), it still agrees quite well with the experimental observations.

To verify that the fiber fracture occurs within a short time interval when the temperature is raised from 75°C to 125°C, two additional experiments were conducted. In both of these specimens, the fibers were pretensioned to about 70% of their expected failure load. Such pretension loads are expected to produce fiber failure during the standard cure cycle. In one of the specimens the test was terminated after the first temperature hold, i.e. before starting the temperature ramp. The specimen was removed and immediately examined under an optical microscope. No fiber crack was detected in this specimen. The other specimen was removed at the end of the heating ramp and was immediately examined under the microscope. This specimen did show a fiber crack as that shown in Figure 2.15. This suggests that the fiber failure occurred during the heating ramp from 75°C to 125°C.

For a given upper cure temperature limit, there may be many cure cycles which complete the cure. The resulting residual stresses will not be the same since different cycles mean different amounts of *effective* volume changes and different extents of stress relaxation. The following example shows how changing the cure cycle can change cure induced stresses. Figure 2.16 shows the change in the fiber stresses during a

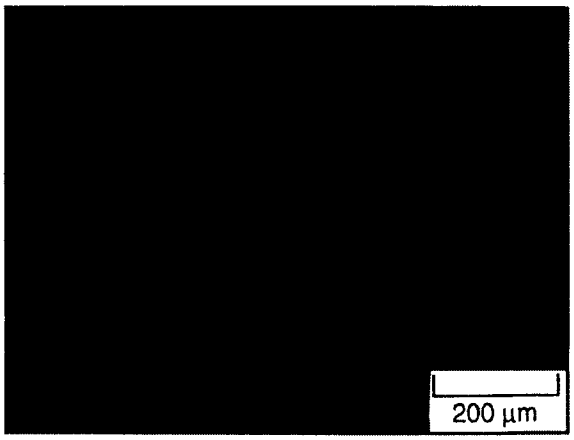

Figure 2.15 Cure induced stresses produced fiber fracture in a pretensioned fiber.

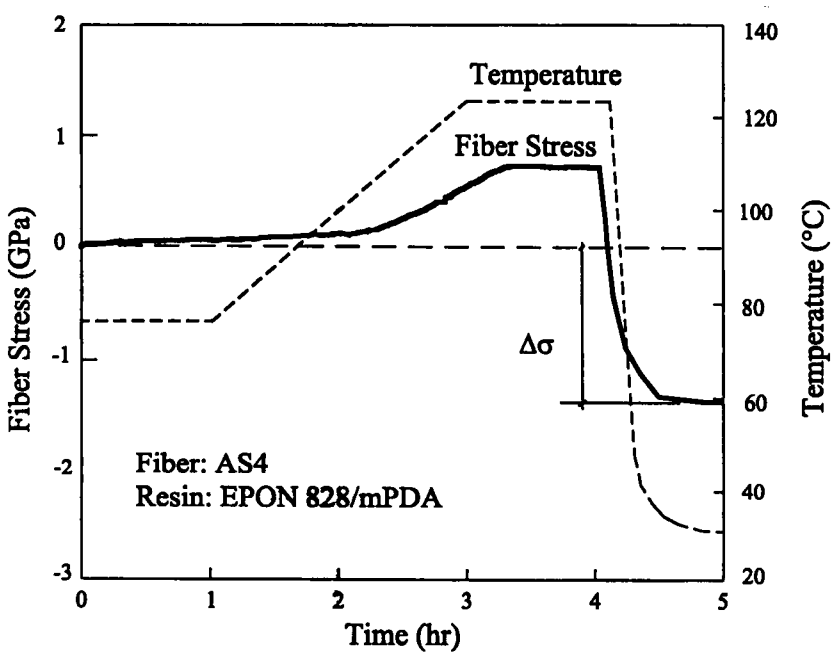

Figure 2.16 Variation in fiber stresses during the modified cure cycle.

modified cure cycle. The heating rate during the heating ramp from the first to the second dwell temperatures was reduced arbitrarily to allow for more balance between chemical shrinkage and the thermal expansion. Also, the slow heating rate allows for more stress relaxation. Moreover, the gradual heating applies more thermal expansion towards the end of the cure cycle which causes thermal expansion to be *effective*. The modified cycle results in more uniform profile for the fiber stress. The maximum value of tensile stress was lower than that in the typical two dwell cure cycle. To further verify the results of Figure 2.16, another CIST was conducted with the fiber prestressed to 1.8 GPa. No fiber fracture was detected when the cure cycle shown in Figure 2.16 was used. The final value of the tensile stresses in the fiber at the end of the cure, just before cool down, was higher than that in the standard cure cycle. As discussed earlier, tensile stresses that develop during cure counteract part of the stresses developed due to the thermal shrinkage and thus reduce the final residual stresses. In this case, the new cycle is expected to produce less residual stresses after cool down is completed. This can be seen by comparing final value of fiber stresses at the end of each cycle ($\Delta\sigma$ in Figures 2.14 and 2.16).

2-3 MODIFICATION OF CURE CYCLES USING TRIAL AND ERROR METHOD

To study the effect of changing the cure cycle on fiber tension profile, several tests were performed on AS4/3501-6 graphite/epoxy. The objective was to find a modified cure cycle that minimizes the stresses development in the fiber during cure. Such a cure cycle

will produce ultimately a flat fiber tension curve. The parameters are, initial heating temperature and the subsequent heating rate/s. Maximum temperature was set as that of the standard cure cycle. Trial and error approach was used to explore the existence of such a cycle. Figure 2.17 shows corresponding fiber tension profile during one of the intermediate trial cycles. It is clear that changing the cure cycle affect the variation in the fiber tension. The trial and error was continued until the cycle shown in Figure 2.18 was obtained. The obtained cure cycle almost completely eliminates the variation in the fiber tension during cure. The cure cycle was terminated when the temperature reached the highest cure temperature hold and the fiber tension remained constant for 30 minutes during temperature hold. The new cure cycle produces an almost flat fiber tension curve and it is shorter than the standard cure cycle.

Figure 2.19 shows volume change data during such a cycle. There is a good agreement between polymer volume change and fiber tension. There is no change in the fiber tension during the initial part of the cure cycle where the resin viscosity is low. As the polymer viscosity increases, the thermal expansion combined with stress relaxation act to cancel stresses due to crosslinking shrinkage and thus fiber tension remains constant. To check the completeness of resin cure, the glass transition temperature of the specimens cured using the standard and the modified cure cycles were measured. Results indicate that the glass transition temperature is almost the same, Table 2.1. Also, the T_g remained unchanged for specimens cured for 30 and 60 minutes longer at the highest temperature in the modified cycle. This indicates that the modified cure cycle satisfies the cure requirement while keeping cure induced stresses to a minimum.

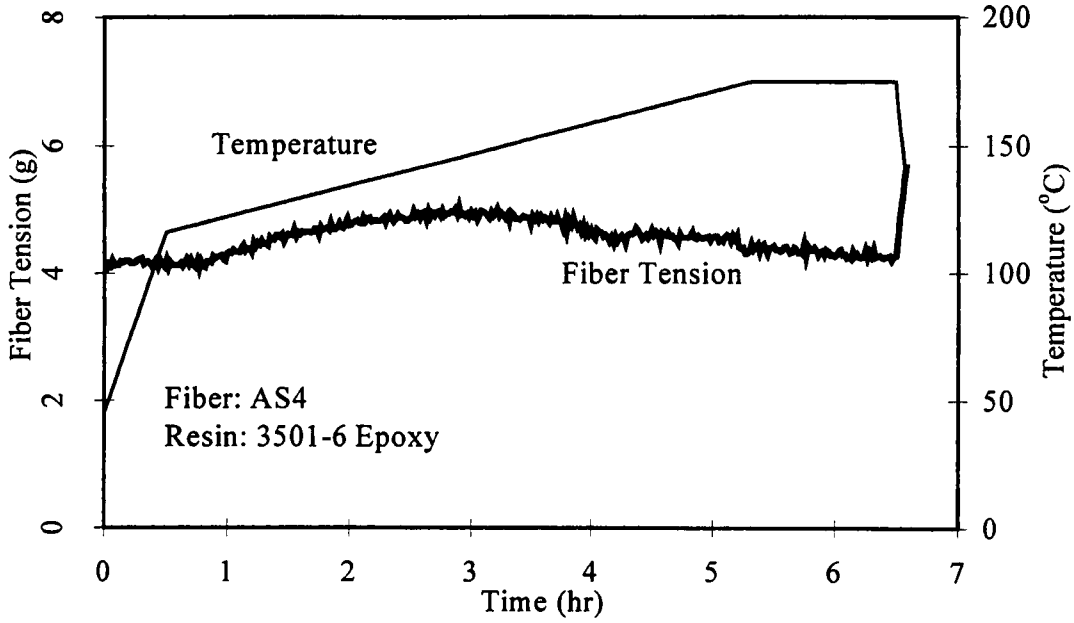

Figure 2.17 Fiber tension during an intermediate cure cycle obtained using trial and error modification method.

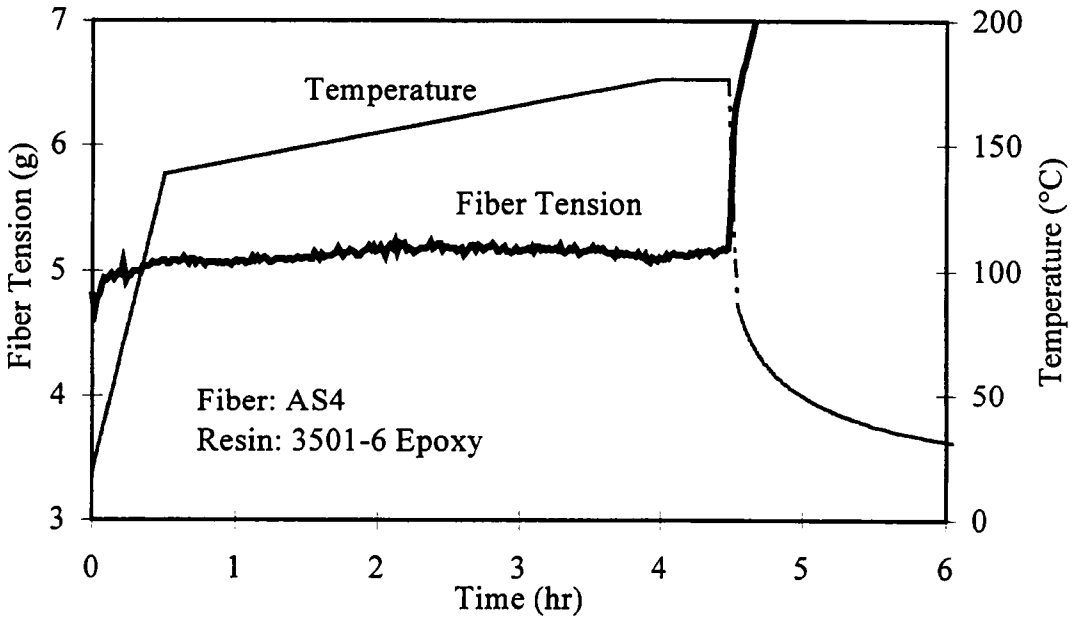

Figure 2.18 Fiber tension during a modified cure cycle of 3501-6 epoxy obtained using trial and error modification method.

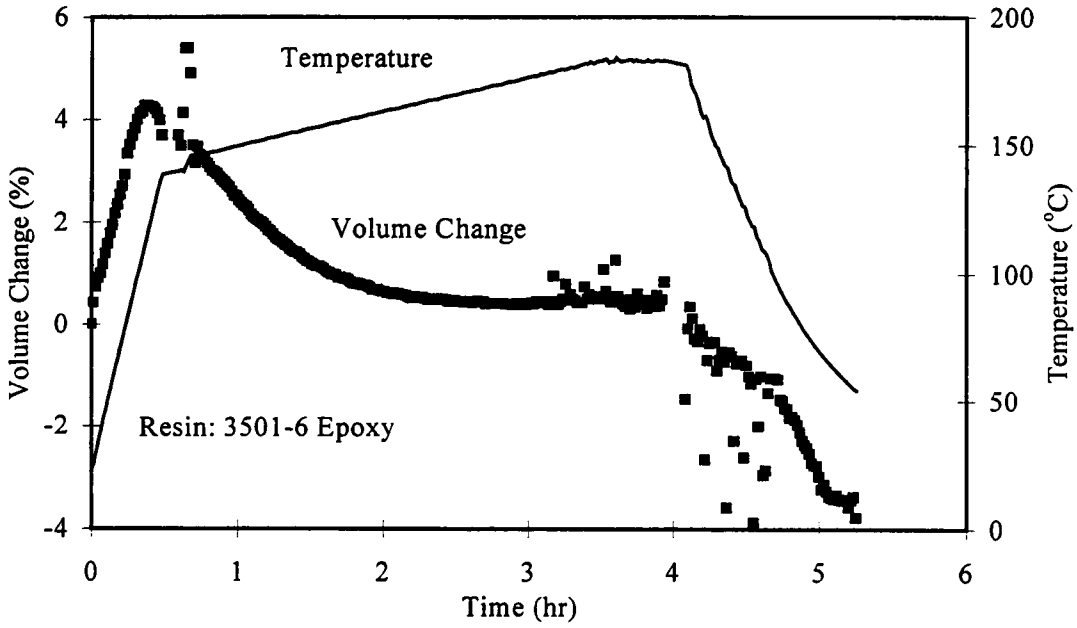

Figure 2.19 Volume changes during the modified cure cycle of 3501-6 shown in Figure 2.18.

Table 2.1 Glass transition temperature for 3501-6 epoxy specimens cured using different cure cycles.

Cure Cycle	Standard Cycle	Modified Cycle	Modified Cycle + 30 min.	Modified Cycle + 60 min.
Glass Transition Temperature	170°C	171°C	172°C	171°C

In the above modified cycle, it was intended to cancel stresses developed during cure cycle. Another approach is to develop tensile stresses inside the composite during cure and maintain these stresses until the cool down. These tensile stresses will counteract part of the compressive stresses resulting from the thermal shrinkage. To develop tensile stresses during cure, the *effective* thermal expansion should be increased. This can be done by developing more thermal expansion after the polymer attains high viscosity. This implies that cure should be carried at a low temperature for long time before heating to a higher temperature to complete the cure. Thermal expansion that occurs during this part of the cure cycle will produce larger tensile stresses than if the heating was applied early in the cure cycle. Figure 2.20 shows typical results of 3501-6 epoxy when this approach is considered. This cure cycle was chosen arbitrarily with the first dwell extended for three hours (versus 1 hr in the standard cure cycle). The drop in the fiber tension during the heating ramp between first and second dwell temperatures in this cycle is larger than that in the standard cycle (Figures 2.6 and 2.20). As a result of this

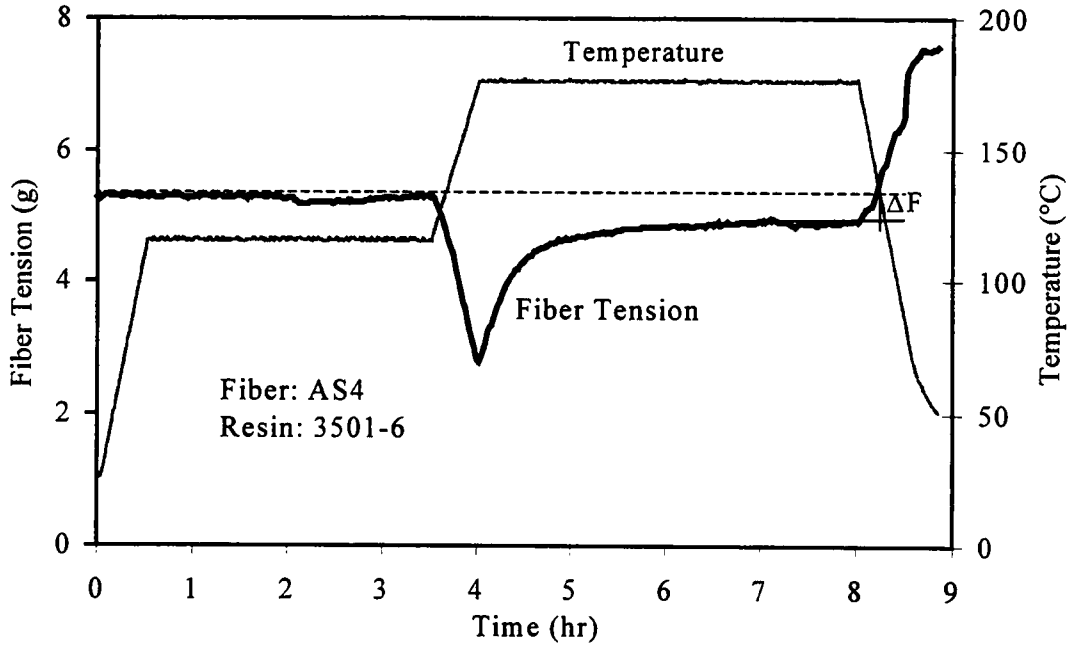

Figure 2.20 Variation in fiber tension during another modified cure cycle of 3501-6 epoxy.

large drop, the fiber tension at the end of the cure cycle, prior to cooling down, was still smaller than the initial fiber tension (ΔF in Figure 2.20). This decrease in the fiber tension corresponds to the development of net tensile stresses in the fiber running inside the polymer. These tensile stresses will offset part of the compressive stresses produced during cool down and hence reduce the final residual stresses. It should be noted that this type of cycle is longer than the standard cycles. The parameters in this approach include, first dwell temperature, number of dwells, duration of these dwells, and heating rates between dwells. The proper choice of these parameters can result in cycles with lower final residual stresses but the cure cycle will be longer.

2-4 MODIFICATION OF CURE CYCLES USING CLOSED LOOP FEEDBACK CONTROL SYSTEM (CLFS)

Effects of residual stresses generated during the cure are reflected in the mechanical properties and dimensional stability of the composite parts. Different cure cycles result in different patterns of volume changes in the polymers during cure. Thus, changing cure cycles can affect residual stress development in composites. In section 2-3, CIST was used to determine modified cure cycles which reduced cure induced stresses in single fiber composites. The approach was to use trial and error to obtain such a cycle. Although the trial and error approach answered the question regarding the existence of such cycles, it was not practical to use with different composites systems since many trials may be involved. This calls for the development of a feedback control system. The idea is to appropriately adjust the volume changes in the polymer and utilize the

viscoelastic stress relaxation to minimize the variation and the values of the cure induced stresses.

As mentioned before, volume expansion and shrinkage occur in the polymer during different periods of the cure process. Before polymer gelation, stress relaxation is very effective and fiber stresses are not likely to build up. As the polymer approaches gelation, the increase in the viscosity causes relaxation of stresses to occur over longer time spans and stresses may start to build up due to cure shrinkage. These stresses can be reduced by inducing thermal expansion in the polymer. In the current study, the CLFS was developed to determine modified cure cycles that reduce cure shrinkage stresses for various composite systems. In this feedback system, the unrelaxed part of stresses developed due to polymerization shrinkage is simultaneously canceled by proportional thermal expansion.

Since *effective* expansion produces tensile stresses, it will counteract a fraction of the compressive stresses due to shrinkage, and thus it reduces final residual stresses. Therefore, it is desirable to suitably increase the *effective* thermal expansion. *Effective* thermal expansion is not a constant for a given resin. It depends mainly on the temperature where gelation occurs. The objective of this research work is to develop a simple procedure to reschedule the cure cycle to produce maximum cancellation of stresses due to *effective* shrinkage with *effective* expansion and stress relaxation.

2-4-1 Optimization Procedure

A computer program was developed to automatically adjust the heating rate during cure to minimize the variation in the fiber tension. The method is based on searching for a heating path that results in a maximum cancellation of the unrelaxed stresses. Thus, when the CLFS detects an increase in fiber tension (as a result of crosslinking shrinkage in the resin), it will increase the temperature such that the resulting thermal expansion suffices to cancel the stresses produced by the chemical shrinkage. On the other hand, a decrease in fiber tension implies excessive thermal expansion in the resin due to rapid heating. In such cases, the program will start to decrease the heating rate proportionally. The check for the change in the fiber tension is done at certain time intervals that are long enough to allow for some stress relaxation. The test is considered complete when the fiber tension stops increasing for a certain period during a temperature hold at the maximum cure temperature. This period (typically from 20 to 40 minutes) varies according to the resin type. A block diagram of the CLFS is shown in Figure 2.21.

2-4-2 Optimization Parameters

The time interval and the heat increment applied by CLFS determine the heating rate at a particular moment in the cure cycle. The time interval is chosen by the user. The longer the time interval, the more stress relaxation is allowed (for same temperature increment). However, a longer time interval means longer cure cycle. For most polymers at high temperature, stress relaxation is inevitable but its extent may vary depending on time and temperature. Stress relaxation can be utilized together with *effective* thermal expansion

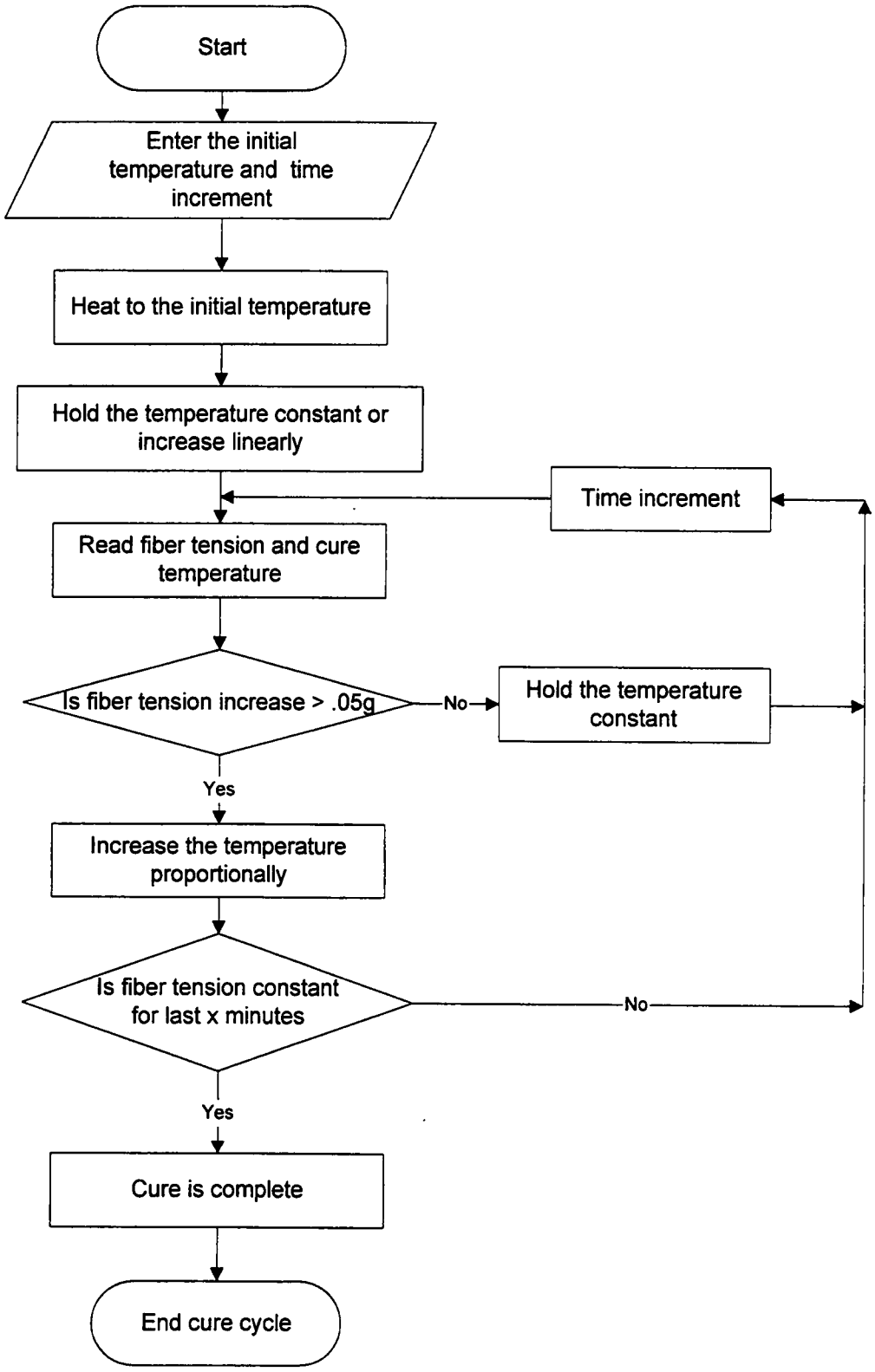

Figure 2.21 Flow chart of the Closed Loop Feedback System (CLFS) used to obtain cure cycles with reduced cure induced stresses.

to minimize stresses due to chemical shrinkage. In practical cure cycles, most of thermal expansion is consumed during initial heating and hence there is a small amount of *effective* thermal expansion. In such cases, stress relaxation should be allowed as much as possible (without significantly prolonging the cure cycle) together with increasing thermal expansion to balance shrinkage stresses. The time interval should not be shorter than that required to allow the effect of the heat increment on matrix thermal expansion to occur completely. The heat increment is proportional to the change in the fiber tension from a reference value, which is taken as the initial fiber tension.

The proportionality constant that determines the extent of heat increment corresponding to a certain change in the fiber tension can be determined approximately by running the CIST with a cure cycle in which temperature is increased in steps. In this study, the initial value of this constant was taken as the ratio of the temperature increase during the ramp between the first and second dwells and the corresponding drop in the fiber tension of the standard cure cycle ($\Delta T/\Delta F$ in Figure 2.6). The proportionality constant was found to change with the degree of cure. The larger the degree of cure, the larger the value of the proportionality constant. This may be attributed to the decrease in the contribution of stress relaxation at higher degree of cure to cancel the change in stresses. In the CLFS, only approximate initial value is required, then the program uses continuously measured fiber tension and temperature change data to adjust this ratio to accommodate for the possible effects of degree of cure and temperature.

The test starts with raising the temperature from room temperature to an initial temperature after which the feedback system starts to control the heating rate. The program scans the load cell reading 1000 times every minute and records their average,

which is then compared to a reference value to determine the change in the fiber tension. A threshold value of the fiber tension change, below which no adjustment in the heating rate is applied, was taken as 0.05 gm to account for the possible small environmental fluctuations.

2-4-3 Typical Results

Figure 2.6 shows the fiber tension profile during the standard cure cycle of AS4/3501-6 graphite/epoxy composites. A noteworthy observation is that the final value of the fiber tension prior to cool down is higher than the initial fiber tension value. As discussed in earlier sections, this net increase in the fiber tension corresponds to the development of compressive stresses in the fibers. These stresses will be added to the stresses produced during cool down resulting in more residual stresses. In the following discussion, results of the modified cure cycles obtained by CLFS are presented.

Figure 2.22 shows the cure cycle obtained from CLFS for the AS4/3501-6 graphite/epoxy. Recall that the feedback system constantly adjusts the heating rate to keep the changes in the fiber tension to a minimum. Consequently, the resulting fiber tension curve is almost flat. Figure 2.23 shows the volume change data obtained from the volumetric dilatometer for the 3501-6 epoxy for a cycle in which the obtained modified cure cycle was approximated with linear segments. The resin volume change curve is almost flat after about 1.5 hours. It is believed that the polymer volume change before 1.5 hours has a minor effect on the fiber tension because polymer viscosity is low and, hence, stress relaxation is very effective to cancel developed stresses. After 1.5

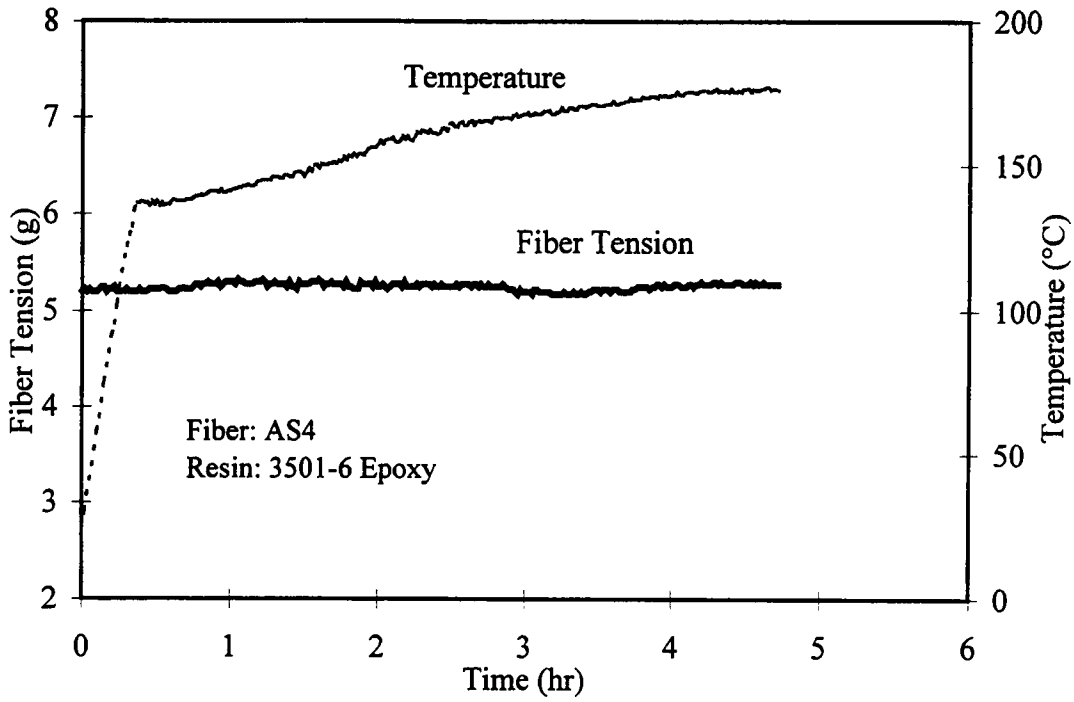

Figure 2.22 Fiber tension data during a cure cycle modified using CLFS.

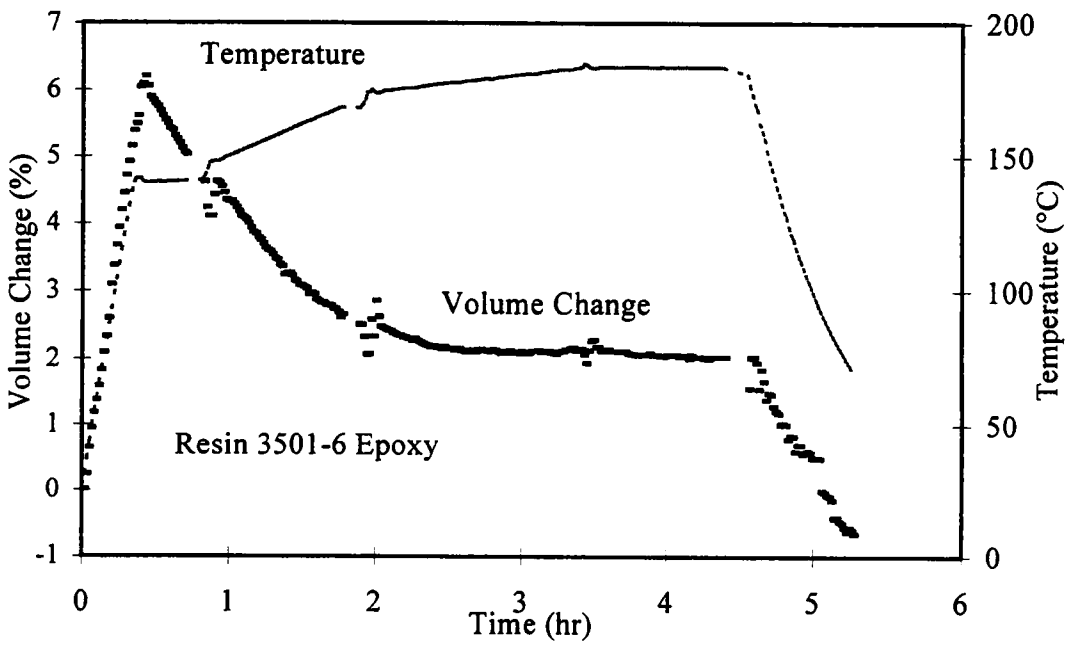

Figure 2.23 Volume change data during a cure cycle modified using CLFS.

hours, the thermal expansion appears to balance the crosslinking shrinkage to keep the polymer volume almost constant. The initial temperature beyond which the computer starts to change the heating rate was 138°C which was taken from the trial and error results. Starting at a lower temperature will increase the duration of the cure cycle. On the other hand, starting from higher temperature will reduce the total amount of thermal expansion that may be needed to the balance the crosslinking shrinkage. The effect of initial temperature will be discussed in Chapter 3. It should be noted that the total duration of the modified cure cycle was shorter than the standard cycle.

Table 2.2 shows the Glass Transition Temperature (T_g) obtained using TMA for 3501-4 epoxy specimens cured using the standard and the modified cure cycles. The values of the T_g for the standard and the modified cycles are almost the same. The modified cure cycle was extended by 30 minutes to study the effect of such increase. The extension of the modified cure cycle does not increase the T_g and hence the cure was considered complete.

Table 2.2 Glass transition temperature for 3501-6 epoxy specimens cured using different cure cycles.

Cure Cycle	Standard Cycle	Modified Cycle	Modified Cycle + 30 min.
Glass Transition Temperature	170°C	171°C	172°C

2-5 SUMMARY

A new test method to monitor the development of cure induced stresses in thermoset polymer composites was modified to study several materials systems. Test results were shown to be highly reproducible. Good qualitative agreement between test results and independently measured polymer volume change data was seen.

The test method was modified with a closed loop feedback control system to modify the cure cycles to produce less cure induced stresses. The modified cure cycles were found to produce less cure induced stresses compared to standard cure cycles while maintaining same glass transition temperature and in some cases shorter cure time.

CHAPTER 3

EFFECT OF CURE CYCLE ON CURE INDUCED STRESSES

3-1 INTRODUCTION

In chapter 2, CIST method was presented. Sample results were demonstrated and it was shown that the test method can be used to monitor the cure induced stresses in single fiber thermoset polymer composites. The test method was modified with a closed loop feedback control system (CLFS) to alter the time temperature schedule to reduce the cure induced stresses.

In this chapter, results of applying CIST and CLFS to different thermoset systems are shown. The CIST was used to study the development of fiber stresses during the cure of several thermoset polymers using cure cycles recommend by resin manufactures. The resins included were 3501-6 and 934 epoxies, 977-3 toughened epoxy, LTM-45 ELD and X343-59 low cure temperature epoxies, and 5250-4 bismaleimide (BMI). Fibers mainly were AS4 graphite and, for comparison, S2 glass in some cases. The CLFS was used to modify such standard cure cycles to reduce cure induced stresses. The results were analyzed and cure cycles were classified according to their effect on the cure induced stresses. The cure cycles obtained from the CIST were applied to cure composite laminates in vacuum hot press to demonstrate the applicability of such cure cycles to processing of composites.

3-2 STANDARD CURE CYCLES

In this section, fiber tension data are shown for different materials during their standard cure cycles. Volume change data whenever available are also shown for verification.

3-2-1 3501-6 and 934 Epoxies

Volume change data during standard cure cycle of 3501-6 epoxy was shown in Figure 2.3. Typical fiber tension data for AS4/3501-6 graphite/epoxy single fiber composite was shown in Figure 2.6. For comparison purpose, the test was repeated with S2 glass fibers instead of the AS4 graphite fibers. The resulting fiber tension profile is shown in Figure 3.1. The trends of the results are similar for the two different fibers. The values of the fiber tension changes are different which may be attributed to the difference in the fiber dimensions, mechanical properties, and interface properties.

Standard cure cycle of 934 epoxy resin consists of: heating from room temperature to 116°C in 30 minutes; holding at 116°C for 60 minutes; raising temperature from 116°C to 177°C in 25 minutes; holding at 177°C for 240 minutes followed by cooling down to room temperature. Figure 3.2 shows the volume change data of this resin during such a cure cycle. There is crosslinking shrinkage during the first dwell temperature indicating the onset of cure. The crosslinking shrinkage increases significantly during the second dwell. Figure 3.3 shows the variation in an AS4 fiber tension during such a cure cycle. The trend of the results is similar to that 3501-6 epoxy. However, the values of the fiber tension change are different for these two resins as should be expected because of the differences in the volume change characteristics of the resins and fiber/matrix interface

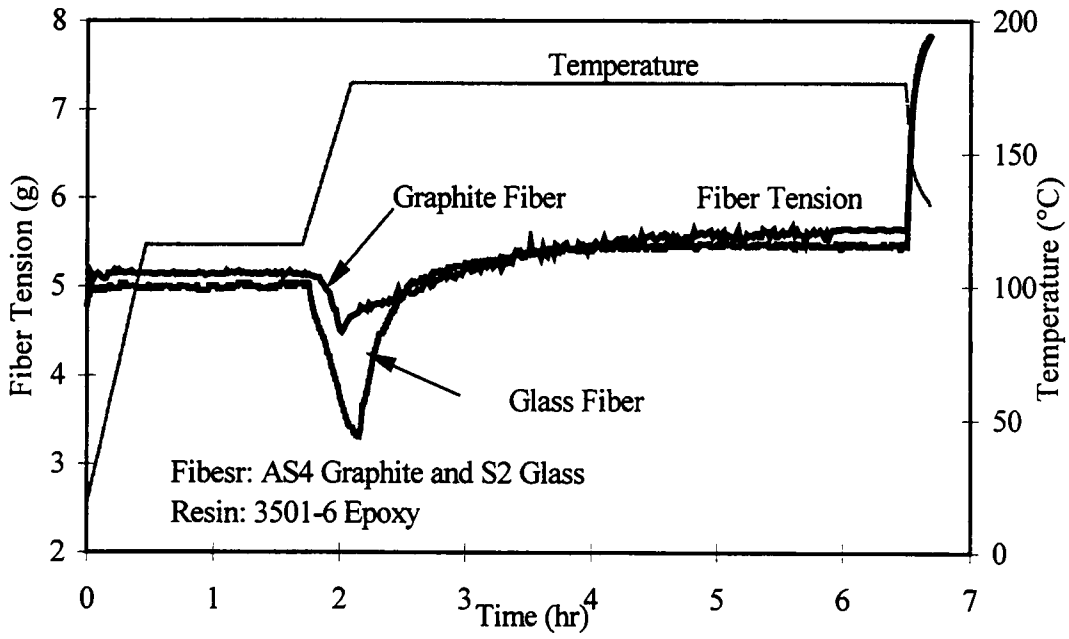

Figure 3.1 Variation in the fiber tension during the standard cure cycle of 3501-6 epoxy.

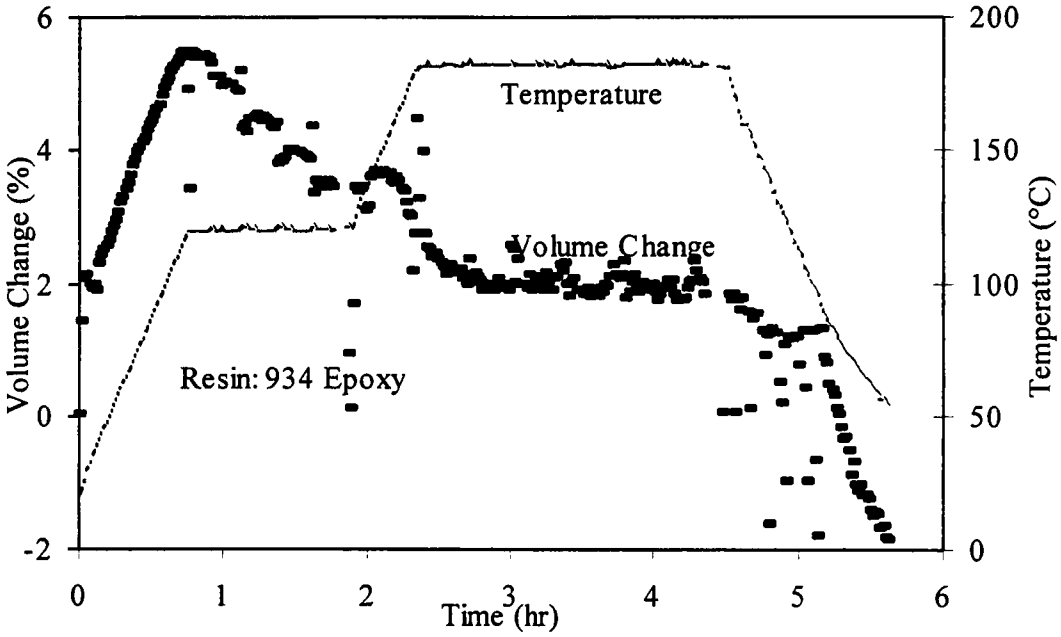

Figure 3.2 Volume change of 934 epoxy during the standard cure cycle.

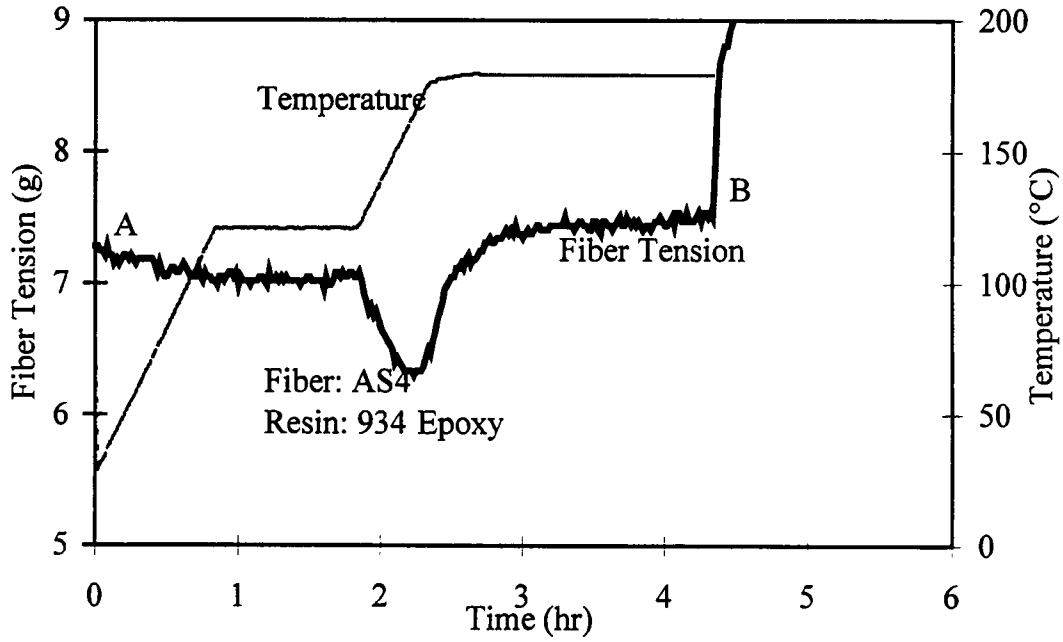

Figure 3.3 Variation in the fiber tension during the standard cure cycle of 934 epoxy.

properties. A comparison between Figures 3.2 and 3.3 shows that volume changes occurring during the first dwell have no effect on fiber stresses. In this case, cure induced stresses are governed by the chemical shrinkage during the second dwell only. There is a good agreement between volume change data (Figure 3.2) and fiber tension data (Figure 3.3), i.e. after the polymer has achieved relatively high viscosity, thermal expansion causes a drop in the fiber tension where as shrinkage causes an increase. Figure 3.3 shows that the value of the fiber tension prior to the onset of the cool down (point B) is larger than that of the initial tension (point A) indicating the development of net compressive stresses in the fiber due to cure shrinkage.

3-2-2 974-3 Toughened Epoxy

Standard cure cycle of 977-3 toughened epoxy consists of: heating from room temperature to 180°C in 30 minutes; holding at 180°C for 360 minutes followed by cooling down to room temperature. Volume changes of this resin during the standard cure cycle are shown in Figure 3.4. There is volume expansion during the initial heating from the room temperature to the maximum cure temperature. The crosslinking shrinkage dominates the volume changes during the temperature hold at 180°C. Figure 3.5 shows fiber tension profile during the same cycle. Clearly, thermal expansion during the initial heating does not change fiber tension due to low polymer viscosity during this stage. As the resin starts to cure, its stiffness develops during the temperature hold at 180°C and chemical shrinkage causes fiber tension to increase. The rate of increase in the fiber tension diminishes gradually as the cure approaches completion. Finally, there is an increase in the fiber tension during cool down due to thermal shrinkage.

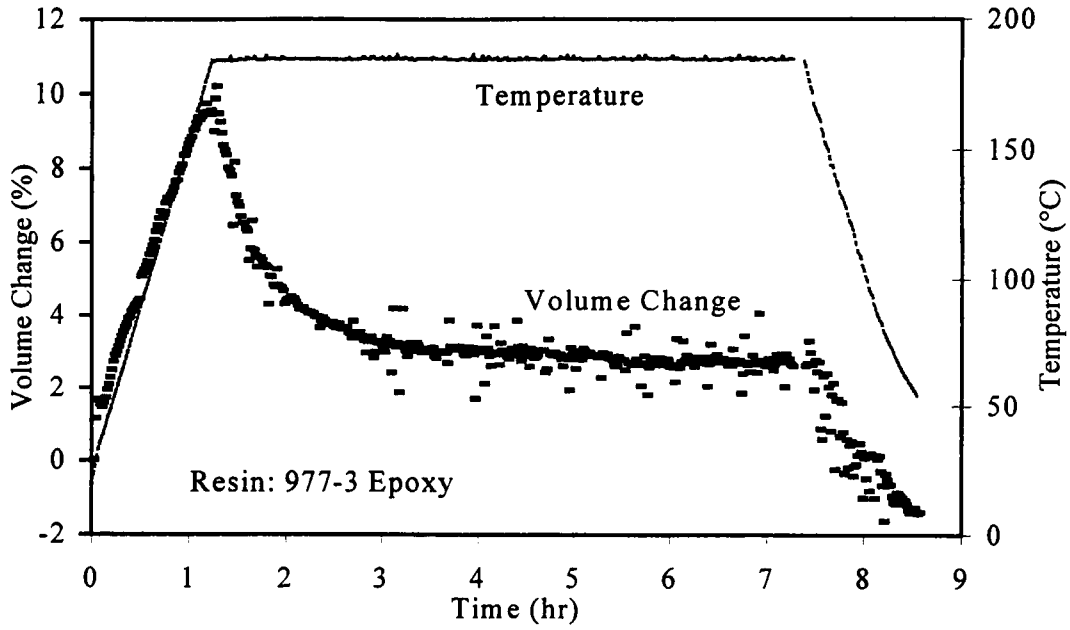

Figure 3.4 Volume change of 977-3 epoxy during the standard cure cycle.

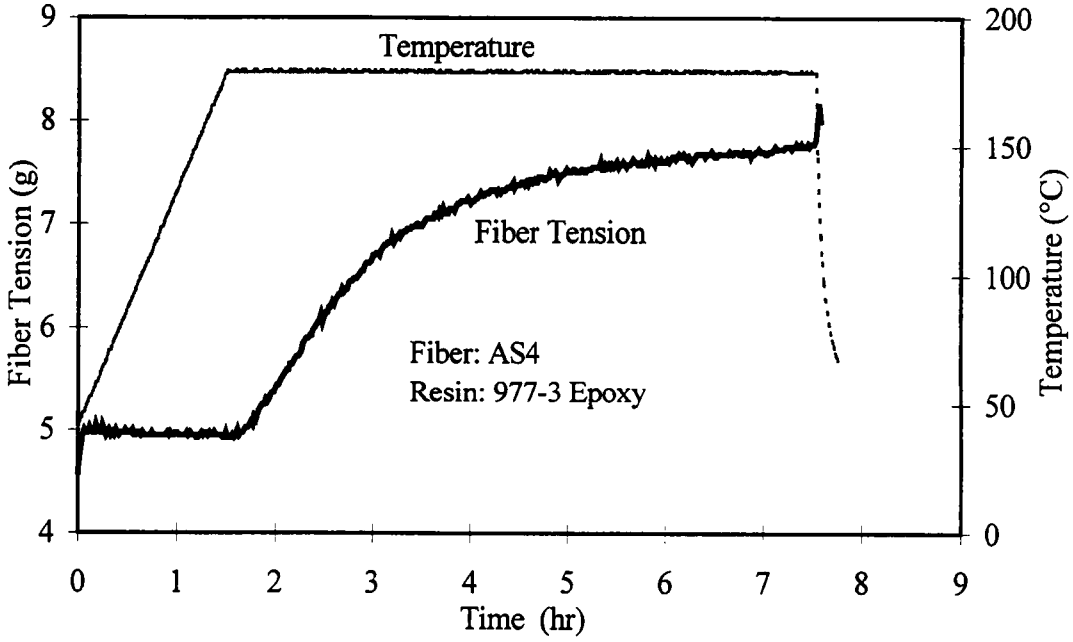

Figure 3.5 Fiber tension data during the standard cure cycle of 977-3 epoxy resin.

3-2-3 5250-4 BMI

For the 5250-4 BMI resin, the standard cure cycle is divided into two parts: initial cure and post cure. Only the first part will be presented here (section 3-4 shows results for an alternative cure cycle for 52550-4 BMI including post cure). This cycle consists of: heating the sample from room temperature to 121°C in 35 minutes; holding at 121°C for 45 minutes; raising temperature from 121°C to 177°C in 25 minutes; holding at 177°C for 360 minutes followed by cooling down to room temperature. Figure 3.6 shows the volume change of 5250-4 BMI during the first part of the standard cure cycle. Figure 3.7 shows the fiber tension profile for AS4 in 5250-4 BMI matrix during the same cure cycle. The trends of the results are similar to those of the epoxy resins shown above. A comparison between Figures 3.6 and 3.7 shows that there is a good correlation between polymer volume change and fiber tension change during cure, i.e. once the polymer has developed significant stiffness, an increase or decrease in the polymer volume produces a decrease or increase, respectively in the fiber tension.

3-2-4 X343-59 and LTM-45 ELD Low Cure Temperature Epoxies

The standard low temperature cure cycle for X343-59 resin consists of: heating from 30°C to 66°C at 1.5°C/min; holding at 66°C for 840 minutes; cooling to 30°C at 2.5°C/min; heating to 177°C at 1.5°C/min; holding for 120 minutes; and cooling to 30°C at 2.5°C/min. The standard low temperature cure cycle for LTM-45 ELD consists of: heating from 30°C to 60°C at 0.5°C/min; holding at 60°C for 960 minutes; cooling to 30°C at 1.5°C/min; heating to 177°C at 0.25°C/min; holding for 120 minutes; and

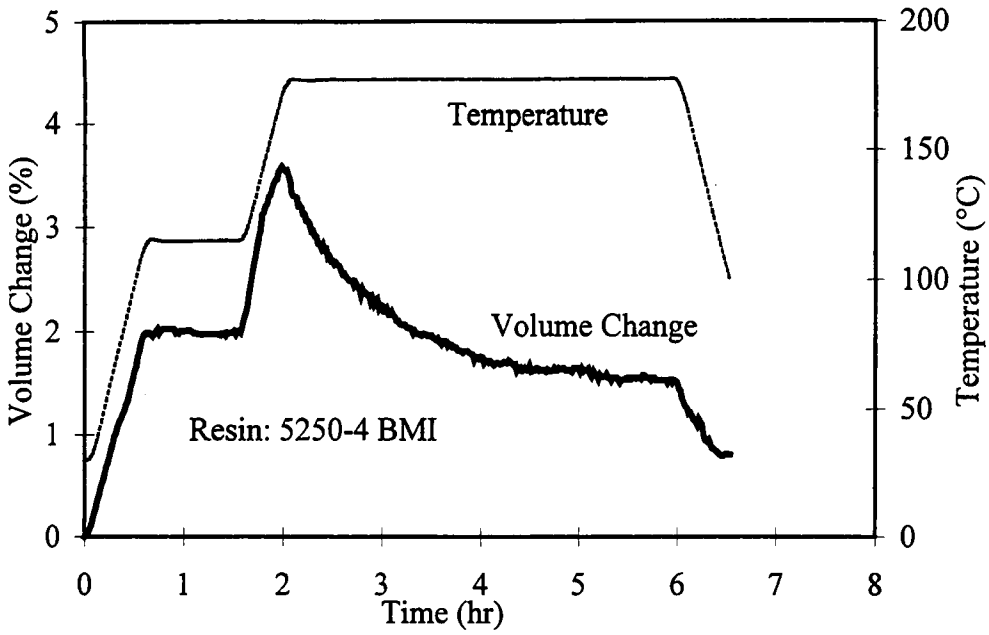

Figure 3.6 Volume change data of 5250-4 BMI resin during the standard cure cycle.

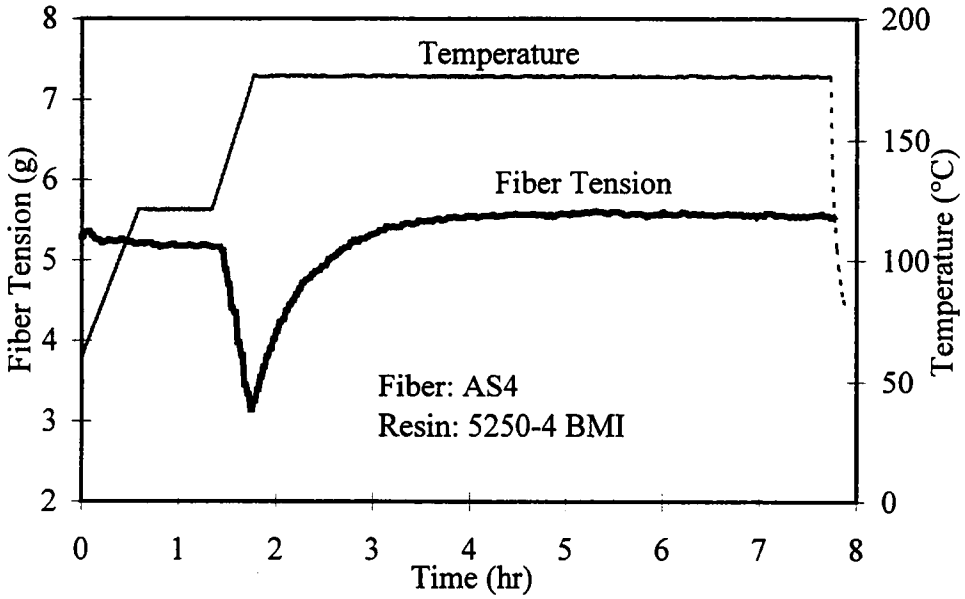

Figure 3.7 Variation in the fiber tension during standard cure cycle of 5250-4 BMI.

cooling to 30°C at 1.5°C/min. In a different set of experiments, these two resins were cured using an autoclave cure cycle that used for 3501-6 epoxy. That cycle consists of: heating from room temperature to 116°C in 30 minutes; holding at 116°C for 60 minutes; heating from 116°C to 177°C in 25 minutes; holding at 177°C for 240 minutes; and cooling to room temperature in 50 minutes. This cycle was proposed by the industry as an alternative to cut cure time of the standard low temperature cure cycles whenever autoclave cure is justified.

Figure 3.8 shows the volume change data of X343-59 during a low temperature cure cycle. Cure shrinkage occurs during the 66°C hold and continues during the 177°C hold. Figure 3.9 shows the variation in the fiber tension during the same cycle. There is a slight gradual increase in fiber tension during the 66°C hold due to cure shrinkage. During cool down from 66°C to 30°C at the end of the 66°C hold, another increase in the fiber tension occurs due to thermal contraction. As the resin is heated to post cure temperature, 177°C, the fiber tension decreases as a result of the thermal expansion. The tension drops below the initial tension value at the end of the heating ramp to 177°C. Some increase in the fiber tension can be seen during the 177°C hold time due to remaining cure shrinkage and stress relaxation as discussed below. Finally, fiber tension increases during cool down from 177°C to room temperature.

Figure 3.9 shows that fiber tension drops below its initial value during heating to post cure temperature. It should be noted that stress relaxation causes decay in any change in fiber tension (increase or decrease) from its initial value. In case of fiber tension drop below its initial value, stress relaxation causes fiber tension to increase again towards its initial value. Therefore, the increase in the fiber tension during the 177°C hold in Figure

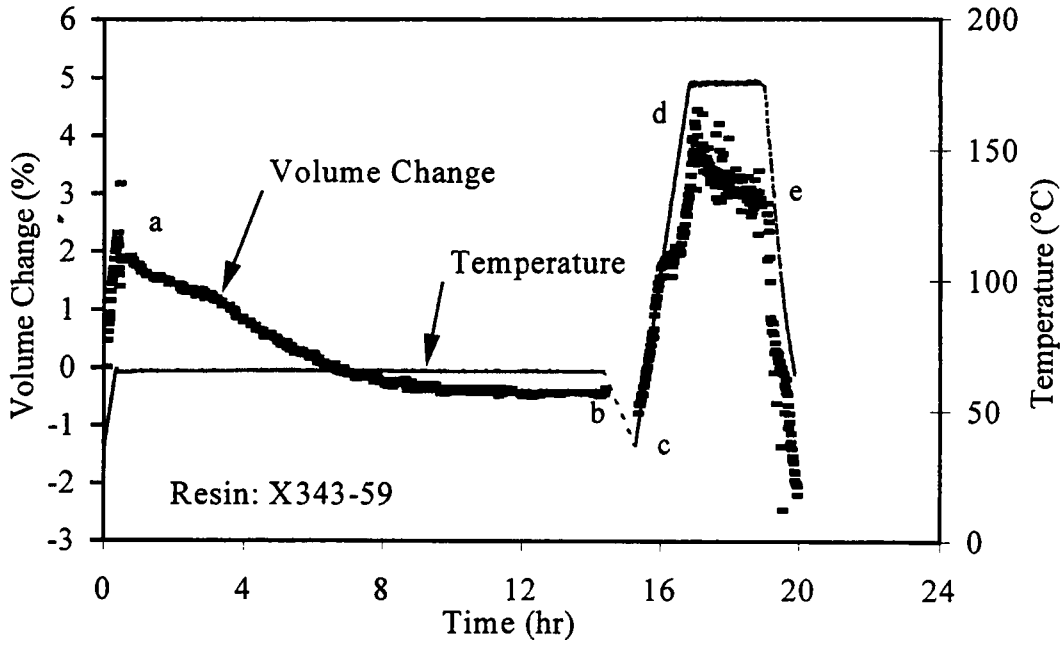

Figure 3.8 Volume change of X343-59 during the standard low temperature cure cycle.

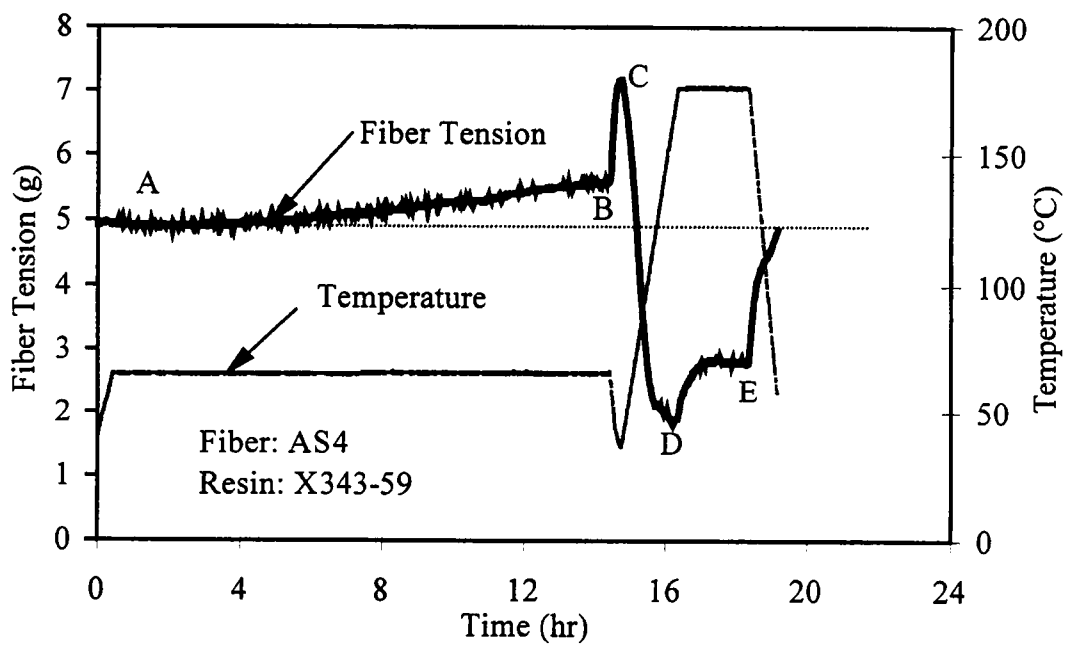

Figure 3.9 Variation in the fiber tension during the standard low temperature cure cycle of X343-59 epoxy.

3.9 is due to a combination of chemical shrinkage and stress relaxation (since fiber tension is below its initial value).

During the above cycle (Figure 3.9), curing at a relatively low temperature for a long time increases the viscosity of the resin. This causes the thermal expansion occurring during heating to post cure temperature, at 177°C, to be *effective* expansion. The term *effective* volume changes was defined in Section 2-2. This *effective* expansion causes a drop in the fiber tension below its initial value. This drop is larger than the increase in the fiber tension during the 177°C hold (compare thermal expansion during the 177°C ramp to that of the cure shrinkage during the 177°C hold in Figure 3.8). The final value of the fiber tension before cool down is still smaller than the initial fiber tension. This indicates that net tensile stresses are developed in the fiber prior to cool down. These tensile stresses will cancel part of the compressive stresses developed during the cool down and thus reduce residual stresses. In this particular case, stress free temperature will be below the post cure temperature. Stress free temperature was defined in Section 1-2.

Figure 3.10 shows the volume change data of X343-59 during the standard autoclave cure cycle of 3501-6 epoxy. A large amount of shrinkage occurs during the first temperature hold and additional shrinkage occurs during the second hold. Figure 3.11 shows the corresponding fiber tension variation. The shrinkage during the first temperature hold causes a significant increase in the fiber tension. The thermal expansion during the second temperature ramp decreases this tension. A slight increase in fiber tension can be seen during the second hold. Finally, cool down shrinkage increases fiber tension. Figure 3.11 shows that the final value of the fiber tension prior

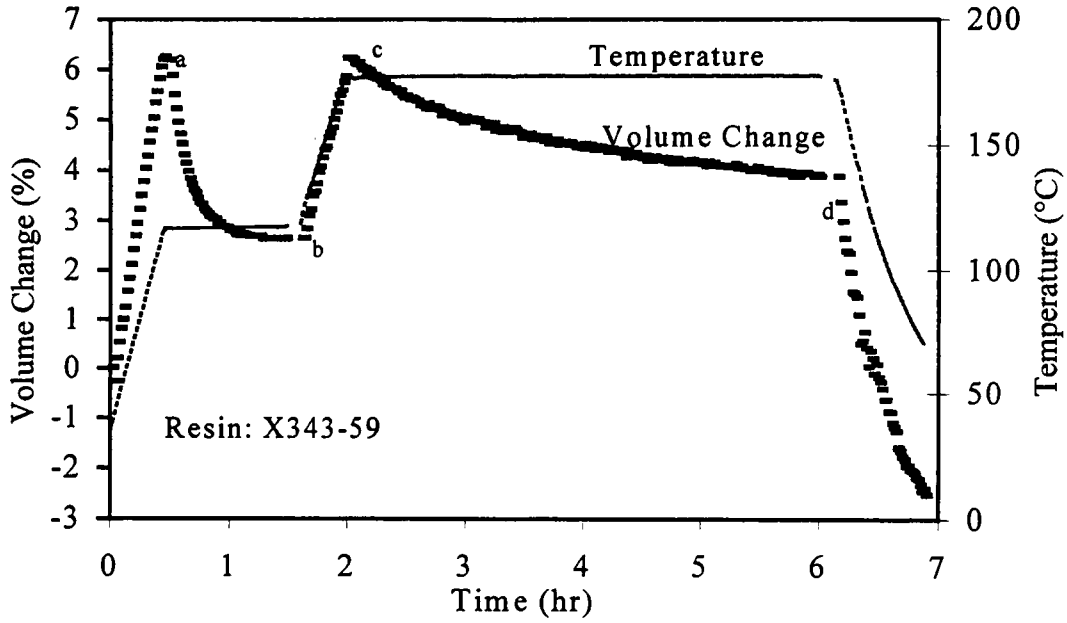

Figure 3.10 Volume change of X343-59 during an autoclave type cure cycle.

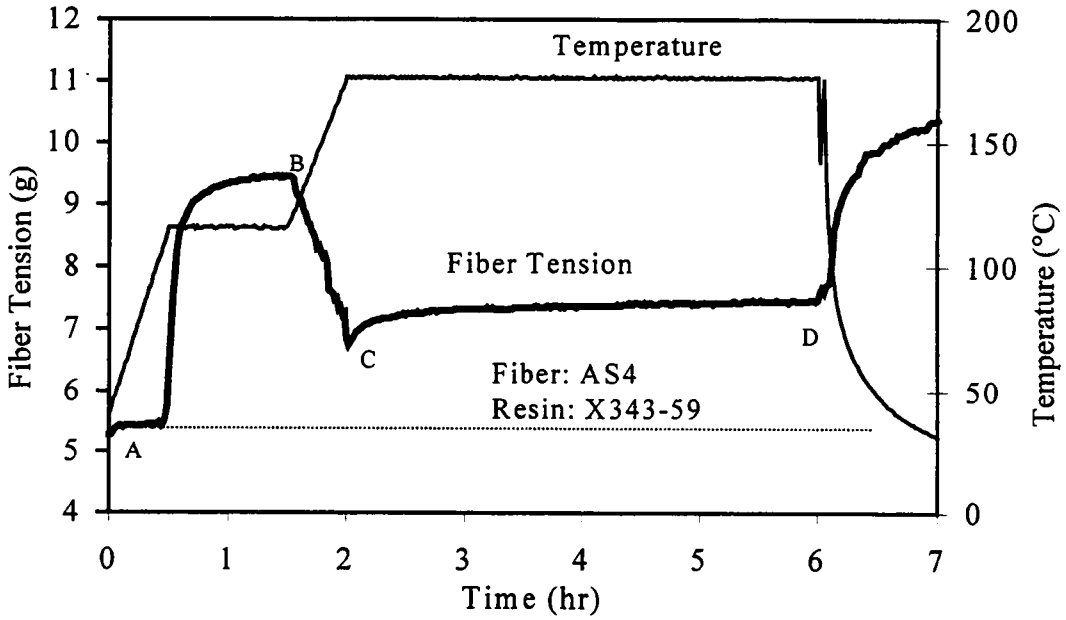

Figure 3.11 Variation in the fiber tension during an autoclave type cure cycle of X343-59.

to cool down is more than its initial value. In this typical autoclave cycle, heating to the relatively high first temperature hold in a short time just melts the resin and causes thermal expansion but does not give rise to tensile stresses in the fiber. This causes the chemical shrinkage to dominate the volume change and its effect will finally be added to cool down shrinkage causing more residual stresses.

Figure 3.9 shows that when the low temperature cure cycle is applied, the fiber is in a tensile stress state just before cool down. These tensile stresses will offset some of the compressive stresses that occur during cool down resulting in less final residual stresses. On the other hand, when typical autoclave cure cycle is applied, the fiber is in a state of compressive stress prior cool down. These compressive stresses combined with stresses developed during cool down produce higher residual stresses. A comparison between the two cycles suggests that the autoclave type cure cycle will result in more residual stresses than the low temperature cure cycle.

Figure 3.12 shows the volume change data of LTM-45 ELD epoxy during its standard low temperature cure cycle. Figure 3.13 shows the corresponding fiber tension profile. Compared to X343-59 resin (Figure 3.9), more stresses are developed during the 60°C hold. There is not much change in the volume during the 177°C hold. This suggests that the cure was almost completed during the slow heating ramp from 30°C to the post cure temperature. Fiber tension data agrees with the volume changes data showing only a slight increase during the post cure temperature hold (which may be due to stress relaxation). Similar to X343-59, the *effective* thermal expansion developed during heating to post cure temperature lowered the fiber tension below the initial value until the end of the cycle, i.e. fiber is under tensile stresses prior to cool down.

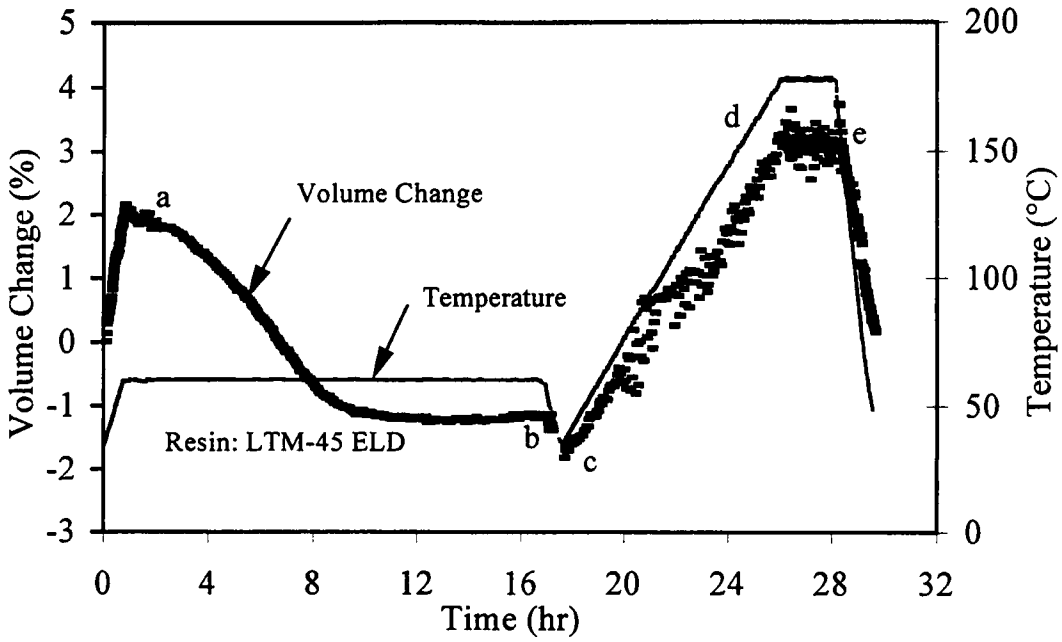

Figure 3.12 Volume change of LTM-45 ELD epoxy during the standard low temperature cure cycle.

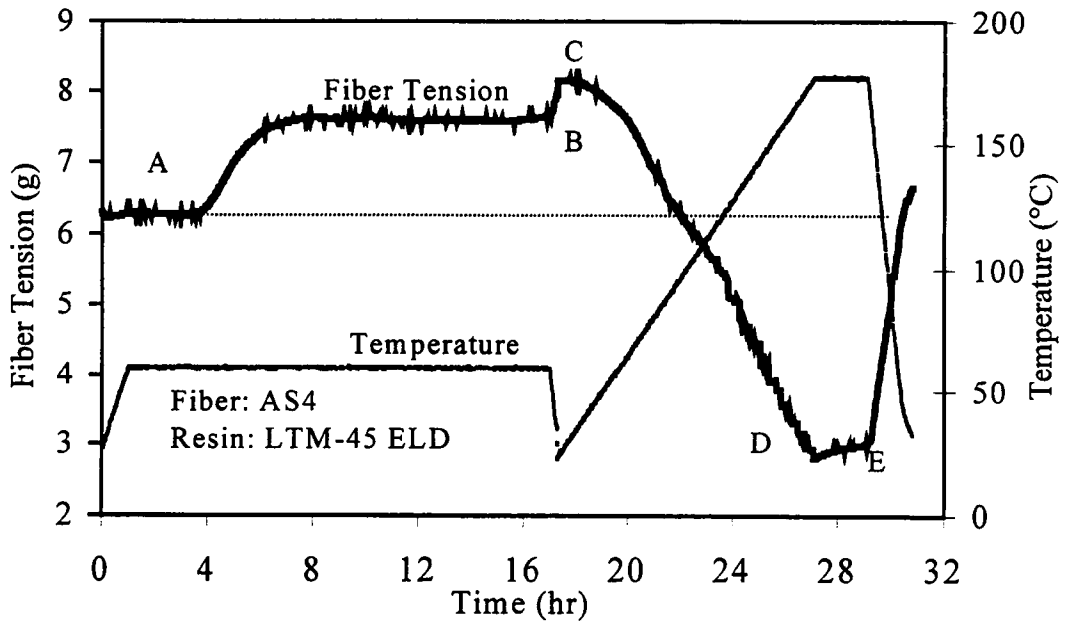

Figure 3.13 Variation in the fiber tension during the standard low temperature cure cycle of LTM-45 ELD epoxy.

Figure 3.14 shows the volume change data of the LTM-45 ELD epoxy under the autoclave type cycle. The behavior of LTM-45 ELD under this cycle is similar to X343-59 under the same cycle, where most of the cure occurs during the first temperature hold. Figure 3.15 shows the corresponding fiber tension profile. Compressive stresses are developed in the composite prior to cool down. Hence, similar to X343-59, low temperature cure cycle is expected to produce less residual stresses than the autoclave type.

3-3 MODIFIED CURE CYCLES

As discussed in Chapter 2, a closed loop feedback control system (CLFS) was developed to obtain modified cure cycles that reduce cure induced stresses. The method is based on searching for a heating path that results in maximum cancellation of the unrelaxed stresses. Typical results of applying the method were demonstrated in Section 2-4-3. Results of applying the CLFS to different composite systems are given below.

3-3-1 3501-6 and 934 Epoxies

Fiber tension data for an AS4 fiber in 3501-6 epoxy during standard cure cycle was shown in Figure 2.6. Results of CLFS for AS4 fibers were shown in Figure 2.22 where a modified cure cycle was shown to minimize change in the fiber tension during cure. The standard cure cycle was repeated again with S2 glass fibers instead of AS4 graphite fibers and results are shown in Figure 3.1. Figure 3.16 shows the modified cure cycle obtained for the glass fiber in 3501-6 epoxy resin as obtained from CLFS. The obtained

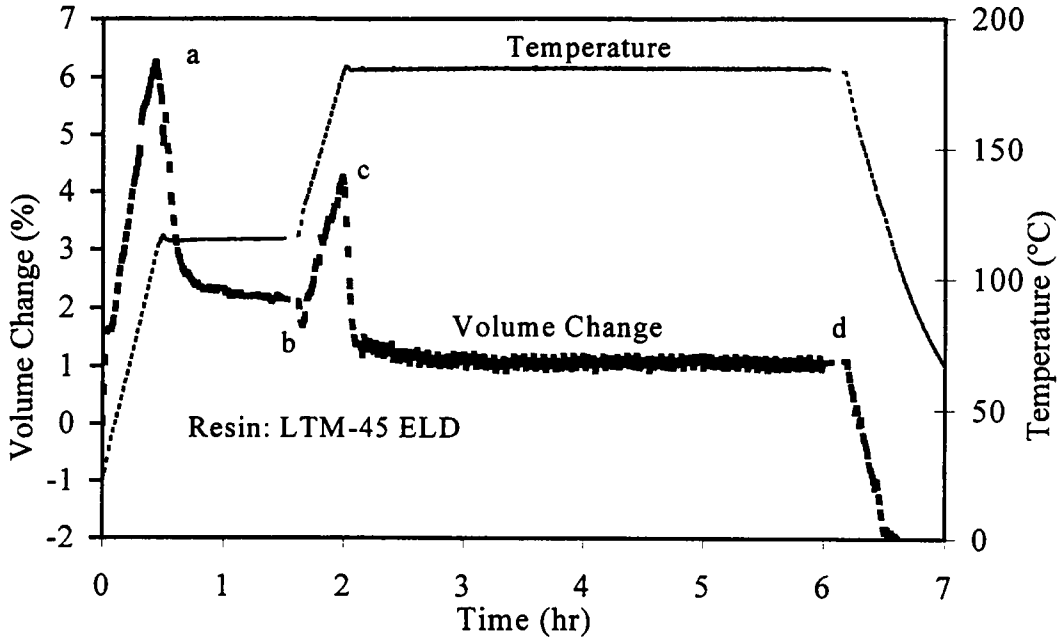

Figure 3.14 Volume change of LTM-45 ELD during an autoclave type cure cycle.

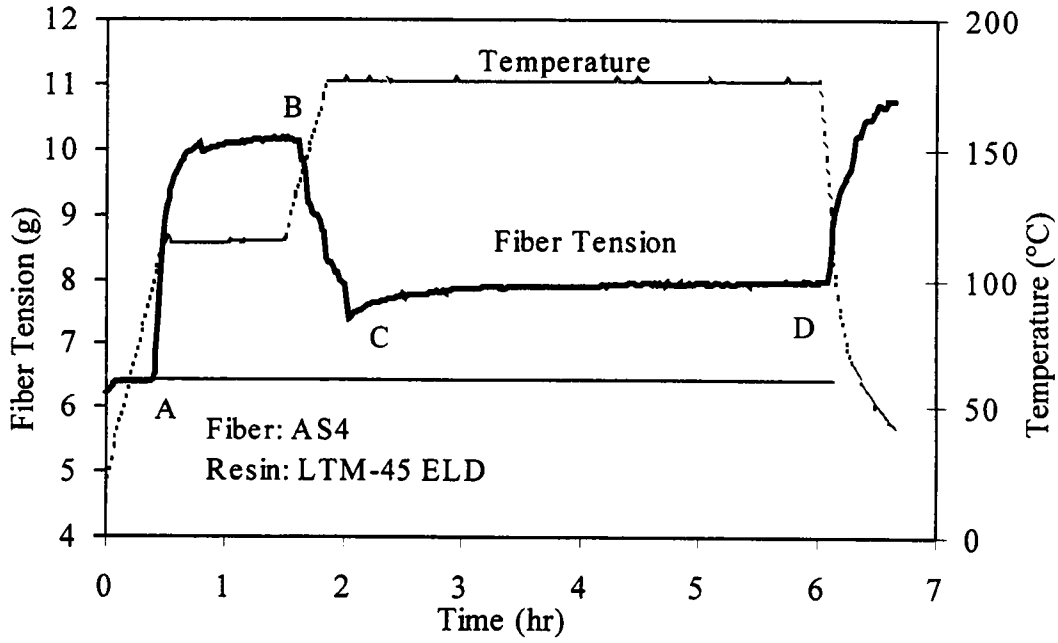

Figure 3.15 Variation in the fiber tension during an autoclave type cure cycle of LTM-45 ELD epoxy.

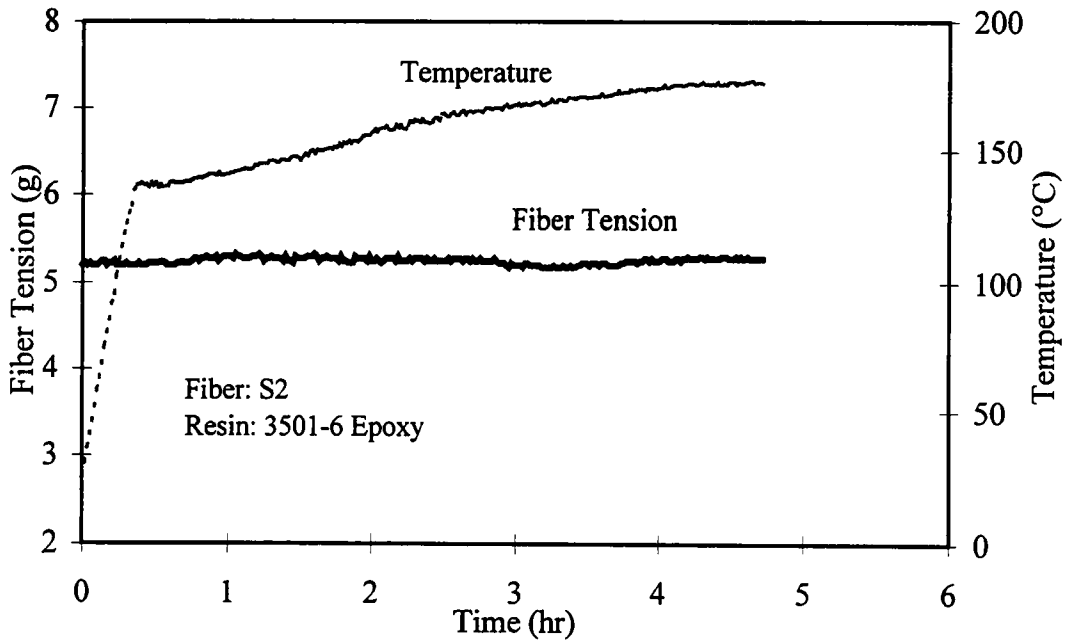

Figure 3.16 A modified cure cycle for S2/3501-6 glass/epoxy system.

cure cycle is similar to the modified cycle of the graphite fiber/3501-6 epoxy system. The slight differences are attributed to the differences in the interface properties. Since the method is based on reducing the strains through rescheduling of volume changes, the fiber properties do not seem to have much influence on the modified cycle.

Figure 3.17 shows a modified cure cycle obtained from the feedback control system for the AS4/934 graphite/epoxy system with the initial temperature taken as 138°C. By comparing the modified cycle with the standard cure cycle (Figure 3.3), it can be seen that the modified cycle reduced fiber stresses during cure. However, the modified cycle is longer than the standard cycle because the cure cycle was extended by CLFS to allow for more stress relaxation of stresses due to chemical shrinkage. Also, results in Figure 3.17 indicate that a significant part of the thermal expansion was used early in the cure cycle (as can be seen from the rapid heating during first 60 minutes beyond initial heating). Applying thermal expansion early in the cure cycle is not recommended from stress cancellation point of view since stresses due to chemical shrinkage are more likely to relax during this period without much temperature increase needed. Consuming thermal expansion during the early part of the cycle may cause chemical shrinkage to dominate the volume changes towards the end of the cycle where stress relaxation may not be very effective to cancel stresses in short time. This suggested introducing a temperature hold before the feedback starts. Another cycle was generated by using CLFS with lower initial temperature to increase the available *effective* thermal expansion (rather than extending the cure cycle to have more stress relaxation) and with a temperature hold.

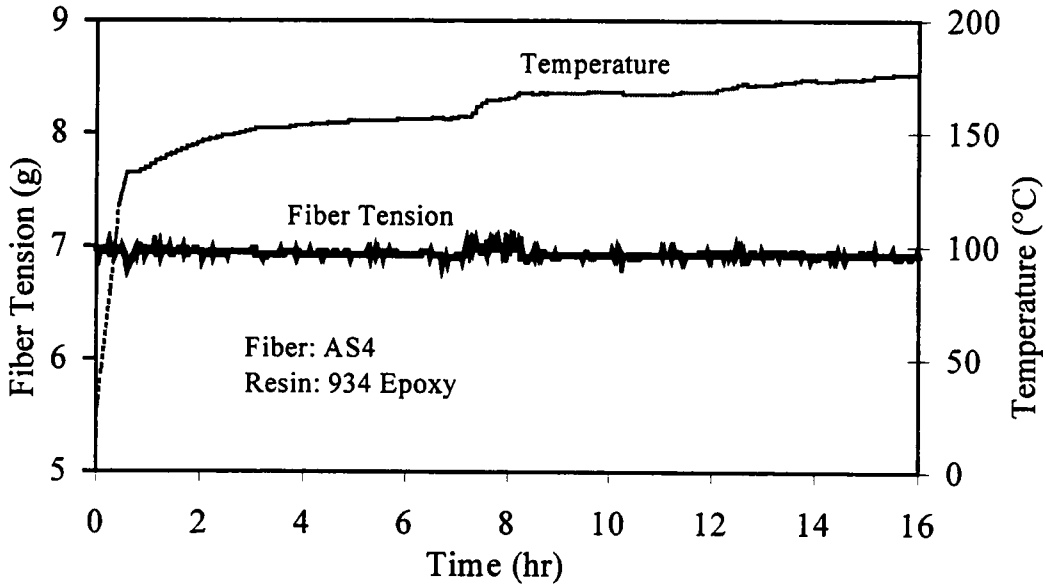

Figure 3.17 A modified cure cycle for AS4/934 graphite/epoxy.

The approach of lowering the initial temperature and introducing the temperature hold leads to a shorter cure cycle with minimum cure induced stresses as shown in Figure 3.18. The initial temperature was taken as 132°C. The new modified cycle results in an almost flat fiber tension curve. Also, the duration of this cycle is within that of the standard cure cycle. Stresses developed during the temperature hold beyond the initial heating are small because of stress relaxation.

3-3-2 977-3 Toughened Epoxy

Figure 3.19 shows one of the modified cycles obtained from the CLFS. Stresses developed during cure are significantly less than that developed in the standard cycle. However, it was not possible to cancel all the stresses developed during cure. For 977-3 epoxy resin, the rate of the chemical reaction is only significant at high temperatures. The initial temperature was chosen as 149°C, which is higher than that used with other resins. In this case, the amount of thermal expansion available at the later part of the cure cycle to counteract the chemical shrinkage will be relatively small. This can be seen from Figure 3.19 where the maximum temperature was reached before the cure was completed (fiber tension still increasing). This causes chemical shrinkage to finally dominate and produce an increase in the fiber tension during the temperature hold at 180°C. At this late stage in the cure cycle, stress relaxation time is long and stresses were not relaxed (as can be seen, the fiber tension prior to cool down is still higher than the initial tension). An alternative approach utilized was to increase the time interval used in the CLFS to allow for more stress relaxation. In addition, the temperature was kept constant for 3 hours after the initial temperature to allow for more stress relaxation and

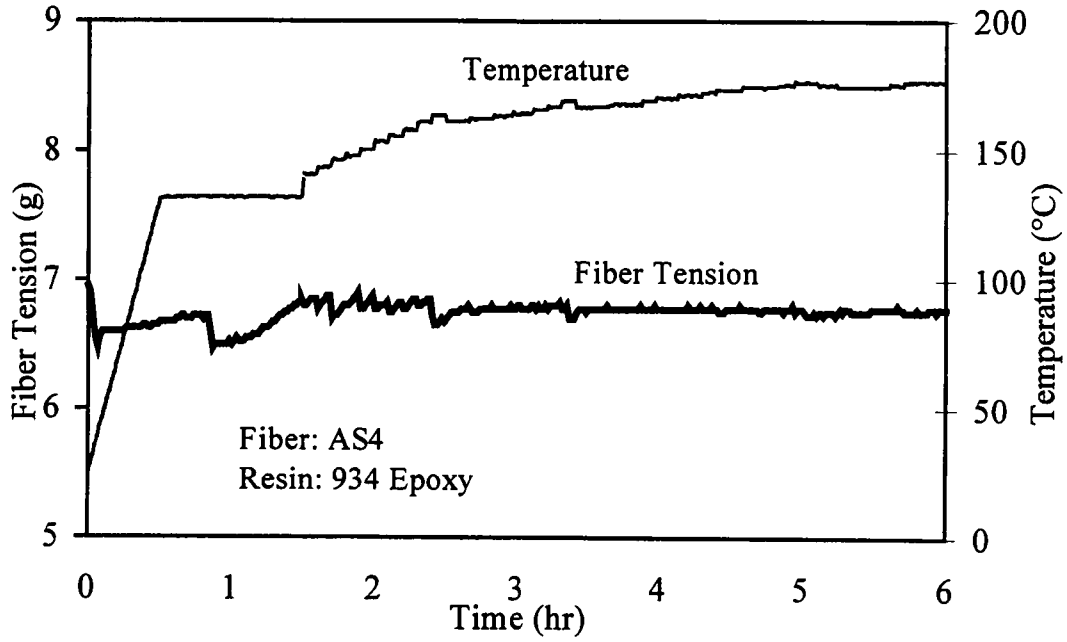

Figure 3.18 Another modified cure cycle for AS4/934 graphite/epoxy.

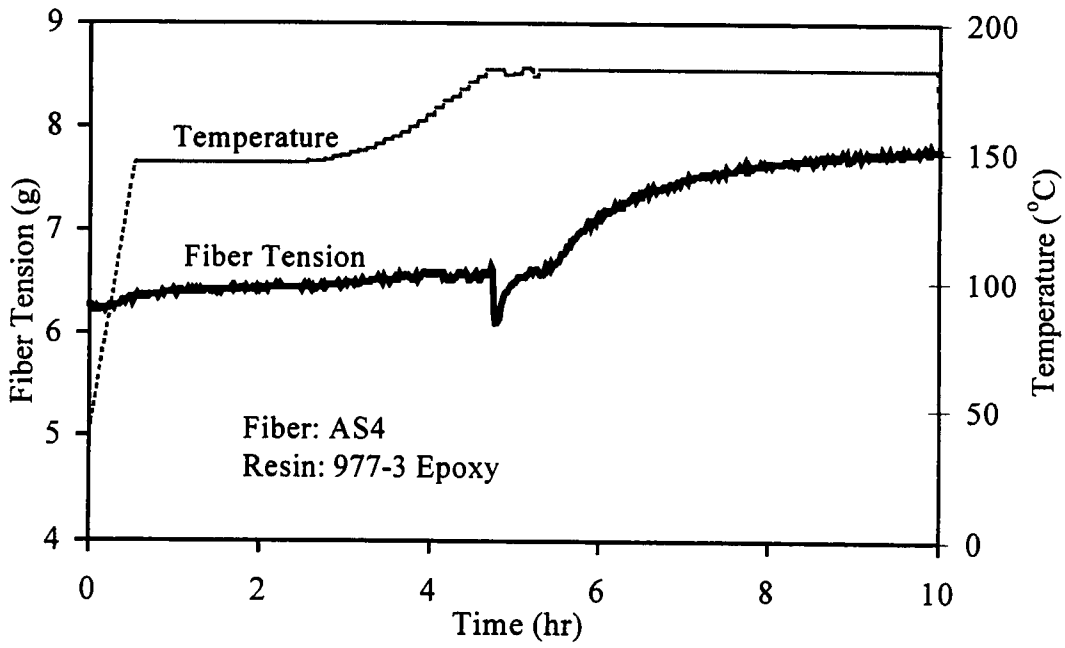

Figure 3.19 A modified cure cycle for AS4/977-3 graphite/epoxy.

increase the *effective* thermal expansion (by lowering gelation temperature). Stresses developed at early part of the cure cycle are more likely to relax during cure than those stresses developed at the later part. Figure 3.20 shows the results of the second modified cycle. It was possible to cancel most of the stresses due to chemical shrinkage. In addition, the duration of the new modified cure cycle is still within that of the standard cure cycle.

3-3-3 5250-4 BMI

Figure 3.21 shows a cure cycle and the corresponding fiber tension profile obtained from the CLFS. The initial temperature was taken as 138°C. The fiber tension profile during the modified cure cycle is much uniform compared to that developed during the standard cycle. Figure 3.22 shows the volume change data of the 5250-4 BMI during the modified cycle. The cure cycle was approximated with linear segments. A good correspondence between fiber tension and volume change data can be seen after the viscosity of the polymer has increased.

To study the effect of the initial temperature, up to which the specimen is heated before enabling the CLFS, tests with different initial temperatures were conducted. Figure 3.23 shows a modified cycle in which the initial temperature was 143°C. The new cycle resulted in a more uniform fiber tension profile during cure. However, compared to the modified cycle shown in Figure 3.21, the new cycle is longer. Starting at high temperature reduces the total thermal expansion available to cancel shrinkage stresses. In this case, slower heat rate has to be applied by the feedback to allow for more stress relaxation. The slower heating rate resulted in longer cure cycle to complete the cure. A

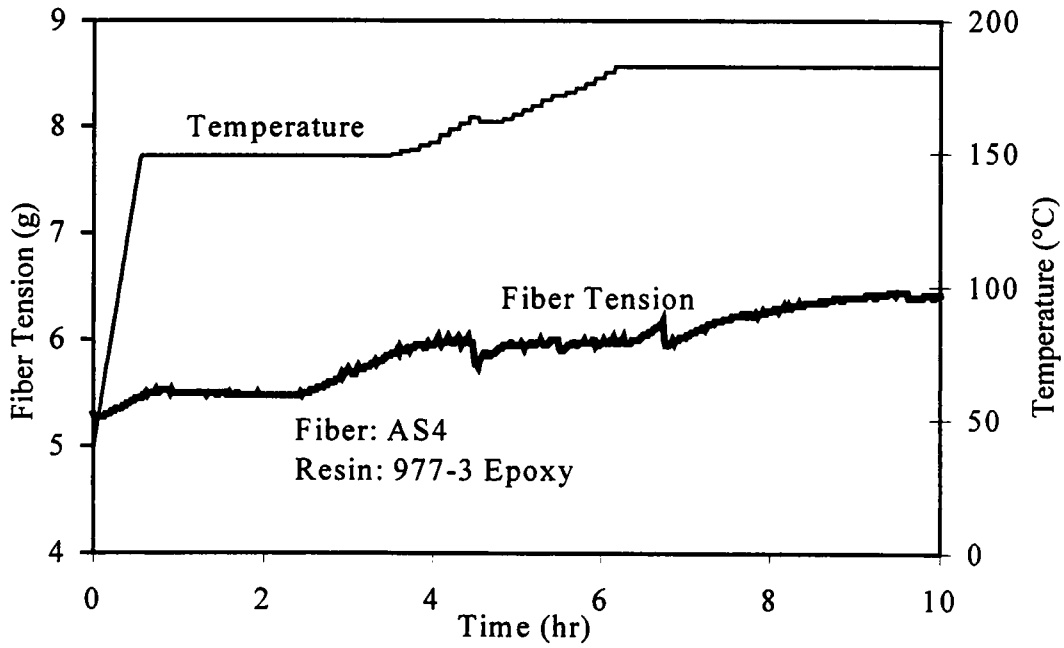

Figure 3.20 Another modified cure cycle for AS4/977-3 graphite/epoxy.

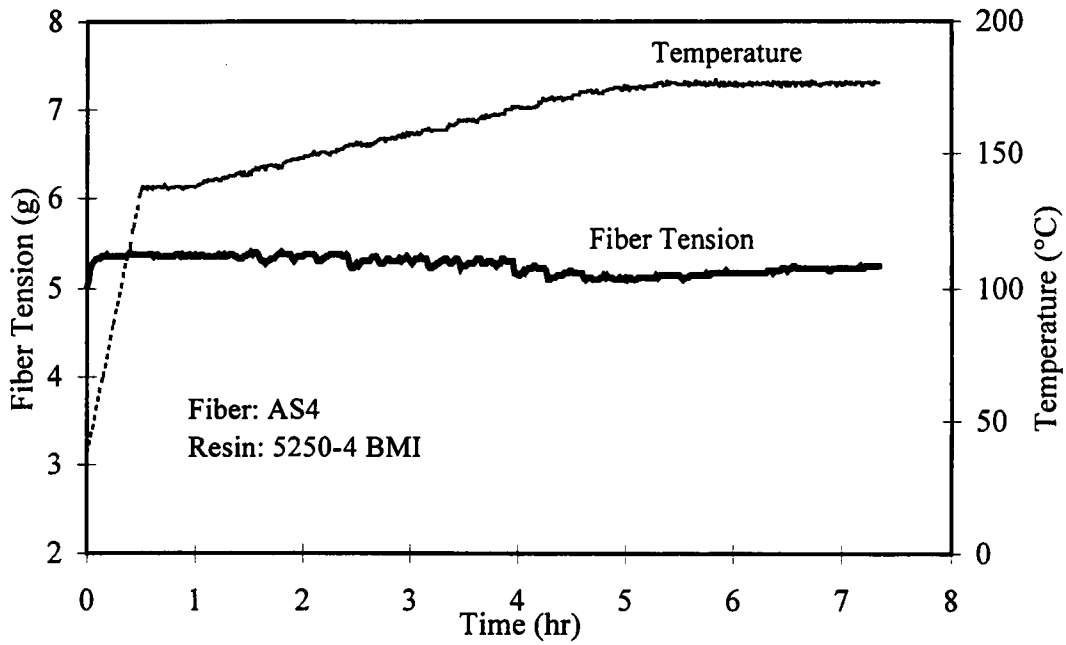

Figure 3.21 A modified cure cycle for AS4/5250-4 graphite/BMI.

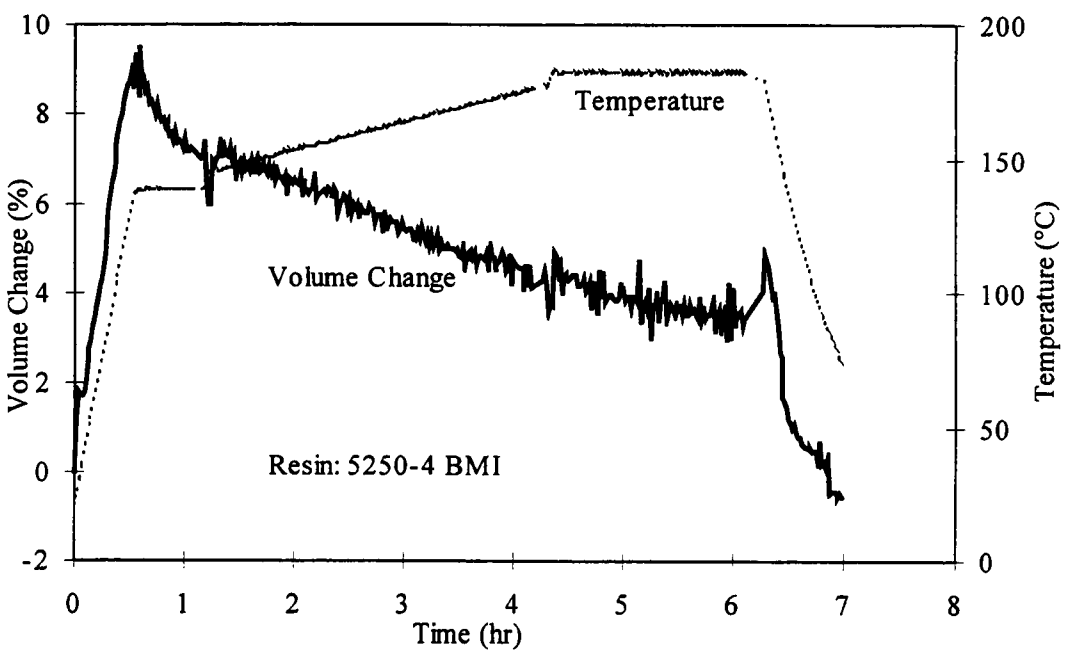

Figure 3.22 Volume change data of 5250-4 BMI during the modified cure cycle shown in Figure 3.21.

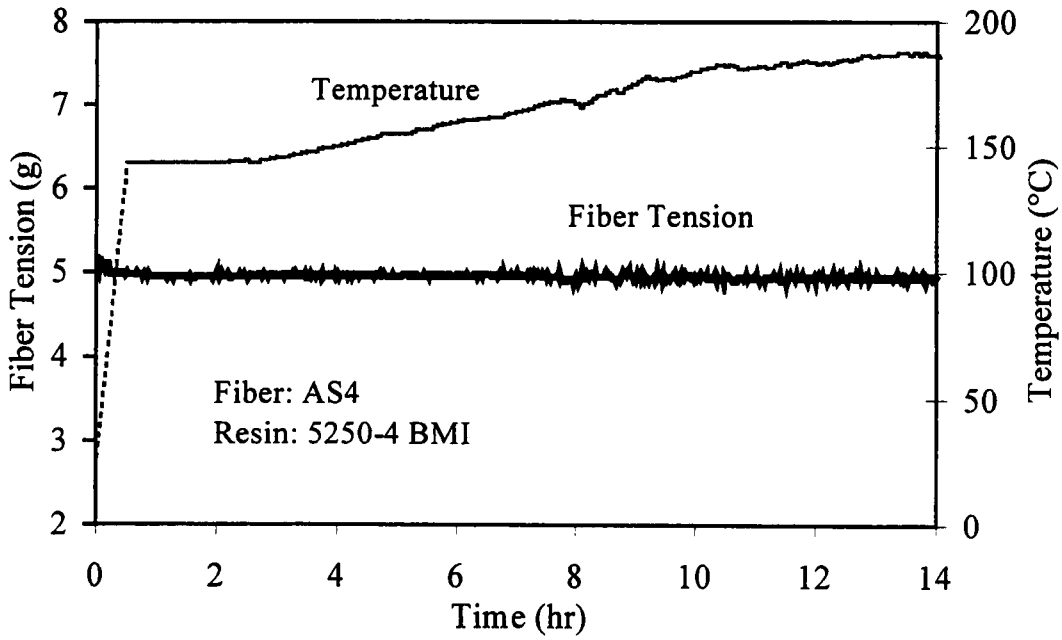

Figure 3.23 Another modified cure cycle for 5250-4 BMI with higher initial temperature.

comparison between the two modified cycles shows the importance of choosing the initial temperature since it affects the combination of thermal expansion and stress relaxation required to cancel the chemical shrinkage.

The T_g data for 5250-4 BMI resin cured using the different cure cycles are shown in Table 3.1. For few experiments, the modified cure cycle was extended to study the effect of cure time increase. The value of T_g increases as the cure cycle is extended indicating that the cure is not completed. As was mentioned earlier, the 5250-4 BMI resin requires post cure at high temperature to complete the cure. Because the resin cure and hence shrinkage continues until the end of the cycle, Figures 3.21 and 3.22 show a steady continuous decrease in the resin volume and corresponding increase in the fiber tension towards the end of the cure cycle.

Table 3.1 Glass transition temperature for 5250-4 BMI specimens cured using different cure cycles.

Cure Cycle	Standard Cycle	Modified Cycle	Modified Cycle + 30 min.
Glass Transition Temperature	165°C	153°C	163°C

3-3-4 X343-59 and LTM-45 ELD Low Cure Temperature Epoxies

The CLFS was used to modify the cure cycles of single fiber composites with X343-59 and LTM-45 ELD resins and AS4 fibers to reduce cure induced stresses. It should be

noted that a major assumption in determining the required thermal expansion to cancel unrelaxed stresses is that the applied temperature increase will not change the polymer chemical reaction rate greatly. For low cure temperature epoxies, the chemical reaction is very sensitive to the increase in temperature. Hence, the temperature increment applied by the feedback control may greatly increase the rate of the reaction causing more chemical shrinkage. To cancel the additional shrinkage, the feedback control will apply more temperature. The new temperature increment will further increase the reaction rate and generate more shrinkage and so on. In such cases, equilibrium at each point may not be possible. In this situation, cancellation of stresses may be achieved by allowing more stress relaxation rather than heating. However, increasing time intervals to allow for more stress relaxation will extend the cycle duration and may lead to vitrification preventing completion of the cure. Vitrification slows down the chemical reaction significantly and as a result the CLFS will stop raising the temperature (since there is no shrinkage to cancel). In such cases, the cure cycle will be stopped before the cure is complete.

For X343-59 resin, Figure 3.9, most of stresses were developed during the post cure, so the feedback control was enabled only during this part of the cure cycle. The objective of the feedback control here is to apply the heat incrementally in such a way that the fiber tension remains constant at a certain value until the resin is cured. This kind of incremental heating prevents *effective* cure shrinkage from developing compressive stresses in the fibers during cure. Also, applying the temperature incrementally prevent large decay of tensile stresses due to thermal expansion by the stress relaxation. Reducing stress relaxation of tensile stresses should finally reduce residual stresses.

The long hold at low temperature was applied as is. Then the temperature was increased linearly to 130°C. At this point, feedback control was enabled. This temperature was high enough to start continue the chemical reactions and also to reach the 177°C limit in reasonable time. Figure 3.24 shows the obtained cure cycle and the corresponding fiber tension. As can be seen, controlling the temperature through the feedback control does not cancel shrinkage stresses completely and the curve is not flat. As discussed above, the increase in the temperature appears to also increase the chemical shrinkage through enhancing the reaction rate. This will result in net increase in the fiber tension instead of canceling it. As the reaction advances, its rate appears to decrease allowing the thermal expansion to start canceling the chemical shrinkage. However, the 177°C limit is reached before the tension returns to the initial value. The completion of the cure was checked by measuring Tg. The obtained cycle gives 171°C versus 174°C for the standard low temperature cure cycle. The difference appears to be statistically insignificant since the highest temperature 177°C is applied in both cases for similar time.

Figure 3.25 shows the case where feedback control was enabled at arbitrarily chosen lower temperature (110°C). Better control over the reaction was possible resulting in an almost flat curve. So starting at low temperature gives the advantage of slower reaction rate but the reaction may stop before the cure is completed because of vitrification. It should be noted that starting at higher temperature is expected to increase the reaction rate and complete it in shorter time but offers less control as was seen when the feedback control was enabled at 130°C.

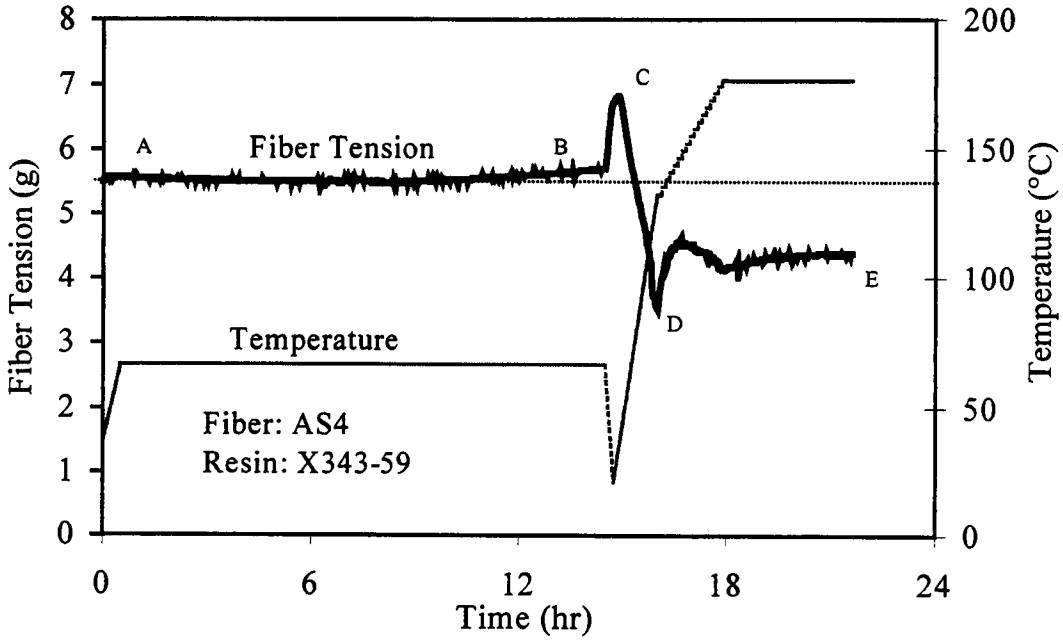

Figure 3.24 Variation in the fiber tension during a modified low temperature cure cycle for AS4/X343-59 graphite/epoxy.

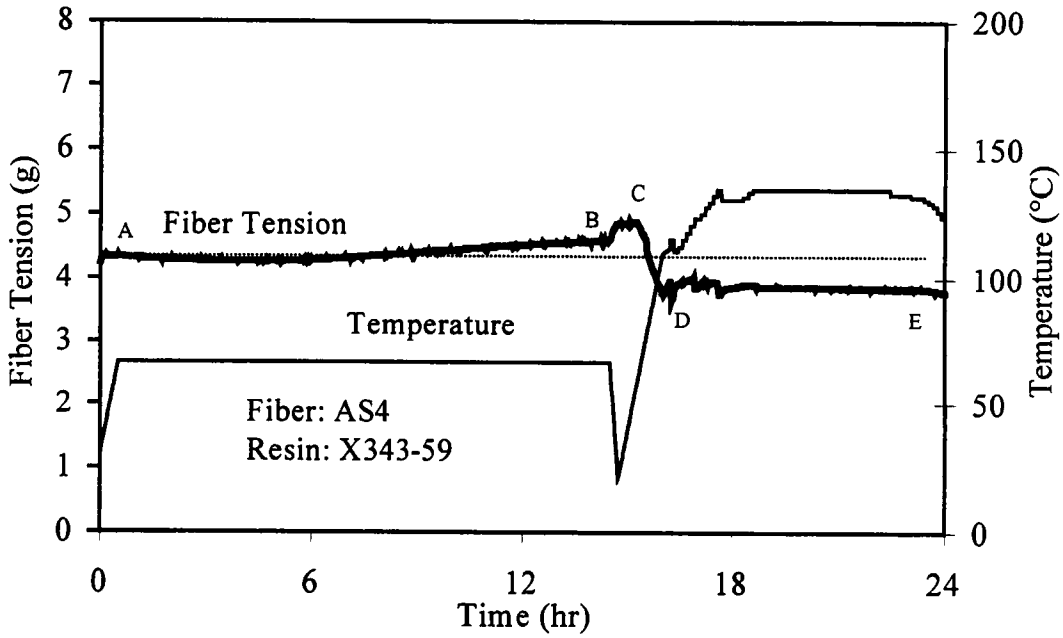

Figure 3.25 Variation in the fiber tension during another modified low temperature cure cycle for AS4/X343-59 graphite/epoxy.

Other optimization runs were performed to find autoclave type cure cycles with minimum residual stresses. Figures 3.26 and 3.27 show the obtained fiber tension and resulting volume change, respectively. Again, at one stage in the cure cycle there is a region in which the feedback control does not cancel stresses because the chemical reaction rate also increases greatly as the temperature increases. However, the final value of the fiber tension is almost identical to initial value. This indicates that there are no cure induced stresses developed during such a cycle in the composite. Such an optimized cycle will produce less residual stresses than typical autoclave cure cycle shown in Figure 3.4 in which final value of the fiber tension is more than the initial tension value. The increase in the fiber tension above the initial value indicates compressive cure stresses in the composite. These compressive stresses will be added to the compressive stresses developed during cool down producing more residual stresses. Glass transition temperature for such a cycle is 176°C which means that the reaction is complete

Using the optimized autoclave type cycle (Figure 3.26), the resin can be cured in a shorter time than for the optimized low temperature cure cycle, Figure 3.24. However, a comparison between the two cycles shows that the optimized low temperature cure cycle has the advantage of developing tensile stresses in the composite during cure versus almost zero stresses in the optimized autoclave type cycle. These tensile stresses will decrease the final residual stresses in the composite.

The feedback control was also used to obtain an optimized low temperature cure cycle for LTM-45 ELD resin with AS4 fibers. Similar to the case with X343-59, during the feedback control, the temperature increase also increases the reaction rate significantly

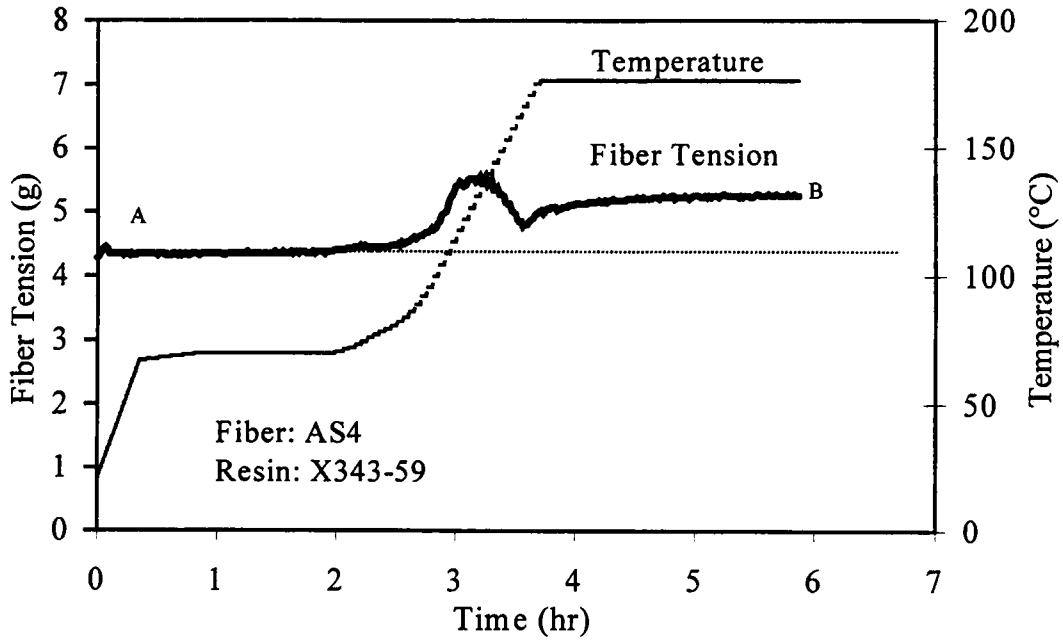

Figure 3.26 Variation in the fiber tension during a modified autoclave type cure cycle for AS4/X343-59 graphite/epoxy.

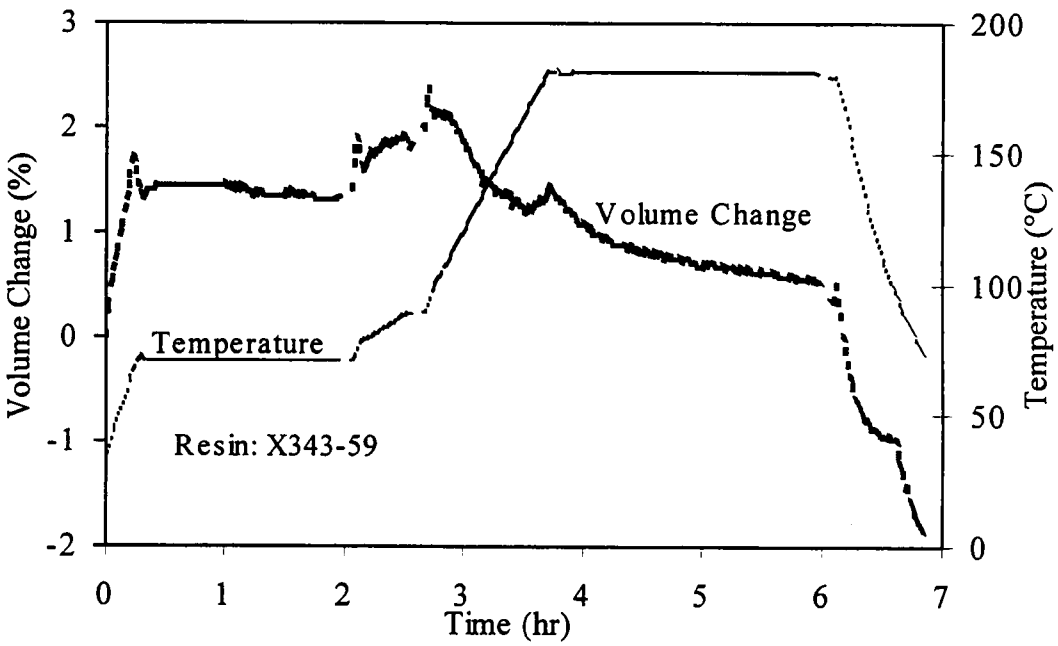

Figure 3.27 Volume change of X343-59 during the modified cure cycle shown in Figure 3.26.

preventing canceling chemical shrinkage stresses completely. After some trials, the cycle shown in Figure 3.28 appears to decrease stresses during the first stage of the cure cycle. The post cure was used as is since there is no significant variation in fiber tension. Figure 3.29 shows the corresponding volume change data.

The optimized cure cycle shown in Figure 3.28 produces almost zero stresses during the first part of the low temperature cure cycle. This may be helpful to maintain dimensional stability of the parts during this stage (before post cure at higher temperature). Also, when this optimized cycle is compared with typical low temperature cure cycle (Figure 3.13), the typical cycle results in compressive stresses at the end of the first stage of the cycle (as indicated by the increase in the fiber tension prior to cool down from 60°C to 30°C). These compressive stresses will reduce the tensile stresses that will be developed during the heating ramp to post cure temperature. As discussed earlier, tensile stresses help to reduce residual stresses. The optimized cycle has the advantage of almost zero stresses developed during the first stage. Thus, it keeps more tensile stresses in the composite (which would be used to cancel stress due to shrinkage during the first stage) and hence less final residual stresses.

3-3-5 Applications

Results of the CIST and CLFS indicate that the modified cycles can effectively reduce stresses produced during cure of single fiber model composites. However, composite laminates contain high fiber volume fraction. Also, during manufacturing there may exist gradients in the temperature and degree of cure across laminate thickness especially in thick parts. These factors and others should be considered to modify cure cycles for

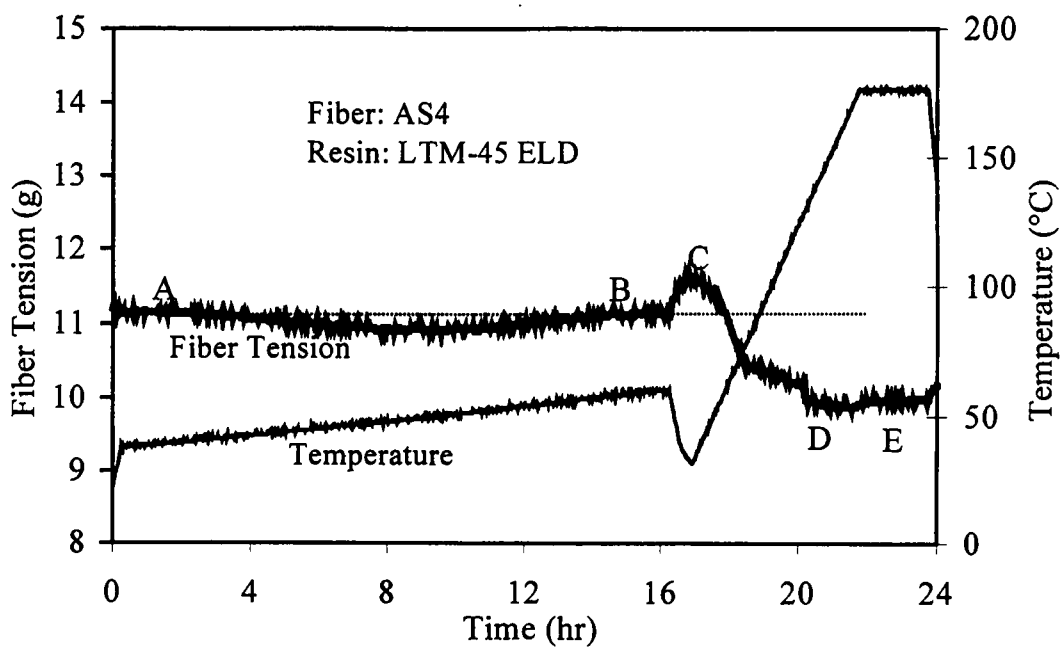

Figure3.28 Variation in the fiber tension during a modified low temperature cure cycle for LTM-45 ELD.

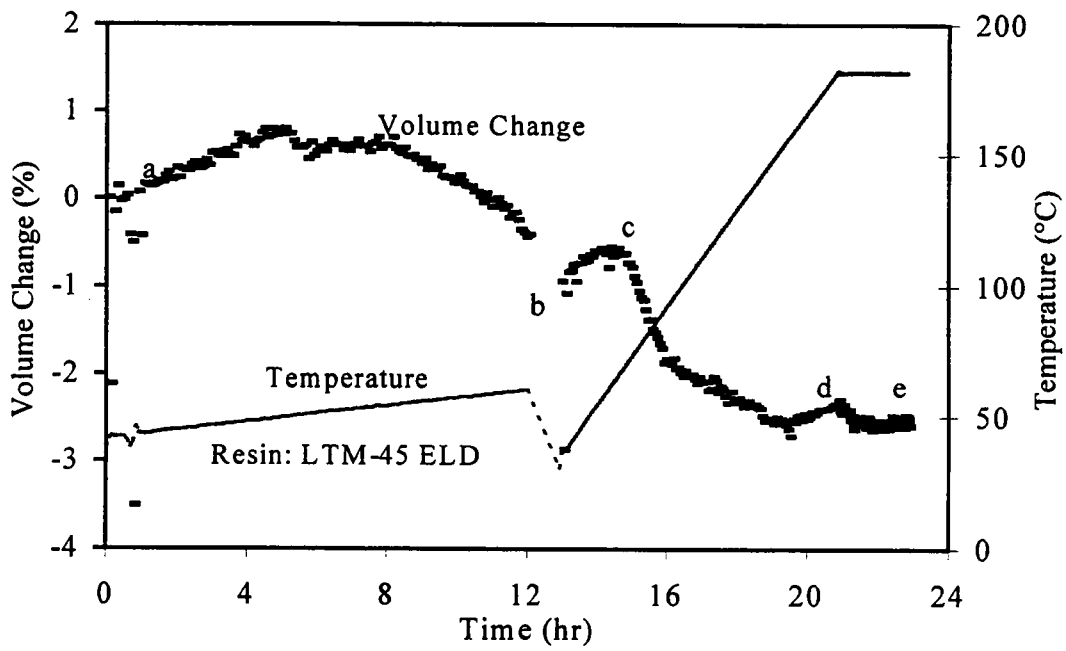

Figure 3.29 Volume change of LTM-45 ELD epoxy during the modified cure cycle shown in Figure 3.28.

composite laminates to reduce residual as will be addressed in chapter 4. In this part of the study, the modified cure cycle as obtained from the CLFS was applied to composite laminates without any changes.

The curvature of unsymmetric laminate was used as a measure of the total residual stresses. The material used was 3501-6/AS4 graphite/epoxy prepreg from Hercules. The composite laminates were cured in a vacuum hot press. Six unsymmetric 1X10 inches $[0^{\circ}_4/90^{\circ}_4]$ strips were cured using the standard cure cycle (Figure 2.2) and another six strips were cured using the modified cycle as obtained from the CLFS (Figure 2.22). The same values of the pressure, vacuum, and cool down rate were used in both the cure cycles. The specimens were made narrow to limit the effect of the curvature in the 90° direction. No machining on the specimens was done to avoid any stress relaxation. The dimensionless curvature of the specimens was calculated as follows [22]

$$Dimensionless\ Cuvature = \frac{8tD}{4D^2 + L^2} \qquad (6)$$

where D, L, and t are the midpoint deflection, projected length of the specimen, and thickness of the specimen respectively. A photograph of two representative specimens cured using the two cycles is shown in Figure 3.30 (a). The modified cycle reduces the specimen curvature. A plot of the dimensionless curvature (Equation 6) shows that the modified cycle reduces the curvature of the unsymmetric laminates by about 14% (Figure 3.30 (b)). The modified cycle was also shown to complete the cure as measured by the glass transition temperature. Additional modification of the cure cycle to account

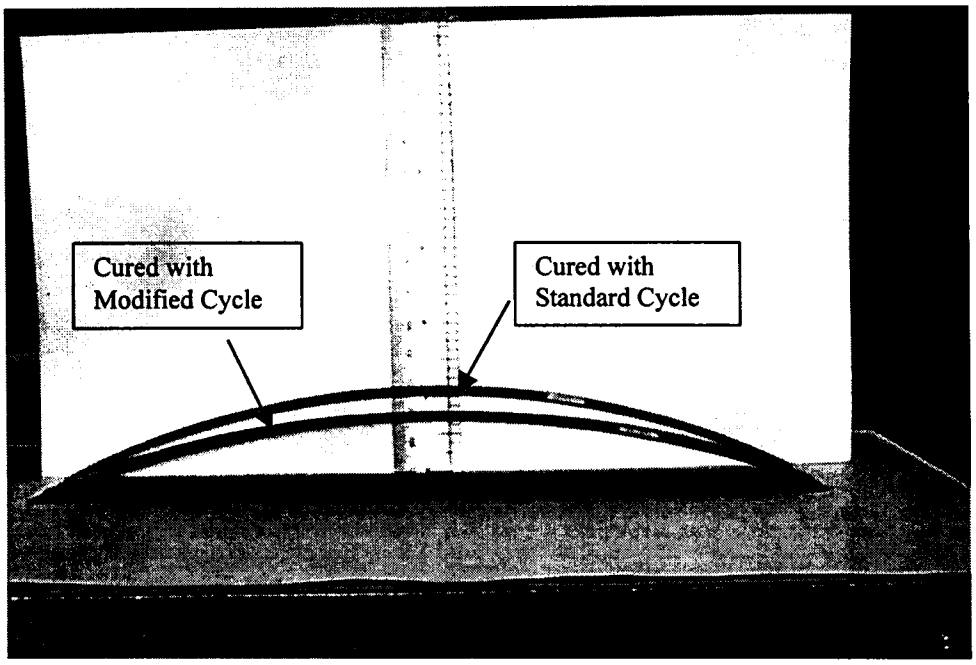

(a) Photograph.

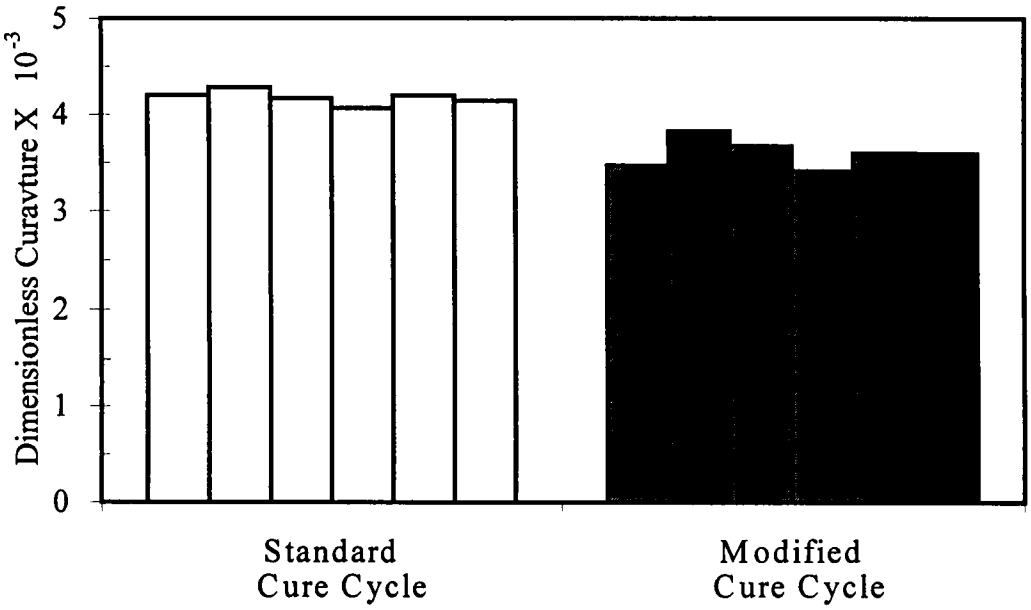

(b) Curvature data.

Figure 3.30 Curvature of unsymmetric AS4/3501-6 graphite/epoxy laminates cured with different cure cycles.

for the effect of possible temperature and cure gradients and fiber volume fraction in the laminates may further reduce the final residual stresses.

3-4 EFFECT OF POST CURE AND COOL DOWN RATES

Stresses may develop in fibers during cure, post cure, and cool down. In the above sections, results of CIST and CLFS were shown mainly for stresses develop during cure. In this section, results of CIST for fiber tension changes during post cure and cool down are presented. The materials used in this section are AS4 fibers in 5250-4 BMI. Standard cure cycle for 5250-4 BMI was presented in section 3-2-3. In this section, an alternative cure cycle will be used. This cycle consists of: heating the sample from room temperature 177°C in 30 minutes; holding at 177°C for 360 minutes; cooling down to room temperature in 100 minutes. The post cure consists of: heating from room temperature to 205°C in 30 minutes; holding at 205°C for 360 minutes; cooling down to room temperature in 100 minutes.

Figure 3.31 shows the variation in the fiber tension during such a time temperature cycle. During the first part of the cure cycle, the fiber tension increases due to chemical shrinkage and during cool down due to thermal shrinkage. During post cure temperature hold, there is a slight increase in the fiber tension. This increase is the resultant of two opposite actions. The first is the decrease in fiber tension because of heating above previous cure temperature to post cure temperature (from177°C to 205°C). The second is the increase in fiber tension due to additional cure at high temperature. It seems that the increase in the fiber tension due to additional cure shrinkage and thermal expansion due

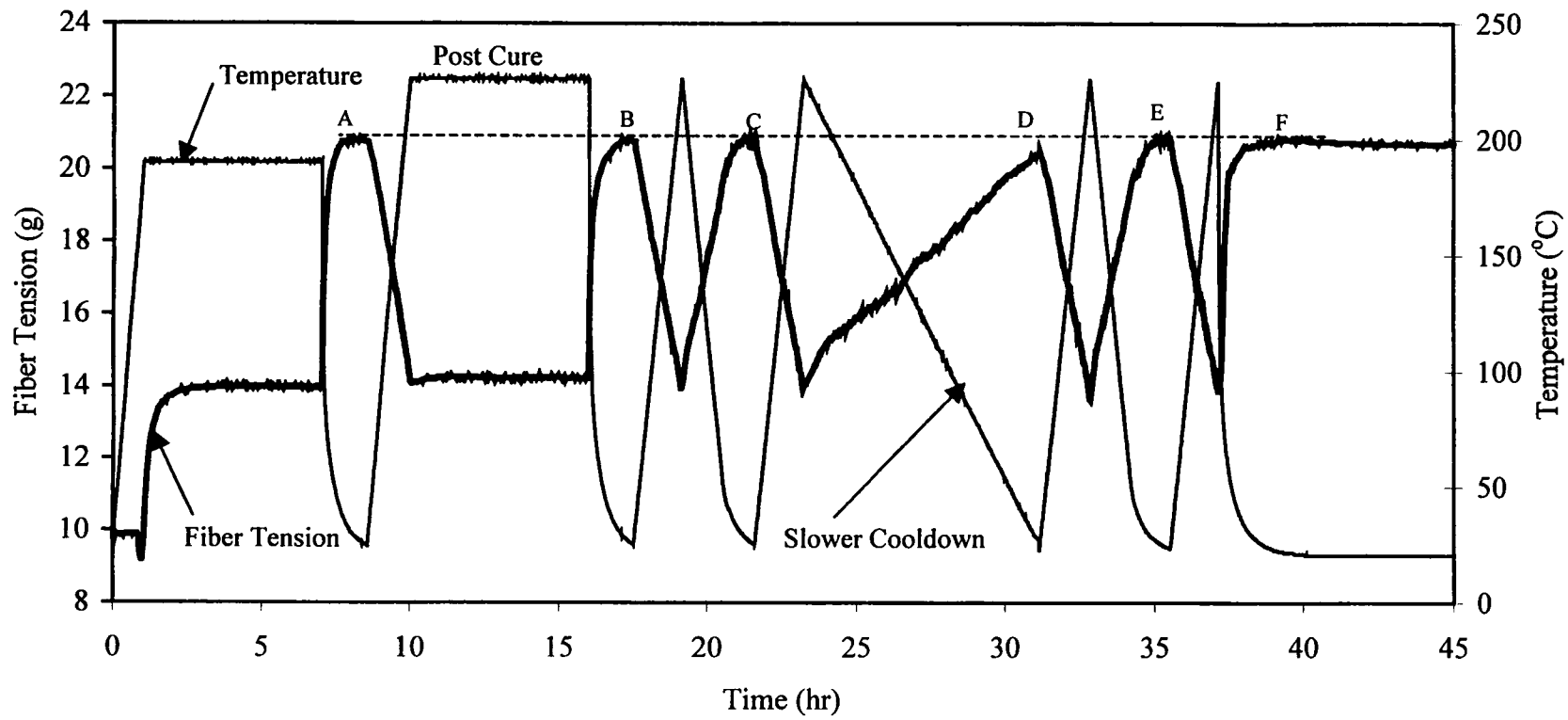

Figure 3.31 Effect of cooldown rate on residual stresses in AS4/5250-4 graphite/BMI single fiber composites.

to additional heating are almost of equal value and as a result, the fiber tension is almost unaffected. The final value of the fiber tension after cool down from posture (point B) is similar to that obtained after cool down from curing at 177°C (point A). Similar findings were reported by White and Hahn for composite laminates subjected to post cure [22].

To study the effect of cool down rate on final fiber tension, after cool down from post cure, the specimen was heated to the same temperature (205°C) and cooled to room temperature at the same previous rate. Same value of final fiber tension was obtained (point C). In the next step, the specimen was heated to the same temperature (205°C) followed by cool down at a slower rate. The final fiber tension at room temperature (point D) is approximately 7% lower than the previous recorded values. To verify that this reduction is due to the enhanced stress relaxation associated with the slower heating rate, the specimen was heated again followed by cool down at same rates as from post cure twice. The reduction in the fiber tension disappeared when cool down rate was increased again (points E and F). The test was repeated and similar results were recorded. Results indicate that slower cool down rate may reduce fiber stresses due to cool down shrinkage. It should be noted that these results are for 5250-4 BMI and can not be generalized. Also, because of the dominant polymer volume fraction in CIST (a single fiber in infinite polymer), polymer viscoelasticity may be more effective than it will be in case of composites with high fiber volume fraction. Constraints applied by fibers on polymer reduce the extent of viscoelasticity as seen in resins.

3-5 CLASSIFICATION OF CURE CYCLES

The results presented in the above section suggest that the major factors affecting such contribution are the amount of *effective* shrinkage and amount of *effective* expansion generated and extent of stress relaxation allowed. *Effective* shrinkage and expansion. For a given thermoset polymer and a given maximum cure temperature, the location of the gelation point is the governing factor that determines the amount of *effective* thermal expansion. The lower the gelation temperature, the larger the *effective* thermal expansion. *Effective* cure shrinkage produces compressive stresses in the fibers. The unrelaxed part of these stresses will be added to the cool down stresses increasing the residual stresses in the composite. The location of the gel point can be lowered to allow for more *effective* thermal expansion. The extent of relaxation of the cure induced stresses depends mainly on time allowed and temperature after gelation before cool down starts. The cure time beyond gelation can be extended by slowing down the heating rate. This may allow for more stress relaxation. Thus, it may be possible to increase the summation of the *effective* thermal expansion and stress relaxation to overcome the stresses generated by the *effective* shrinkage. Depending on the balance between the three factors, the cure cycles can be classified into three types:

Type I: In this case the stresses generated by *effective* shrinkage are larger than the combined effect of the *effective* thermal expansion and stress relaxation. Figure 3.32 (a) shows a schematic of such a cycle as monitored by CIST. The tension prior to the onset of cool down is larger than the initial tension indicating net compressive fiber stresses due to *effective* shrinkage.

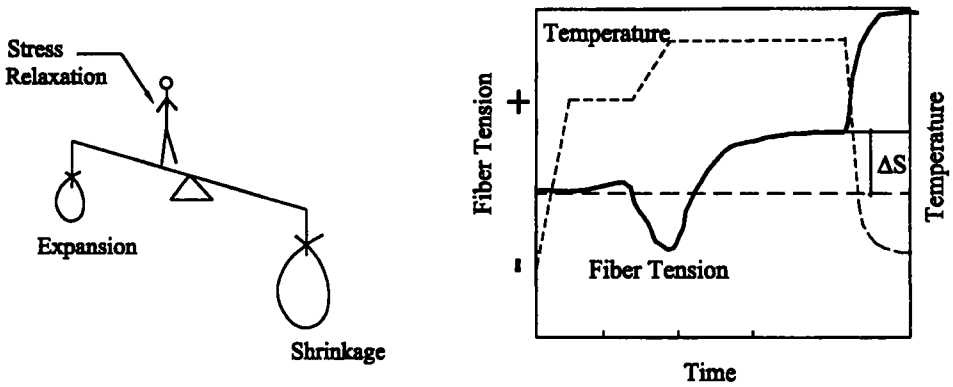

(a) Type I cure cycle

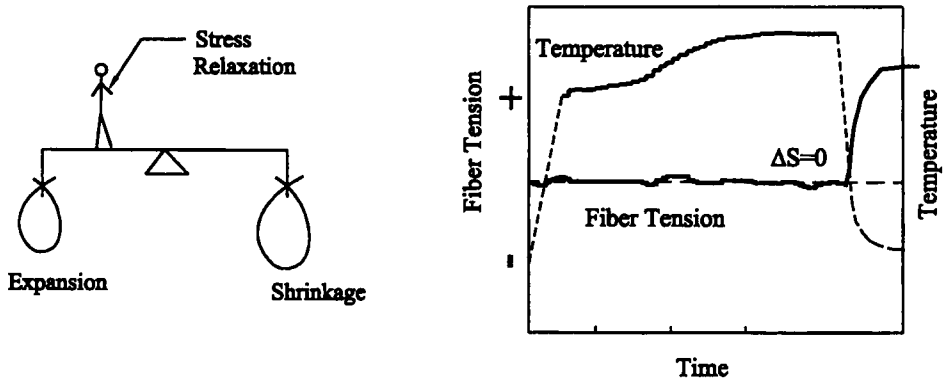

(b) Type II cure cycle

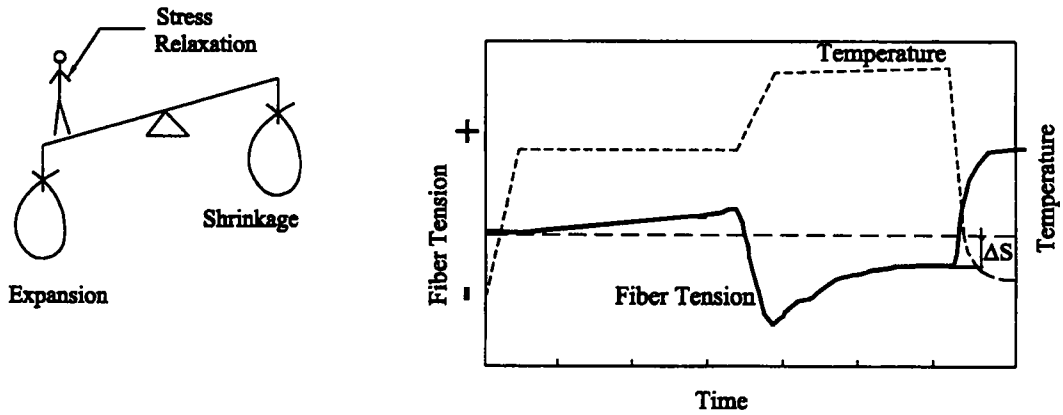

(c) Type III cure cycle

Figure 3.32 Schematic showing the effect of the cure cycle selection on the contribution of cure volume changes to fiber stresses.

Type II: In this case the stresses generated by *effective* shrinkage are equivalent to the combined effect of the *effective* thermal expansion and stress relaxation. Figure 3.32 (b) shows a schematic of such a cycle as obtained by CLFS. The tension prior to the onset of cool down is the same as the initial tension indicating zero net fiber stresses due to cure volume changes. It should be noted that the balance can be generated through the whole cure cycle or just prior to onset of cool down, i.e. allow for increase or decrease in the fiber tension and then cancel these changes through the cycle.

Type III: In this case the stresses generated by *effective* shrinkage are smaller than the combined effect of the *effective* thermal expansion and stress relaxation. Figure 3.32 (c) shows a schematic of such a cure cycle as monitored by CIST. The tension prior to the onset of cool down is smaller than the initial tension indicating net tensile fiber stresses due to *effective* expansion.

Most of the standard cure cycles belong to Type I. This is attributed to the rapid heating to the maximum cure temperature or using short dwell at low temperature. In most of these cycles the gelation temperature is very close to the maximum cure temperature which allows for a small amount of *effective* thermal expansion. Type II cycle can be generated using CLFS as explained above. Type III cycles can be obtained by lowering the gelation temperature to increase *effective* expansion and allowing more stress relaxation. It should be noted that increasing the *effective* thermal expansion by increasing the cure temperature will not help in terms of the final residual stresses since this will increase the cool down shrinkage. So, for a given cure temperature, Type III cycle is basically generated by lowering the gel point and allowing for more stress

relaxation. Results for two typical resin systems, 3501-6 and 977-3 epoxies, are presented here. However, the method can be applied to other resin systems.

3-5-1 3501-6 Epoxy

Figure 3.33 (a) shows a Type I cure cycle of 3501-6 epoxy with corresponding fiber tension changes in an AS4 graphite fiber. This cycle is the standard cure cycle recommended by resin manufacturer. The fiber tension prior to cool down is higher than the initial tension indicating net compressive fiber stresses. Figure 3.33 (b) shows a Type II modified cycle which was obtained using CLFS. The change in the fiber tension through the cure cycle is close to zero. The duration of the modified cycle is shorter than the standard cycle while producing the same glass transition temperature as was shown before in Section 2-4-3. These results were shown before and presented here for convenience.

Figure 3.33 (c) shows a Type III cure cycle. The cure was carried out at a low temperature for longer time to reach gelation at lower temperature. The effect of thermal expansion is larger than that in the standard cure cycle as can be seen by comparing the drop in the fiber tension corresponding to the increase in the temperature from the first to the second dwell temperature. The fiber tension prior to cool down is larger than the initial fiber tension indicating net tensile fiber stresses. These stresses will reduce the residual stresses developed during cool down by thermal shrinkage. The duration of this cycle is longer than the standard cure cycle.

A comparison between the three types of cycles shows that Type II cycle is the shortest and produces less residual stresses than the standard cure cycle. Type III cycle results in

a- Type I cure cycle.

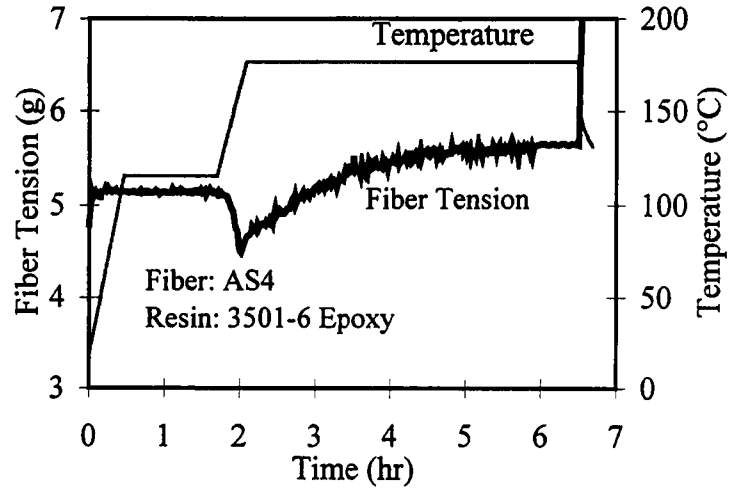

b- Type II cure cycle.

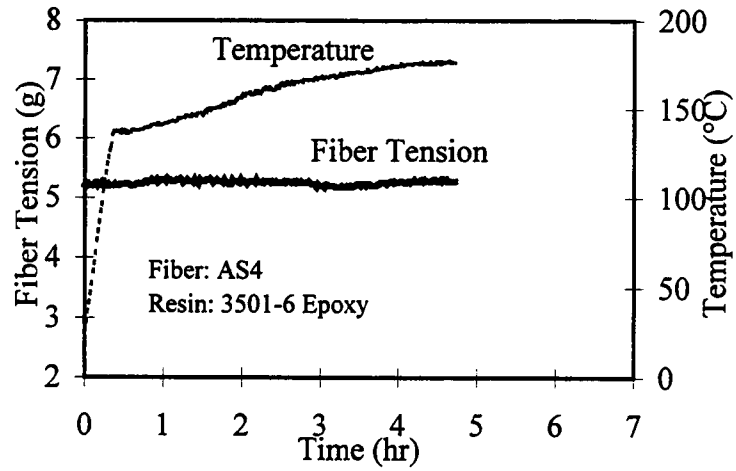

c- Type III cure cycle.

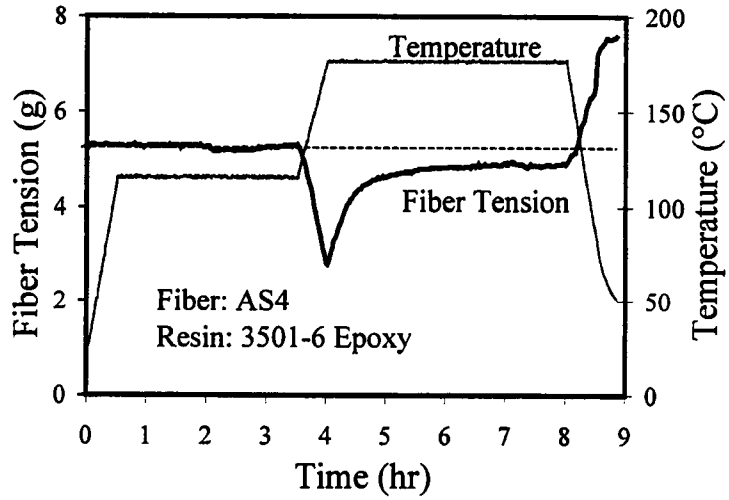

Figure 3.33 Different types of cure cycles for AS4/3501-6 graphite/epoxy.

minimum residual stresses however it is the longest. The three types of cycles produce the same glass transition temperatures (170, 171, and 170°C respectively).

3-5-2 974-3 Toughened Epoxy

The standard cure cycle of 974-3 (Figure 3.34 (a)) is a Type I cycle. The CLFS was applied to obtain Type II and III cycles. The objective in Type II cycle is to have a balance between *effective* shrinkage and the summation of *effective* expansion and stress relaxation. In this case there will be no cure induced stresses and residual stresses will that produced only during the cool down. For Type III cycle, the objective is to increase the summation of the *effective* thermal expansion and stress relaxation more than the *effective* shrinkage.

Standard cure cycle of 977-3 is a Type I cycle (shown in Figure 3.24 (a) for convenience). A Type II was developed using CLFS as shown in section 3-3-2 (shown in Figure 3.24 (b) for convenience). The CLFS was applied to produce Type III cycle with more *effective* thermal expansion and stress relaxation. The initial heating temperature was taken as 118°C. However, at this low temperature a longer temperature hold is required to advance the cure before increasing the temperature (such that thermal expansion will be *effective*). Figure 3.34 (c) shows the Type III cure cycle. The final fiber tension prior to cool down is lower than the initial fiber tension. This indicates the development of tensile stresses in the fiber prior to cool down. These tensile stresses will cancel part of the cool down stresses and hence this type of cycle will produce less residual stresses than the Type I and II cure cycles. However, Type III cycle is considerably longer than the other two types of cycles.

a- Type I cure cycle

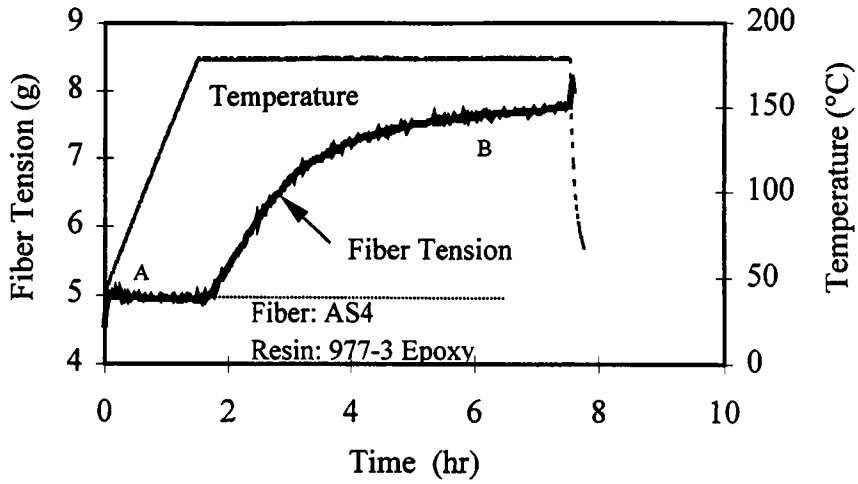

b- Type II cure cycle

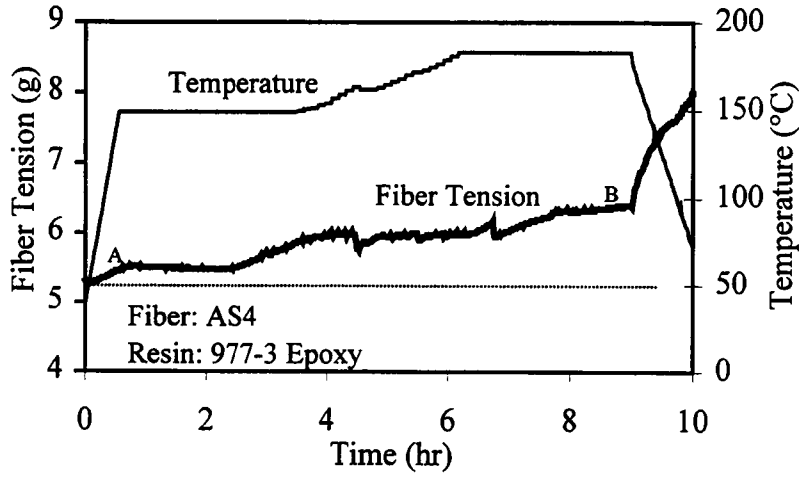

c- Type III cure cycle

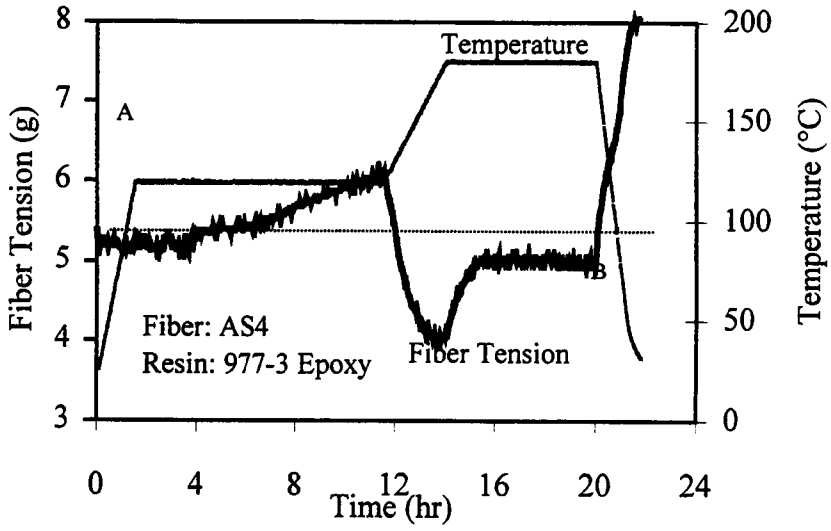

Figure 3.34 Different types of cure cycles for AS4/974-3 graphite/epoxy.

3-5-3 Applications

In this part of the study, the three types of cycles for 977-3 toughened epoxy are applied to cure composite laminates and residual stresses are compared. The composite system used here is IM7/977-3 graphite/toughened epoxy prepreg. The cure cycles are used to cure unsymmetric [$0^o/90^o$] composite laminates. The curvature of the cured laminates was used as an indicator for residual stresses. The laminates were cut and laid up manually and cured in the same location of the single fiber composite specimen to reduce the variation between the cure parameters between CIST and CLFS and the laminates. The dimensions of the specimens are 3/8x3 inches and the lay up is [$0^o_1/90^o_2$]. The cure cycles are shown in Figure 3.34 (a), (b), and (c). The same cool down rate and pressure schedule were used in the three cure cycles. The specimens were made narrow to limit the effect of the curvature in the 90° direction. No machining on the specimens was done to avoid any stress relaxation. Specimens with different layup were tried, however thicker specimens tend to have delamination which may affect the comparison. Curvature of the cured specimens was calculated using Equation 6.

A photograph of representative specimens cured using the three different cycles is shown in Figure 3.35 (a). The modified cycles reduced the specimen curvature. A plot of the dimensionless curvature is shown in Figure 3.35 (b) for the different specimens. Compared to the standard cure cycle, the first modified cycle (Type II) reduced the curvature by about 16% while the second modified cycle (Type III) reduced it by about 19%. The cure was completed in all cases since the glass transition temperatures in all three cases were statistically same (about 205-210°C).

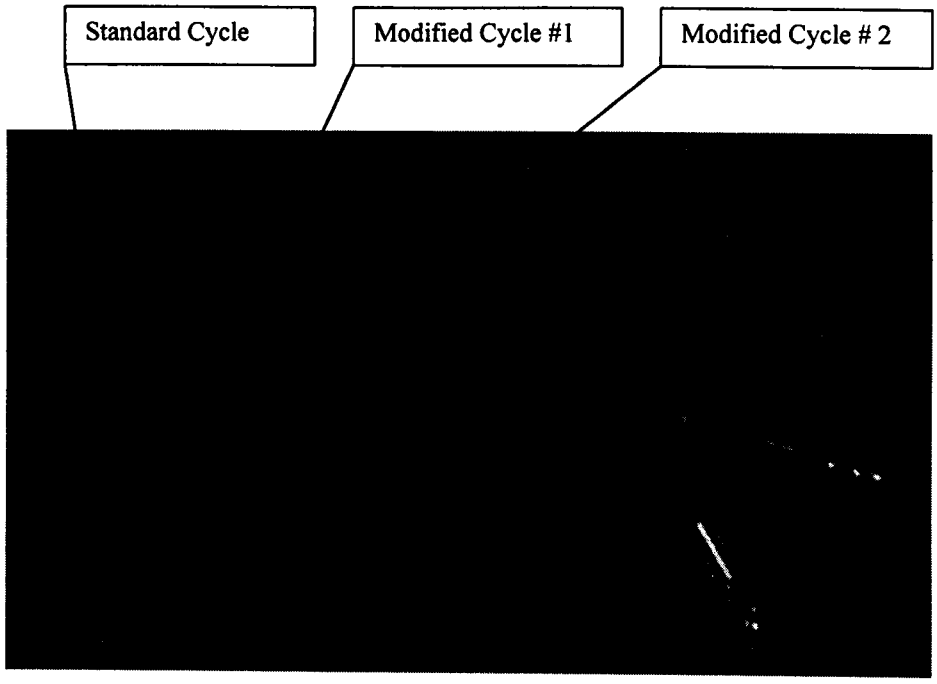

(a) Photograph.

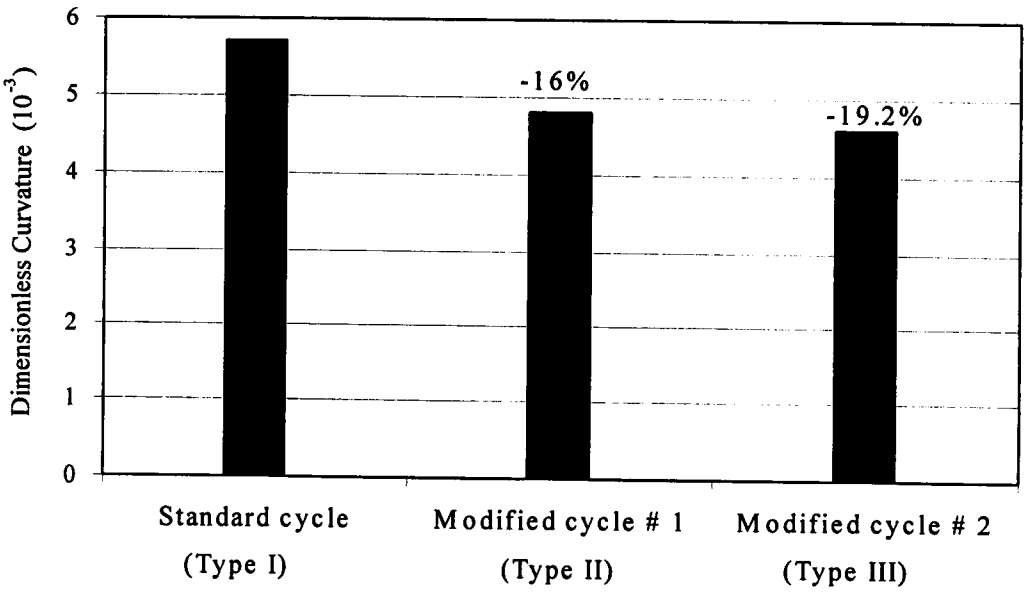

(b) Curvature data.

Figure 3.35 Curvature of unsymmetric IM7/977-3 graphite/epoxy laminates cured using different cure cycles.

3-6 EFFECT OF MODIFIED CURE CYCLES ON MECHANICAL PROPERTIES

The objective here is to investigate the effect of changing the cure cycle on the mechanical properties of the composite laminates which is a major concern for structural applications. The properties affected most by the change in the cure cycle are those which are matrix dependent. The inplan shear strength and shear modulus were chosen as representative mechanical properties.

The composite system used in this part of the study is IM7/977-3 graphite/toughened epoxy prepreg. Symmetrical specimens (10.5X10.5 inches; $(45^{\circ}_{2},-45^{\circ}_{4},45^{\circ}_{2})$) were cut and laid and cured in a vacuum hot press. The cured laminates were then cut to 1X10 inches strips and tested in tension in a universal testing machine (MTS machine). Strain gauges were used to measure strains in 0° and 90° directions. Load and strain data were collected at close intervals to allow for the determination of the stiffness. Six specimens of each cycle were tested and shear strength and shear modulus were calculated.

Figure 3.36 (a) shows the shear strength data for the specimens cured with the three types of cycles. The Type II cycle increased the shear strength by about 15%. The increase in the shear strength may be due to the reduction in the residual stresses and micodamages caused by residual stresses. Type III cycle reduced the failure shear stress by about 25%. This may be due to the long heating beyond cure of the specimens, which is similar to post curing that was shown to reduce shear strength in epoxy composites [58]. Figure 3.36 shows that the three cure cycles results in approximately the same shear modulus.

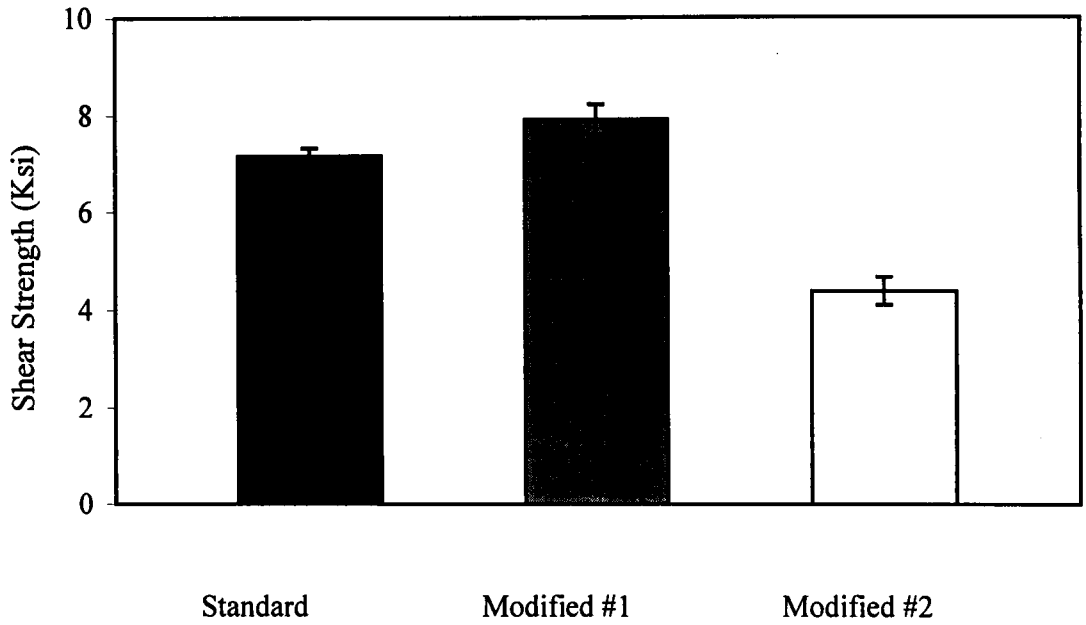

(a) Shear Strength (ksi)

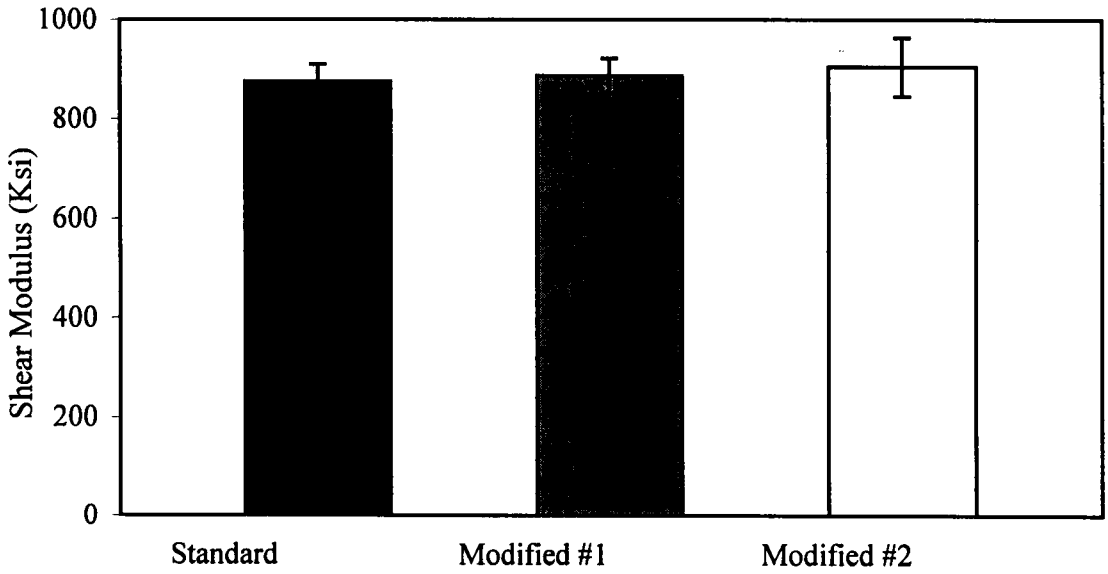

(b) Shear Modulus (ksi)

Figure 3.36 Effect of cure cycle modification on mechanical properties of IM7/977-3 graphite/epoxy composites.

Among the three types of cycles, Type II cycle appears to produce the best results. While the duration is close to the standard cure cycle, it reduces the residual stresses and enhances the mechanical properties.

3-7 SUMMARY AND CONCLUSION

In this chapter, results of a new approach to monitor and reduce cure induced stresses in thermoset polymer composites were presented. The approach utilizes a new test setup and a feedback control system. The method was applied to study the cure induced stresses in several thermoset polymer composites cured using the cure cycles recommended by prepreg manufacturers. Modified cure cycles that reduce cure induced stresses were demonstrated. It was shown that the modified cure cycles not only reduce residual stresses in composite laminates but might enhance the matrix dominated mechanical properties as well, while maintaining the glass transition temperature as those of the standard cure cycles.

A general classification of the cure cycles according to their cure induced stresses was presented and demonstrated with two examples. The classification can be used to compare qualitatively between different cure cycles to reduce cure induced stresses.

CHAPTER 4

CURE CYCLE OPTIMIZATION MODEL AND COMPUTER PROGRAM

4-1 INTRODUCTION

In Chapter 3, it was shown that the approach of controlling the volume changes of the thermoset polymers together with utilizing stress relaxation during cure can effectively reduce residual stresses in single fiber composites as well as in composite laminates. Although the modified cycles were obtained from single fiber composites they were shown to reduce stresses in composite laminates as well. In this part of the study, a mechanical optimization model was developed and used to obtain modified cure cycles that reduce cure induced stresses in composite laminates. The approach is similar to that of the CLFS as shown in Chapters 2 and 3 while consideration was given to the differences between single fiber composites and composite laminates. The major differences between single fiber composites and composite laminates include the existence of gradients in the temperature and degree of cure over the laminate thickness. Also, composite laminates contain high volume fraction of fibers, which is not the case in single fiber model composites. Temperature and degree of cure gradients are determined using models. The effect of fiber volume fraction was included in the determination of effective mechanical and thermal properties of the composite and the flow of the resin.

The developed model includes a procedure for evaluation and minimization of cure induced stresses. The goal is to minimize residual stresses in composite laminates due to cure volume changes. The model was used to determine cure cycles that maximize the cancellation of cure shrinkage stresses by a combination of stress relaxation and thermal expansion beyond gelation. The key assumptions adopted in developing the model include

1- Flat laminate geometry to simplify the analysis.

2- The length and width of the plate are assumed to be relatively large compared to the thickness. This allows using one-dimensional analysis for the resin and heat flow across the laminate thickness.

3- In addition to assumption number 2, the length is assumed to be greater than 10 times the width, which allows for one dimensional analysis of stresses.

4- Only volume changes beyond gelation cause fiber stresses (*effective* volume changes as defined in Chapter 2).

5- The mechanical properties of the matrix and composite are fully developed beyond gelation point.

Other assumptions included in the sub-models and analysis methods will be discussed later. The sub-models include, degree of cure, viscosity, mechanical properties, cure shrinkage, thermal expansion, etc. Numerical solvers were used in the analysis to obtain solutions of the nonlinear coupled equations involved. Viscoelastic laminate theory was used to evaluate stresses as a result of volume changes. The major components of the model are shown in Figure 4.1. First, properties of the polymer are evaluated. Then strains (due to polymer volume changes) and material properties are evaluated. Then

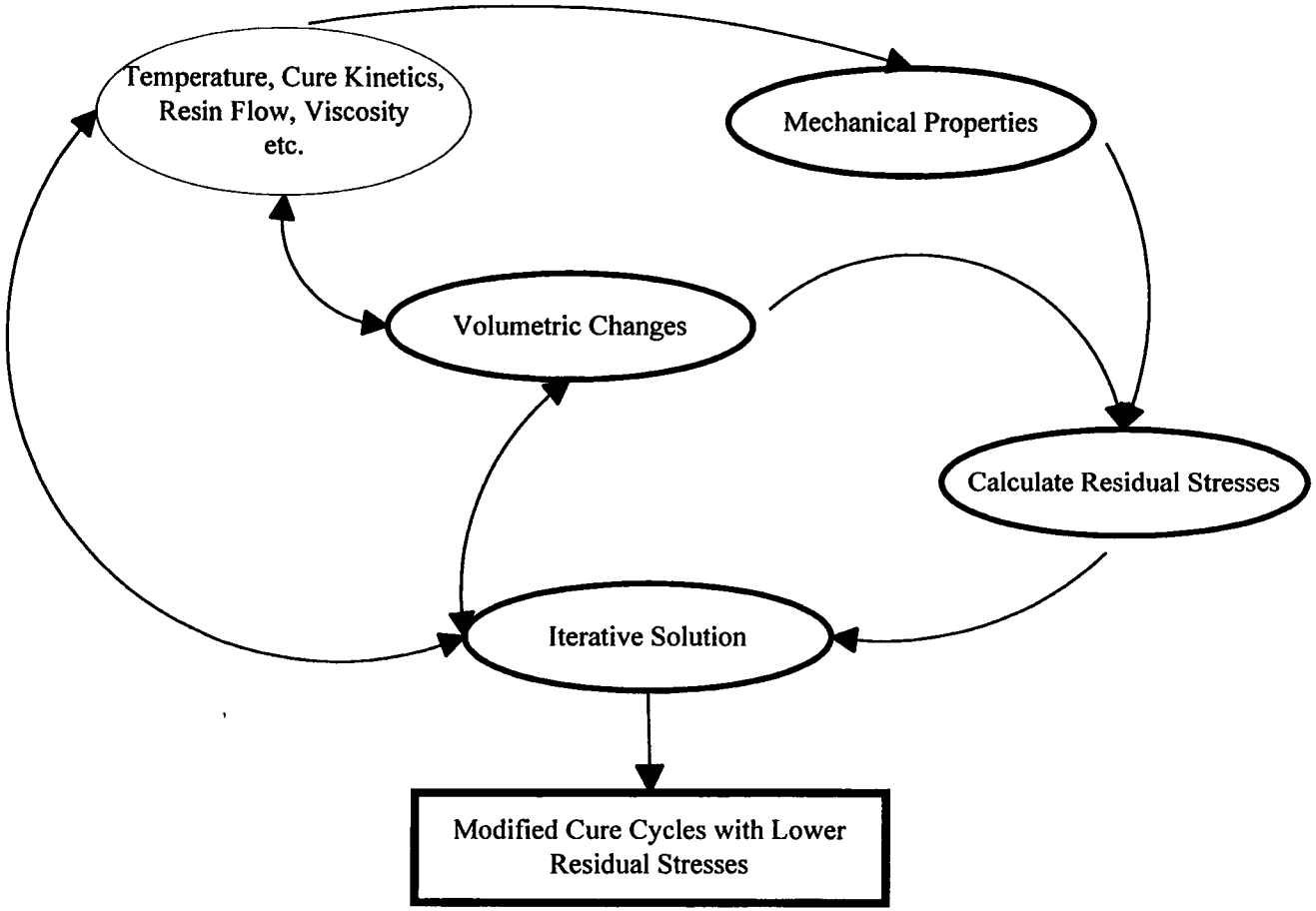

Figure 4.1 Flow diagram of OPTICURE.

stresses are calculated and a criterion, such as curvature of unsymmetric laminates, is used to determine cure cycles with reduced residual stresses. A computer program called OPTICURE (OPTIMUM CURE) was written to perform the procedure. The program runs under Windows and Unix systems. A flow chart of the program is shown in Figure 4.2. Sub-models are discussed first followed by some key elements of the computer program and typical results. The model is general, however, for demonstration purpose the model was applied to AS4/3501-6 graphite/epoxy composite and typical results are presented. Findings of the model correlate well with results obtained from CIST and CLFS.

4-2 SUB-MODELS

Sub-models are used to calculate the changes in the material properties and stresses at any time during the cure cycle. This includes cure kinetics, polymer volume changes, polymer viscosity, and polymer stiffness. Another set of sub-models are used to describe the changes in the composite laminate including heat flow, resin flow out of the composite, thermal properties of the laminates, and laminate stiffness. Because of the nonlinear inter-dependency among variables, incremental numerical solutions are used.

4-2-1 Temperature Distribution

The objective here is to obtain the temperature distribution over the thickness of laminate. The temperature at each layer is needed to calculate resin degree of cure,

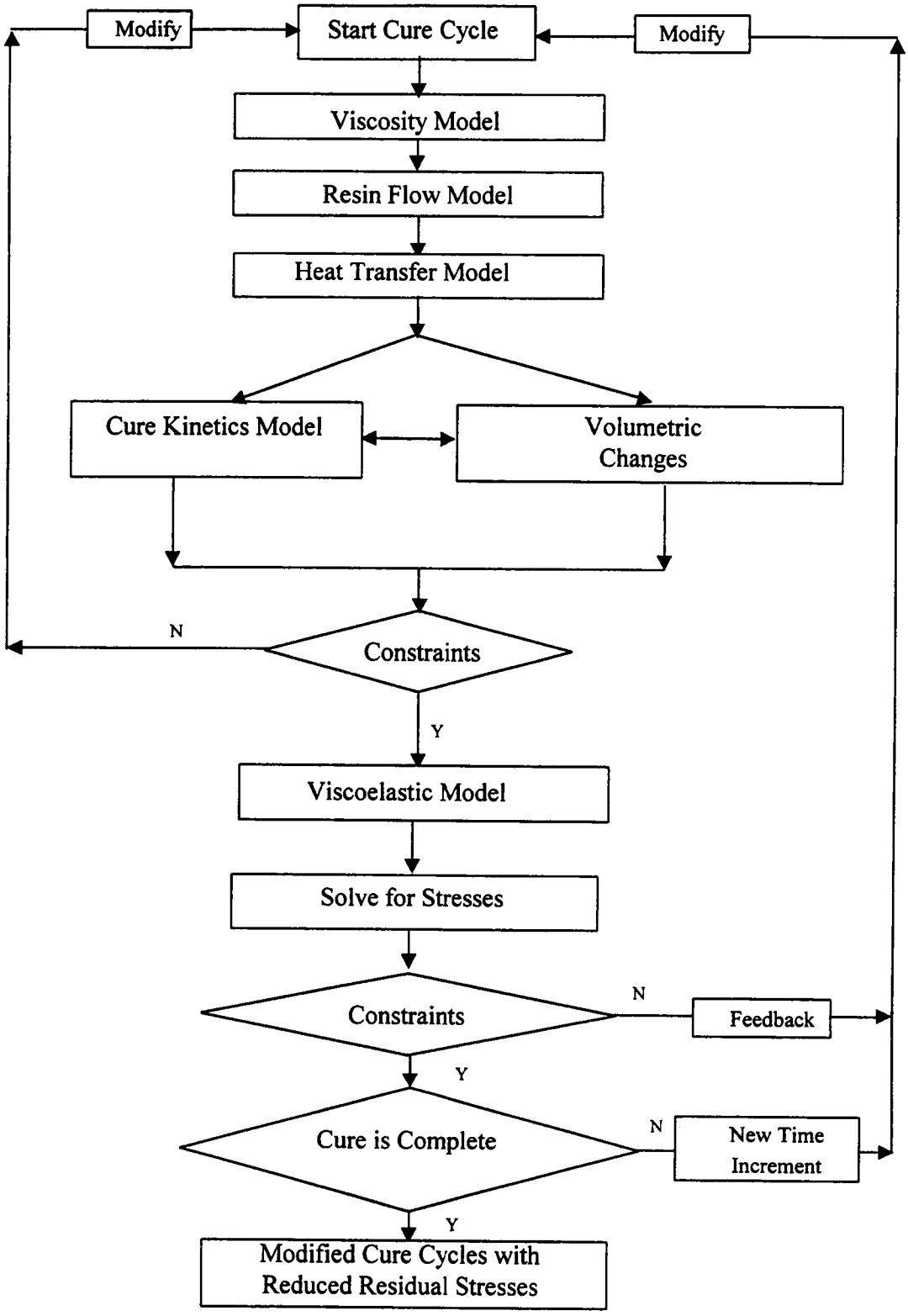

Figure 4.2 Diagrammatic flow chart of OPTICURE.

viscosity, and stiffness. One dimensional heat transfer model is used. The governing PDE of the problem is written as

$$\frac{\partial(\rho\, C\, T)}{\partial t} = \frac{\partial}{\partial z}\left(K\frac{\partial T}{\partial z}\right) + \rho\, \dot{H} \qquad (7)$$

$$\dot{H} = \frac{d\alpha}{dt} H_R$$

where

H_R total heat of reaction

C specific heat of the composite

ρ composite density

K thermal conductivity of the composite

T temperature

α degree of resin cure

The values of the specific heat and density of the composite are calculated in terms of resin and fiber properties by using the rule of mixture. The thermal conductivity of the composite is evaluated from the properties of its constituents using micromechanics as shown by Springer and Tsai [59]. Finite differences method is used to obtain the temperature distribution. Boundary conditions are taken as prescribed temperatures at the top and bottom of the layup assembly. These temperatures are determined by the cure cycle.

4-2-2 Cure Kinetics

Cure kinetics model is used to determine the polymer degree of cure at any time in the cure cycle. The model and the computer program allow for the following general form for cure kinetics

$$d\alpha / dt = f(T,\alpha)$$
$$\alpha = \int_0^t f(T,\alpha)dt \qquad (8)$$

where

α degree of resin cure

T absolute temperature

The equation is integrated numerically to obtain the degree of cure at each point at any time interval during the cure cycle. For the particular case of 3501-6 epoxy, the following model was developed by Loos and Springer [60]

$$d\alpha / dt = (k_1 + k_2\alpha)(1-\alpha)(B-\alpha) \qquad \alpha \le 0.3 \qquad (9)$$
$$d\alpha / dt = k_3(1-\alpha) \qquad \alpha > 0.3$$

Where

$k_1 = A_1 exp(-\Delta E_1 / RT)$

$k_2 = A_2 exp(-\Delta E_2 / RT)$

$k_3 = A_3 exp(-\Delta E_3 / RT)$

$A_1 = 2.101x10^9\ min^{-1}$

$A_2 = -2.014x10^9\ min^{-1}$

$A_3 = 1.960x10^5\ min^{-1}$

$\Delta E_1 = 8.07x10^4\ J/mol$

$\Delta E_2 = 7.78x10^4\ J/mo$

$\Delta E_3 = 5.66x10^4\ J/mo$

$B = 0.47$

The initial conditions are taken as $\alpha=\alpha_b$ at t=0 where α_b is the degree of cure of the b-staged prepreg.

4-2-3 Resin Flow Model

Resin flow model is needed to calculate instant volume fractions of matrix at different times in a cure cycle. One-dimensional consolidation model as suggested by Loos and Springer [61] was used. The model allows for resin flow in the direction perpendicular to the plane of the laminate. The flow in this direction is dominant in composite parts where thickness is relatively small compared to width and length. Equations of the model are shown below.

$$V_r(t) = V_0 - \int_0^t \frac{A_z S_c}{\int_0^{h_c} \mu dz} \left(\frac{P_o - P_b}{1 + G(t)} \right) dt \qquad (10)$$

$$G(t) = \frac{S_c}{S_b} \frac{\mu_b h_b}{\int_0^{h_c} \mu dz}$$

$$h_b = \frac{1}{\phi_b A_z} \int_0^t \frac{dV_r}{dt} dt$$

$$h_c = n_c h_l$$

where

V_r resin volume fraction

V_o initial resin volume fraction

A_z laminate area perpendicular to the flow direction

S_c apparent permeability of the composite

S_b apparent permeability of the bleeder

$G(t)$ parameter

μ viscosity of the resin

n_c number of compacted layers

h_l thickness of one compacted layer

h_c thickness of compacted layers in the composite

h_b instantaneous depth of resin inside the bleeder

ϕ_b porosity of the bleeder

P_o applied pressure

P_b pressure in the bleeder

Values of the model parameters for 3501-6 epoxy are given in the above reference. It can be seen that the resin flow depends on polymer viscosity. At gelation the polymer viscosity increases significantly and the flow beyond gelation can be ignored.

4-2-4 Gelation

Gelation is defined by the formation of an infinite network in the thermoset polymer. Gelation is accompanied by a significant increase in the viscosity. Polymer stiffness increases with the viscosity. Before gelation, the polymer viscosity is relaively low at high temperatures and hence the polymer stiffness. Because of the low viscosity, stress relaxation will be very effective to cancel stresses that develop before gelation.

In the current analysis, it was assumed that gelation occurs at a fixed degree of cure, α^*, which is determined experimentally. Figure 4.3 shows degree of cure and polymer

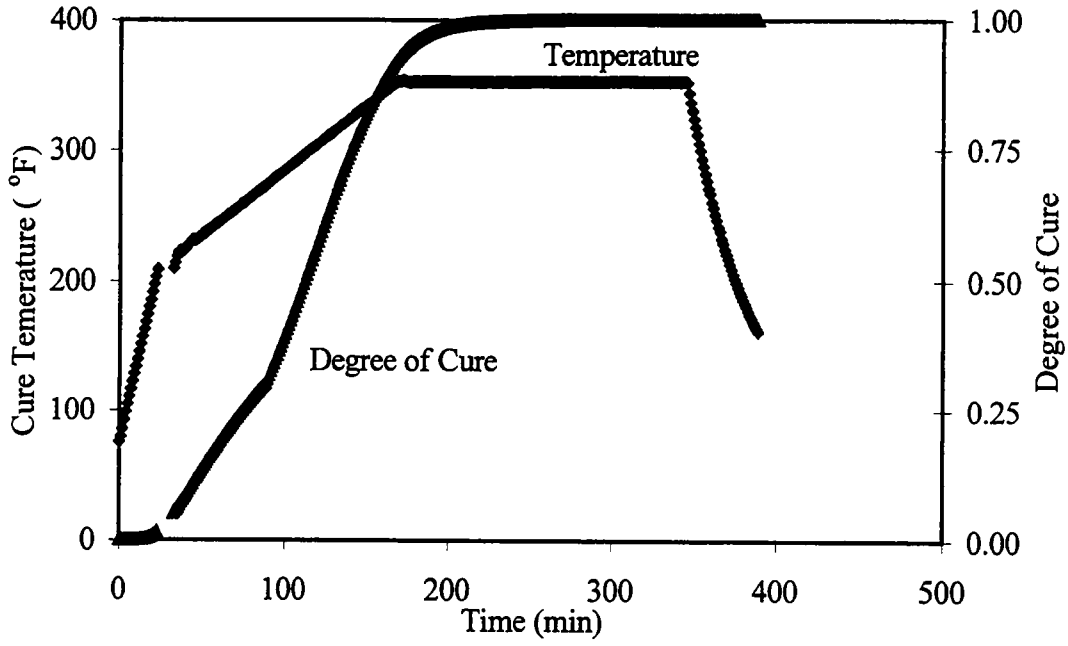

a- Degree of cure

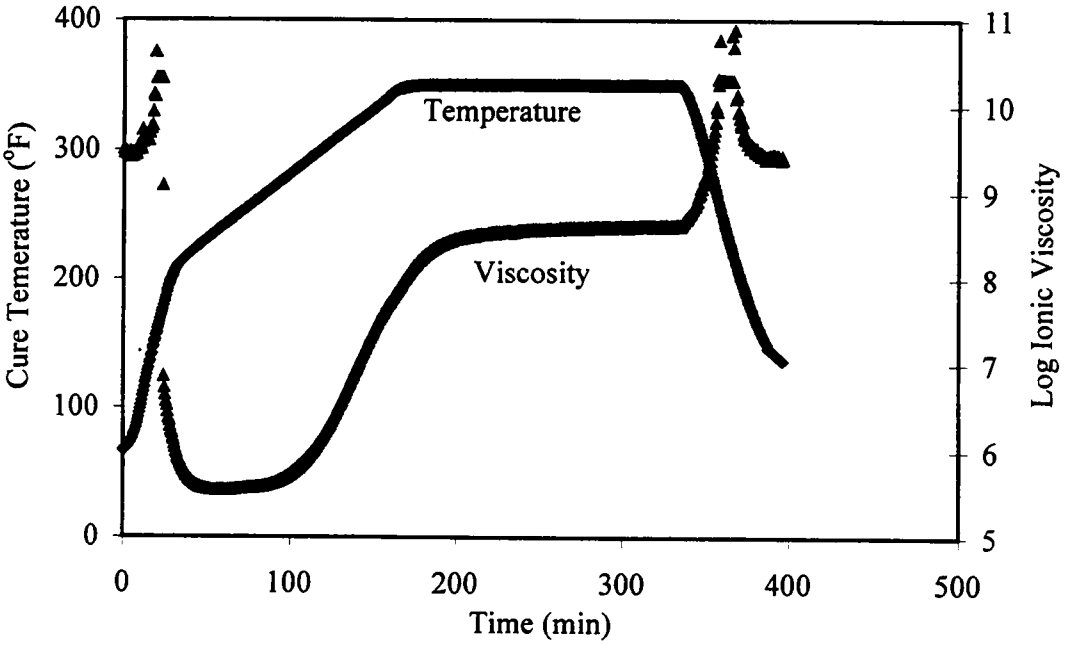

(b) Log ionic viscosity

Figure 4.3 Degree of cure and viscosity during a cure cycle of 3501-6 epoxy.

viscosity during a cure cycle [62]. During heating from room temperature to initial heating temperatures the polymer viscosity decreases significantly. The viscosity of the polymer remains low until the polymer approaches gelation at which it starts to increase rapidly. Gelation is defined as the point at which there is an inflection in the slop during this increase. In that particular example gelation occurs at degree of cure α=0.81. Data from the same reference (5 different cycles) was used to determine an average value of α^*=0.80.

4-2-5 Volume Change Model

Volume changes in thermoset polymers consist of chemical shrinkage due to crosslinking and thermal expansion during temperature changes. Chemical shrinkage is calculated assuming a linear relationship between the degree of cure and amount of shrinkage. Thermal expansion is estimated by determining the polymer thermal expansion coefficient during cure. In general, thermal expansion coefficient of the polymer may depend on the temperature and degree of cure. No models were found in the literature to establish such dependency. Currently, research work is going at the composite materials laboratory at the University of Tennessee to develop such models.

Only thermal expansion beyond gelation is of importance for the current analysis. For 3501-6 epoxy, gelation is assumed to occur at degree of cure α^*=0.80 as discussed above.

Crosslinking shrinkage is calculated as

$$\Delta V_{sh}(\alpha) = \Delta\alpha \; \Delta V'_{sh} \qquad (11)$$

and thermal expansion coefficient is determined as

$$\Delta V_{th} = \Delta V - \Delta V_{sh}(\alpha) \qquad (12)$$
$$\theta(\alpha, T) = \Delta V_{th} / \Delta T$$

where

$\Delta V'_{sh}$	total cure shrinkage from experiments
$\Delta V_{sh}(\alpha)$	increase in the cure shrinkage
ΔV_{th}	thermal expansion after ΔT increase in the temperature
$\theta(\alpha,T)$	thermal expansion coefficient of the polymer at degree of cure α and temperature T
ΔT	temperature increment
ΔV	total change in the polymer volume measured experimentally

The cure kinetics and heat transfer models were used to calculate the change in the degree of cure and temperature at any point in the cure cycle. Since thermal expansion coefficient changes significantly with the change in the polymer state (glassy or rubbery), the polymer state should be determined. When cure temperature is less than the glass transition temperature the polymer is considered to be in a glassy, and when temperature is higher, rubbery state is considered. The following form of Di Benedetto model [63] is used to determine the polymer glass transition temperature as a function of degree of cure

$$\frac{T_g - T_{g0}}{T_{g\infty} - T_{g0}} = \frac{\lambda \alpha}{1-(1-\lambda)\alpha} \qquad (13)$$

where T_g is the polymer glass transition temperature in °K at any degree of cure α. T_{g0} and $T_{g\infty}$ are the glass transition at α=0 and α=1 respectively. In the above equation, λ is a constant which can be approximated as [63]

$$\lambda = \frac{T_{g0}}{T_{g\infty}} \tag{14}$$

For 3501-6 epoxy $T_{g\infty}$ =450°K and T_{g0} = 284°K [64]. Based on these values and considering room temperature of 20°C and cure temperature of 177°C, rubbery state was found to be dominant in almost all practical cure cycles (from cure cycle duration point of view).

The volume change data of the cure cycle shown in Figure 4.4 (a) was used to test the validity of the assumptions adopted in modeling cure shrinkage and thermal expansion. Degree of cure and glass transition temperature were calculated using cure kinetics and glass transition temperature models. Output of the models is shown in Figure 4.4 (b). Volume change during the temperature hold at 350°F was plotted against the degree of cure as shown in Figure 4.5 (a). Volume changes during such holds are attributed to cure shrinkage (since there is no temperature change). The relationship is approximately linear, which agrees with the assumption implied in Equation 11. After correlating cure shrinkage with the degree of cure (Equation 11), thermal expansion was calculated using Equation 12. Using this procedure, thermal expansion was calculated at different points during the heating ramp from gelation point up to the temperature hold at 350°F. Calculated thermal expansion was plotted against temperature as shown in Figure 4.5 (b). The relationship can also be approximated with a straight line. This suggests that it

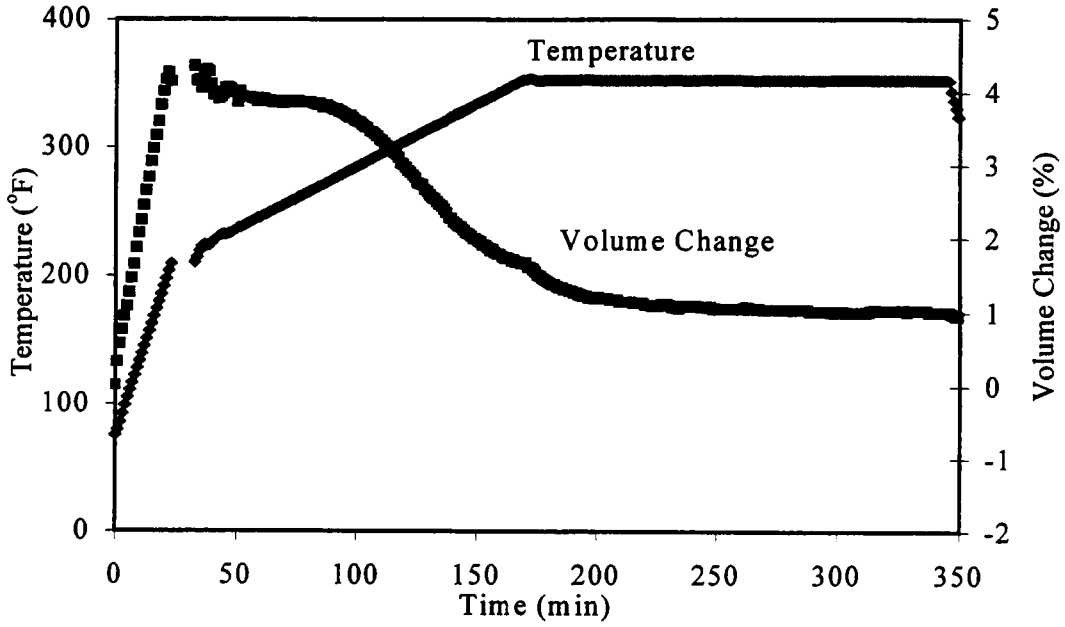

a- Volume changes

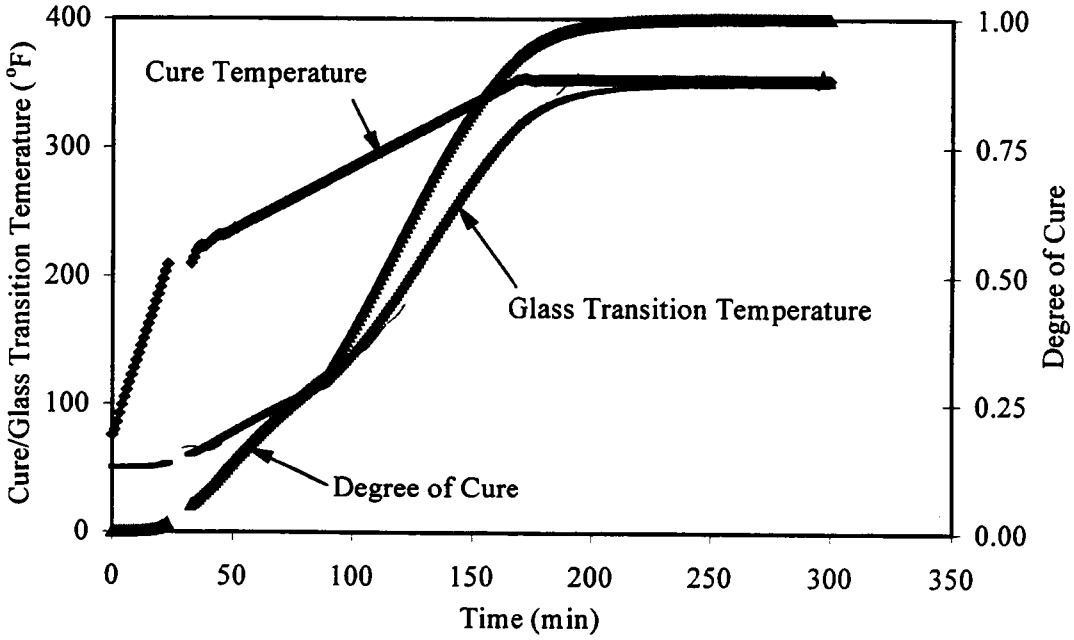

(b) Degree of cure and glass transition temperature

Figure 4.4 Degree of cure, glass transition temperature, and volume changes during a cure cycle of 3501-6 epoxy.

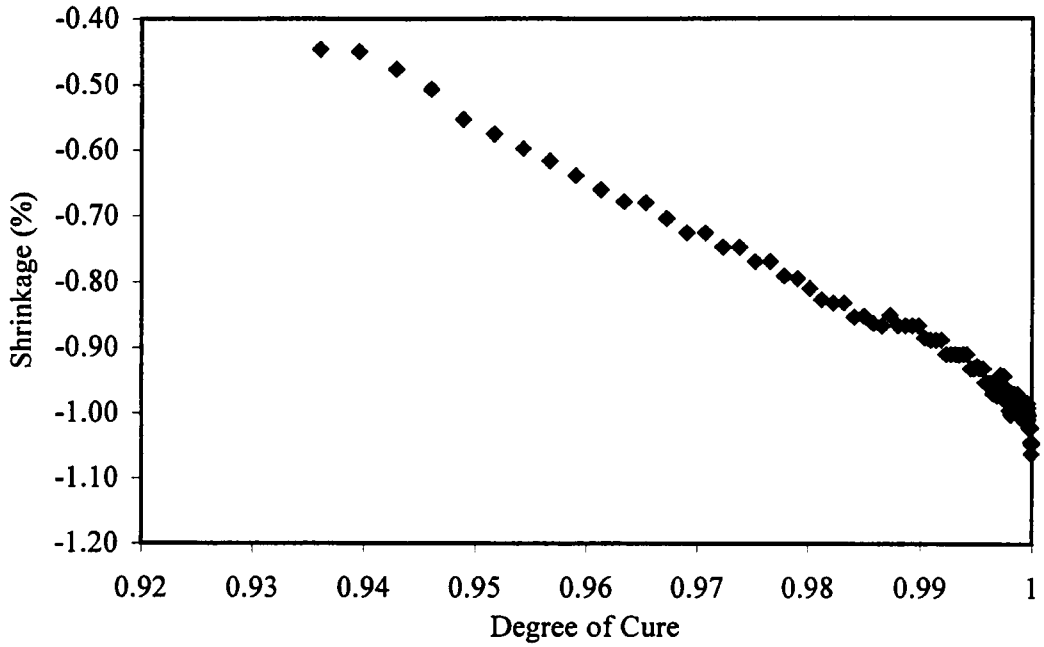

(a) Relationship between degree of cure and cure shrinkage.

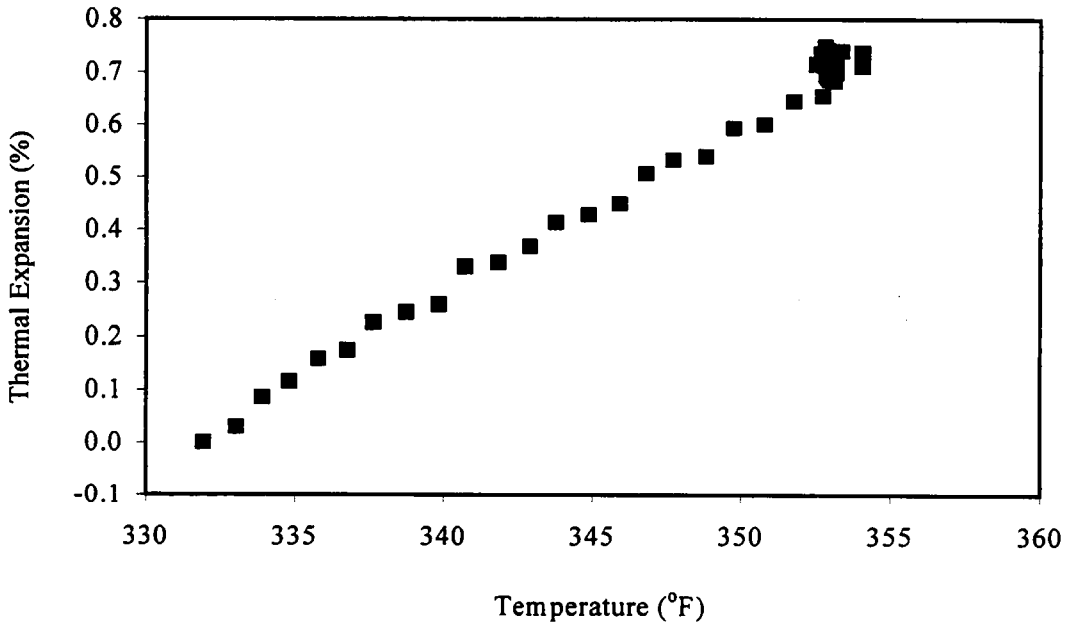

(b) Relationship between temperature and thermal expansion.

Figure 4.5 Variation in cure shrinkage and thermal expansion during cure.

may be justified to use a constant thermal expansion coefficient and ignore any dependency on the degree of cure in the temperature range from gelation to cure temperature.

Cure shrinkage and thermal expansion as predicted from the above correlation were used to predict total volume changes. Figure 4.6 shows comparison between predicted and measured total volume changes. An acceptable agreement exists. It should be emphasized that these results are not general conclusions about the validity of the assumptions or the procedure. Results only indicate that this procedure may be acceptable for 3501-6 epoxy in the range of experimental data for the purpose of stress analysis.

Five different cure cycles [62] were used to obtain average values for the correlation parameters. In all the five cycles, the cure temperature was higher than glass transition temperatures. The value of the total cure shrinkage, $\Delta V'_{sh}$ in Equation 11, was found to change from one test run to another for the same range of degree of cure ($\alpha^*=0.80$ to $\alpha=1$). This was attributed to possible deficiency in the testing procedure, to the choice of parameters, or to the accuracy of measurements but not to the variation in the material properties. In each cycle, to obtain thermal expansion coefficients during transition segments, the value of $\Delta V'_{sh}$ was calculated from the constant temperature segments of the same cure cycle. In cure cycles without any or just small constant temperature holds, an average value of $\Delta V'_{sh}$ was used to yield good correlation. An average value of the thermal expansion coefficient, θ, from different cure cycles was calculated after establishing the correlation and was found to be 2.01×10^{-4} m/m/°F with range of

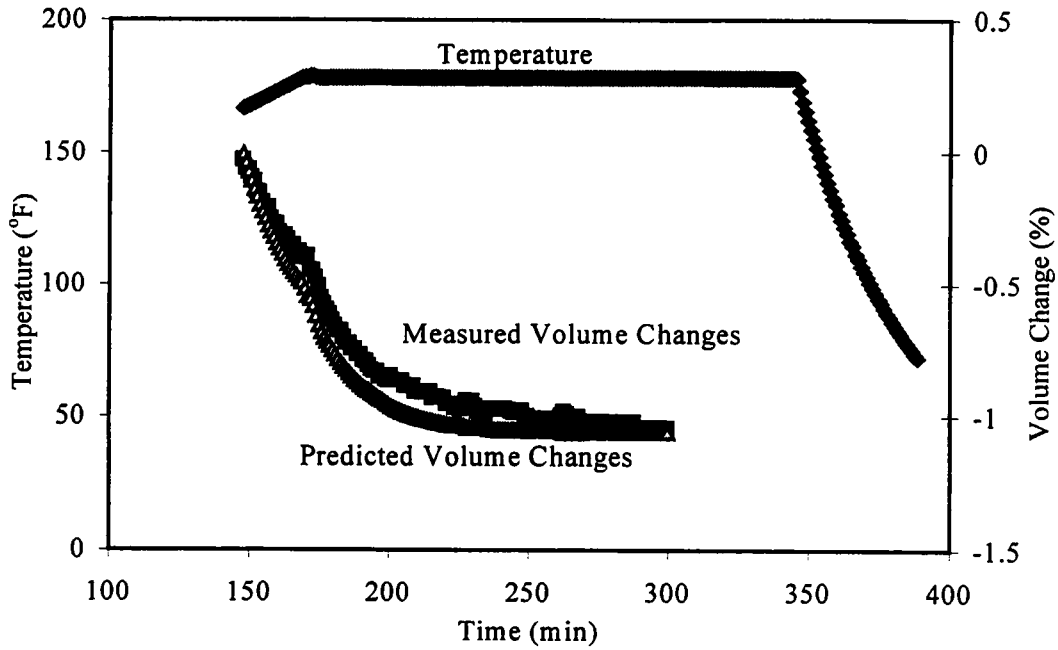

Figure 4.6 Predicted versus measured volume changes beyond gelation.

1.56×10^{-4} to 2.46×10^{-4} m/m/°F. No significant dependency on the degree of cure in the range $\alpha^*=0.80$ to $\alpha=1$ was observed in all five cure cycles. Figure 4.7 shows predicted versus experimental data for a cure cycle in which temperature changes linearly and no temperature holds. An acceptable agreement exists between experimental and predicted values.

4-2-6 Viscosity Model

Resin viscosity is needed to determine the polymer gel point. Gelation is accompanied by sharp increase in viscosity. Viscosity depends on degree of cure and absolute temperature of the polymer. Stresses developed before the gel point are assumed to relax completely. Polymer volume changes occurring beyond the gel point are responsible for producing fiber stresses, and hence these volume changes (both expansion and shrinkage) will be referred to as *effective* volume changes as discussed in Chapter 2. The mechanical model starts to calculate and minimize stresses beyond this point. The general form considered in the model is

$$\mu=f(T,\alpha) \tag{15}$$

where

μ is the polymer viscosity when the cure is complete

T is the absolute temperature

α degree of resin cure

For 3501-6 epoxy, the following relationship was used [60],

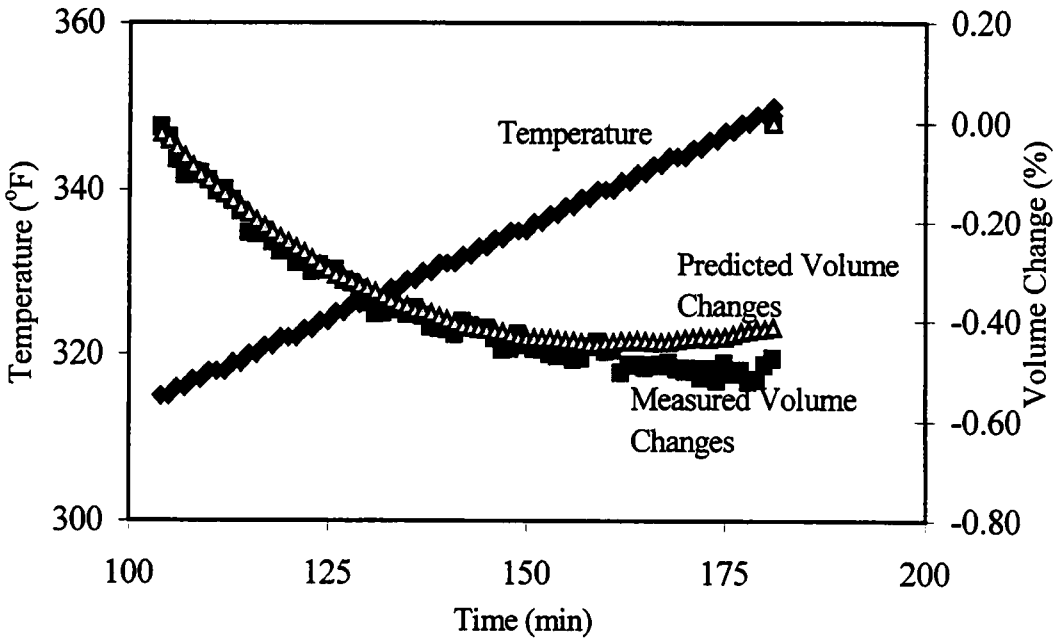

Figure 4.7 Comparison between measured and predicted cure volume changes for linear increase in temperature.

$$\mu = \mu_\infty exp(U / RT + k\alpha) \qquad (16)$$
$$k = 14.1$$
$$\mu_\infty = 7.93x10^{-14}\ Pa.Sec$$
$$U = 9.08x10^{4}\ J/mol$$

4-2-7 Calculation of Stresses

In this section, stresses due to thermal and chemical volume changes were evaluated. Viscoelastic analysis was performed to account for stress relaxation. The viscoelastic solution is based on a quasi-elastic analysis proposed by Schapery [65,66] and applied by Weitsman and Harper & Weitsman [38,39,41] and White and Hahn [29,30]. For comparison purpose, elastic analysis was also performed. Figure 4.8 shows the geometry of the model of the composite laminate under consideration. The layup consists of $[90°_n/0°_n]$ unsymmetric laminates which produces curvature proportional to residual stresses.

4-2-7-1 Elastic analysis

The elastic stress-strain relations for orthotropic laminae under plane stress conditions are

$$\sigma_i = Q_{ij}(\varepsilon_j - e_j) \qquad i=1,2,3 \text{ and } j=1,2 \qquad (17)$$

where σ_i are the stresses, Q_{ij} are the stiffness elements of the lamina, ε_j are the mechanical strains, and e_j are the non-mechanical strains. Non-mechanical strains are

$$e_j = e_j^c + e_j^{th} \qquad i=1,2,3 \qquad (18)$$

where e^c_j and e^{th}_j are the chemical and thermal strains respectively.

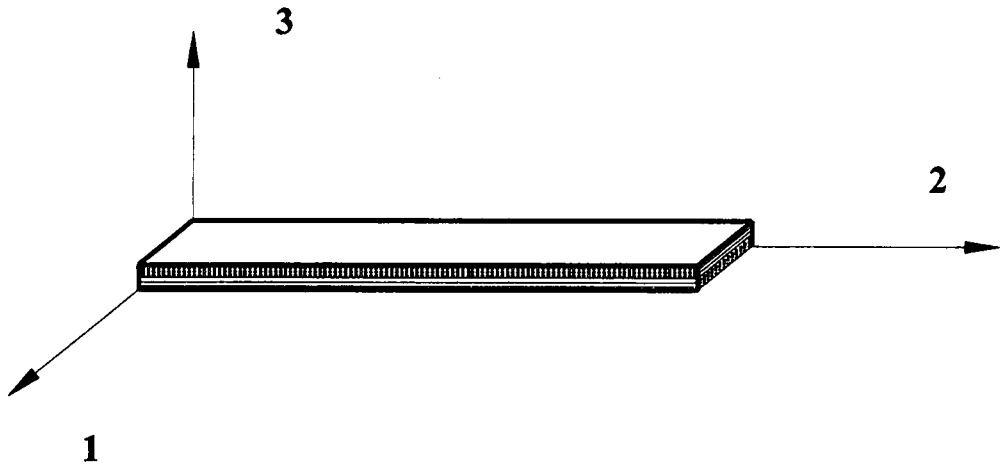

Figure 4.8 Geometry of $[90°_n/0°_n]$ unsymmetric laminate considered in the mechanical model.

During cure cycle, the laminate is held flat and the curvature is zero. Following the analysis presented in reference 29, the resulting moment in the laminate due to non-mechanical strains is given by

$$M_l = h^2 F(e_L - e_T) \tag{19}$$

where

$$F = \frac{Q^2_{LT} + Q_L Q_T}{Q_L + Q_T + 2Q_{LT}} \tag{20}$$

e_L and e_T are the non-mechanical strains in 1 and 2 directions as shown in Figure 4.8 and h is half of the laminate thickness. The stiffness elements of the composite are calculated as

$$Q_L = \frac{S_T}{S_L S_T - S^2_{LT}}$$

$$Q_T = \frac{S_L}{S_L S_T - S^2_{LT}} \tag{21}$$

$$Q_{LT} = \frac{-S_{LT}}{S_L S_T - S^2_{LT}}$$

Where

$$S_L = \frac{1}{E_L}$$

$$S_T = \frac{1}{E_T} \tag{22}$$

$$S_{LT} = \frac{-\nu_{LT}}{E_L}$$

and for AS4/3501-6 graphite/epoxy composites [67]

E_L=144.9 GPa

E_T=9.69 GPa

ν_{LT}=0.30

Using the elastic properties shown above and the non-mechanical strains due to volumetric changes, the moment in the laminate can be calculated at any point in the cure cycle beyond gelation and during cool down.

4-2-7-2 Viscoelastic analysis

It is well established that polymers exhibit viscoelastic behavior at high temperatures. The properties of the composite dominated by the matrix are expected to have similar behavior although to a different extent. Experimental data suggests that for epoxy polymer composites, the transverse modulus depends on time and temperature. For linear thermorheologically simple materials, a single temperature dependent shift factor, $a_T(T)$, is used to account for the change in the temperature. The stresses in the composite laminate at any time beyond gelation is a function of the volume changes and stiffness starting from gelation point and up to the time of interest. Stiffness and compliance of the composite depend on reduced times, $\xi(t)$ and $\xi(\tau)$, which depend on temperature history and calculated as

$$\xi(t)=\int_0^t \frac{ds}{a_T[T(s)]}$$
$$\xi(\tau)=\int_0^\tau \frac{ds}{a_T[T(s)]} \qquad (23)$$

In the above equations, the following shift form for the shift factor is usually used with epoxies

$$a_T(T)=exp\left(\frac{B_1}{T}-B_2\right) \qquad (24)$$

where B_1 and B_2 are constants determined from experimental data.

Usually viscoelastic analysis is too complicated to obtain exact solutions when realistic models are used to describe materials properties. Harper and Weitsman showed that for AS4/3502 graphite/epoxy composites, which belong to the same family of products from Hercules as AS4/3501-6 composites and have similar mechanical properties [67], quasi-elastic and direct inversion methods can be used without significant errors [41]. Following their formulation, the following integral was obtained for the moment in $[90°_n/0°_n]$ unsymmetric laminate at any time t

$$M_1(t)=h^2\int_0^t F[\xi(t)-\xi(\tau)]\frac{d[e_1(\tau)-e_2(\tau)]}{d\tau}d\tau \tag{25}$$

where

$$F(t)=\frac{Q_{LT}^2(t)+Q_L(t)Q_T(t)}{Q_L(t)+Q_T(t)+2Q_{LT}(t)} \tag{26}$$

and

$$Q_L(t)=\frac{S_T(t)}{S_L(t)S_T(t)-S_{LT}^2(t)}$$
$$Q_T(t)=\frac{S_L(t)}{S_L(t)S_T(t)-S_{LT}^2(t)} \tag{27}$$
$$Q_{LT}(t)=\frac{-S_{LT}(t)}{S_L(t)S_T(t)-S_{LT}^2(t)}$$

where

$$S_L(t)=\frac{1}{E_L(t)}$$
$$S_T(t)=\frac{1}{E_T(t)} \tag{28}$$
$$S_{LT}(t)=\frac{-\nu_{LT}(t)}{E_L(t)}$$

To obtain the moment at any time t in the cure cycle, the integral is obtained numerically. The time domain is divided into n equal portions Δt. Initial time $t_1=0$ and $t_{n+1}=t$. It should be noted that according to our assumptions $t_1=0$ corresponds to gelation point. The moment at any time t is given by

$$M_1(t)=\frac{h^2}{2}\sum_{k=1}^{n}\{F[\xi(t_{n+1})-\xi(t_{k+1})]+F[\xi(t_{n+1})-\xi(t_k)]\}\{\Delta e(t_{k+1})-\Delta e(t_k)\}) \tag{29}$$

where

$$\begin{aligned}\Delta e(t_{k+1})&=e_L(t_{k+1})-e_T(t_{k+1})\\ \Delta e(t_k)&=e_L(t_k)-e_T(t_k)\end{aligned} \tag{30}$$

The time increment is taken small enough to yield sufficient accuracy without resulting in too long calculation times or significant round-off errors. Using trial and error, time increments between 10-30 second were found to be appropriate.

4-2-7-3 Materials properties

Only few publications were found to describe the viscoelastic behavior of AS4/3501-6 graphite epoxy [68-71]. The data available in some studies are for $[\pm 45°_n]_s$ laminates and very complicated to use with $[90°_n/0°_n]$ layup under consideration [68-70]. Results published in reference 71 are for 3501-6 resin and can not be used with composites. Data published in reference 41 is for AS4/3502 graphite/epoxy which belong to the same products family from Hercules and having similar mechanical properties [67]. Due to the

lack of information found on viscoelastic properties of AS4/3501-6, properties of AS4/3502 were modified and used in this study.

Following the guidelines in reference 41, the longitudinal modulus and Poisson' s ratio were assumed to be constants and taken from reference 67

$S_L=6.9X10^{-3}$ MPa^{-1}

$S_{LT}=2.07X10^{-3}$ MPa^{-1}

For AS4/3502 composites, the viscoelastic transverse compliance can be expressed in the form

$$Sl_T(t)=Sl_0(t+tl_0)^{ql} \qquad (31)$$

in which

$S1_0=88.2X10^{-6}$ Mpa^{-1} min^{-q}

q1=0.00775

$t1_0$=1 minute.

The following approximate expression is obtained for the transverse compliance in AS4/3501-6 graphite/epoxy

$$S_T(t)=S_0(t+t_0)^q \qquad (32)$$

in which

$S_0=103.0X10^{-6}$ Mpa^{-1} min^{-q}

q=0.00775

t_0=1 minute.

The above relationship yields the same elastic transverse compliance of AS4/3501-6 at time t=0. The shift factor is assumed to be of the following form considering linear thermorheologically simple behavior

$$a_T(T)=exp\ (-T/A+B) \tag{33}$$

in which

A=6.2558

B=45.81

T= temperature in °K

4-3 COMPUTER PROGRAM

In order to simulate the curing process and calculate cure induced stresses, a computer program is required to perform calculations at different times in the cure cycle. This includes calculating temperature distribution, cure kinetics, resin flow, volume changes, stresses, and other parameters and variables. There is interdependency between different variables, hence the numerical solution should be incremental. The objective of the model and the program is to study the effect of modifying the cure cycle on residual stresses. The program was written to allow for iterative solutions and to allow for comparing large numbers of cycles in the same run.

For a given cure cycle to calculate cure induced stresses, the cure cycle is divided into small time intervals. At each time interval, the following variables are calculated at each layer in the composite

- temperature
- degree of cure
- amount of resin flow out

- viscosity
- volume changes
- mechanical properties

The value of the volume change at the mid thickness layer of the layup is used to calculate non-mechanical strains needed to calculate stresses (as represented by moment as shown in section 4-2-7). Note that no stresses are calculated before gelation and no resin flow or viscosity are calculated beyond gelation.

The major factors affecting cure induced stresses are the amounts of *effective* cure shrinkage and *effective* thermal expansion and the extent of stress relaxation. The amount of *effective* cure shrinkage is fixed and corresponds to the increase in the degree of cure from α=0.80 (for 3501-6 epoxy) to α=1.0. The amount of *effective* thermal expansion depends on gelation temperature for a fixed cure temperature (350°F for AS4/3501-6). The lower the gelation temperature, the more the *effective* thermal expansion. Increasing *effective* thermal expansion by lowering gelation temperature will reduce cure induced stresses but will result in a longer cure cycle. Stress relaxation depends on time allowed for stresses to relax, i.e. time from gelation to the end of cure cycle. This time depends on heating rate beyond gelation. Hence, the following two parameters are identified as the governing factors in the amount of cure induced stresses

1- Gelation temperature

2- Heating rate beyond gelation

For a certain layup, the program allows for changing any one or both variables and in each case, cure induced and cool down stresses are calculated. A flow chart of the program is shown in Figure 4.2.

4-4 RESULTS

This section discusses sample results obtained from using OPTICURE to study the effect of cure cycle on the development of residual stresses. The effects of changing gelation temperature and heating rate beyond gelation during cure of AS4/3501-6 graphite/epoxy were studied. In all the cure cycles shown below, the following parameters are held constant unless otherwise mentioned exclusively

1- Cure cycles start by heating from 70°F (room temperature) to 290°F in 30 minutes.

2- Cure pressure schedule is the same as that recommended by prepreg manufacturer.

3- Cure temperature is 350°F. If cure is completed before reaching that temperature (e.g. when very slow heating rates are applied), the cycle is automatically excluded from comparison.

4- All cure cycles should produce degree of cure $\alpha \geqq 0.99$ at all layers in the laminate.

5- All cycles should produce full prepreg compaction otherwise it is ignored.

6- Once cure is complete, cool down starts from 350°F (cure temperature) to 70°F (room temperature) at 3°F/min.

7- The layup consists of $[90°_8/0°_8]$

8- Cure temperature is applied symmetrically at the top and bottom of the layup.

9- Stresses in composite are represented by the moment of unsymmetric laminates. For convenience, positive direction of the moment is taken as the direction of moment produced by net shrinkage.

10- Gelation temperature is taken as the temperature at the mid thickness layer of the layup when gelation is reached at that layer. This may be different from the applied cure temperature as described by cure cycle because of the heat of the chemical reactions and boundary conditions of the layup.

4-4-1 Effect of Gelation Temperature

As discussed above, lowering gelation temperature increases *effective* thermal expansion which offsets *effective* shrinkage. Figure 4.9 shows a typical example of the relationship between gelation temperature and time required to reach gelation at the mid thickness layer of the layup. Lowering gelation temperature results in a longer time to reach gelation. These results were obtained using OPTICURE. Iterative solution of the heat transfer and cure kinetics equations was used to calculate the time required to reach gelation at a particular temperature.

Cure cycles with gelation temperatures in the range 300°F to 340°F followed by heating rate of 0.7°F/min until cure is complete (cure temperature =350°F) were studied. Time required to complete the cure was computed for each cycle. Figure 4.10 shows the relationship between cure cycle time and gelation temperature. Note that each point in the chart represents a complete cure cycle with a particular gelation temperature and hence cure cycle time.

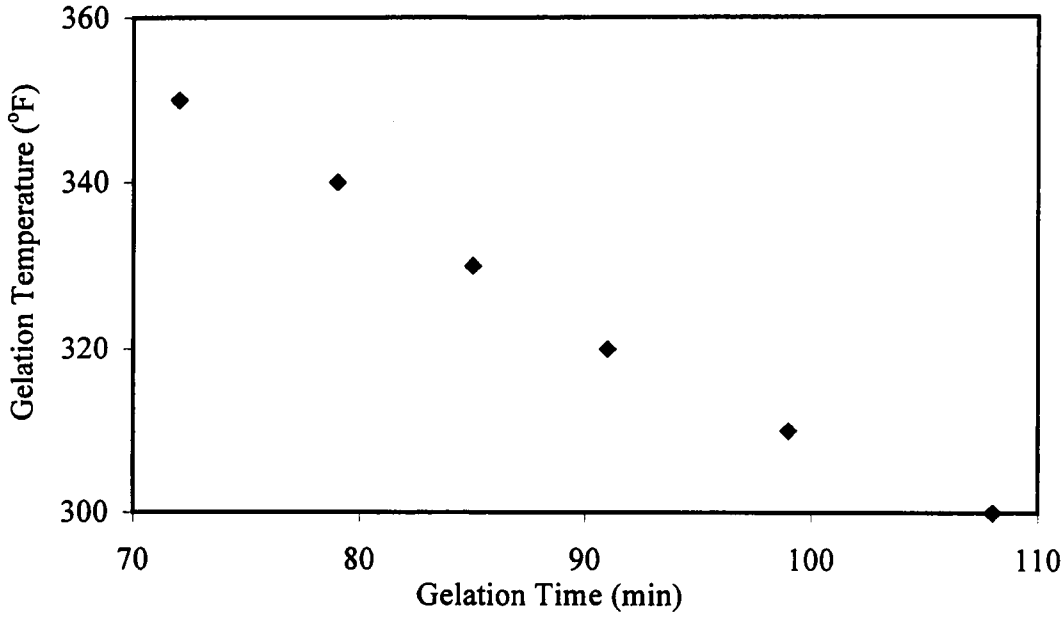

Figure 4.9 Relationship between gelation temperature and gelation time.

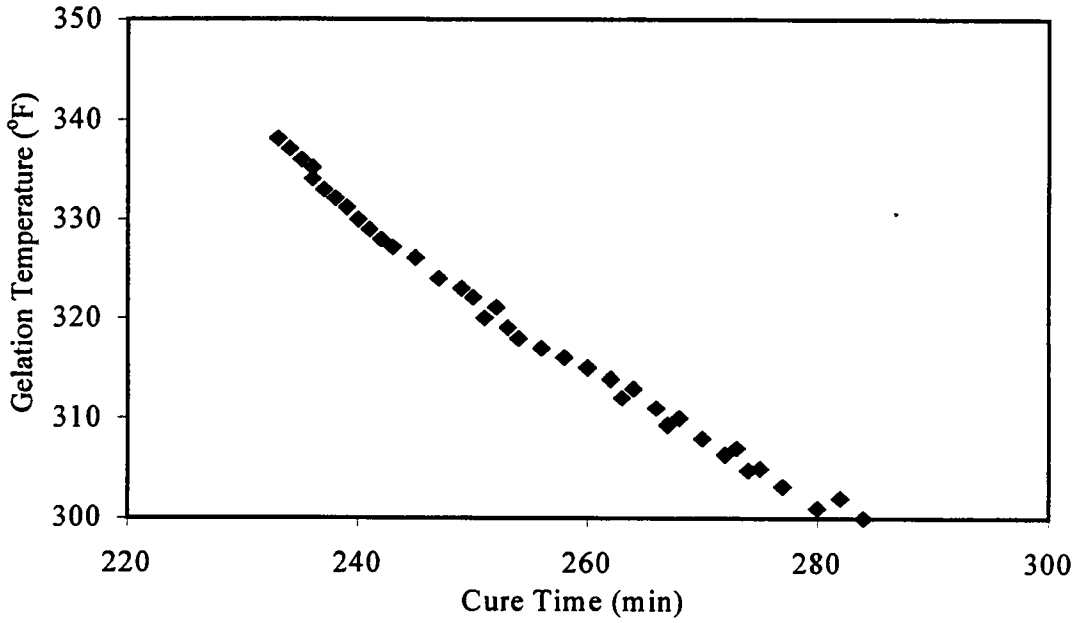

Figure 4.10 Relationship between cure cycle time and gelation temperature.

Using OPTICURE, moments due to cure volume changes were calculated for each cycle. Figure 4.11 (a) shows the relationship between gelation temperature and cured induced moments. The cure induced moments decrease as gelation temperature decrease. Viscoelastic analysis was applied as discussed above to include the effect of stress relaxation. At high gelation temperatures, e.g. 340°F, there is little *effective* thermal expansion and shrinkage is dominant (positive moment due to cure volume changes). This corresponds to type I cycle discussed in single fiber test results in Section 3-5-1. As gelation temperature decreases, more *effective* thermal expansion is generated and lower positive moments are developed. At gelation temperature of 313°F, the moment due to cure volume changes vanishes. This corresponds to type II cure cycle. As gelation temperature continues to decrease, type III cycle is generated in which the combined effect of *effective* thermal expansion and stress relaxation is more than the effect of *effective* shrinkage (negative moment due to thermal expansion).

To study the effect of stress relaxation on stresses developed during cure beyond gelation, moments due to cure volume changes were recalculated assuming elastic behavior (no stress relaxation is allowed). Results are shown in Figure 4.11 (b). Results of the elastic solution exceed the viscoelastic values by about 15-25%. It should be noted that disparity may be a lower bound value since stress relaxation properties of a fully cured composite were utilized for the partially cured composite. Stress relaxation in partially cured polymer is likely to exceed that of a fully cured polymer. Detailed viscoelastic analysis will result in more than the aforementioned percentiles.

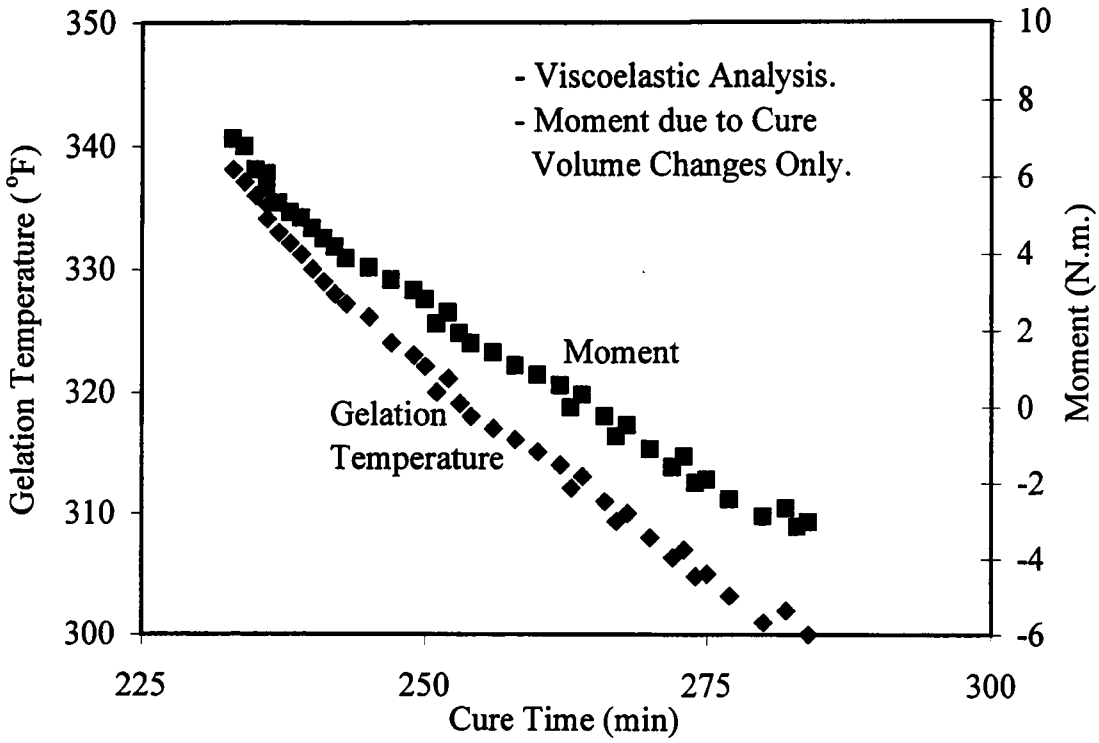

(a) Viscoelastic analysis.

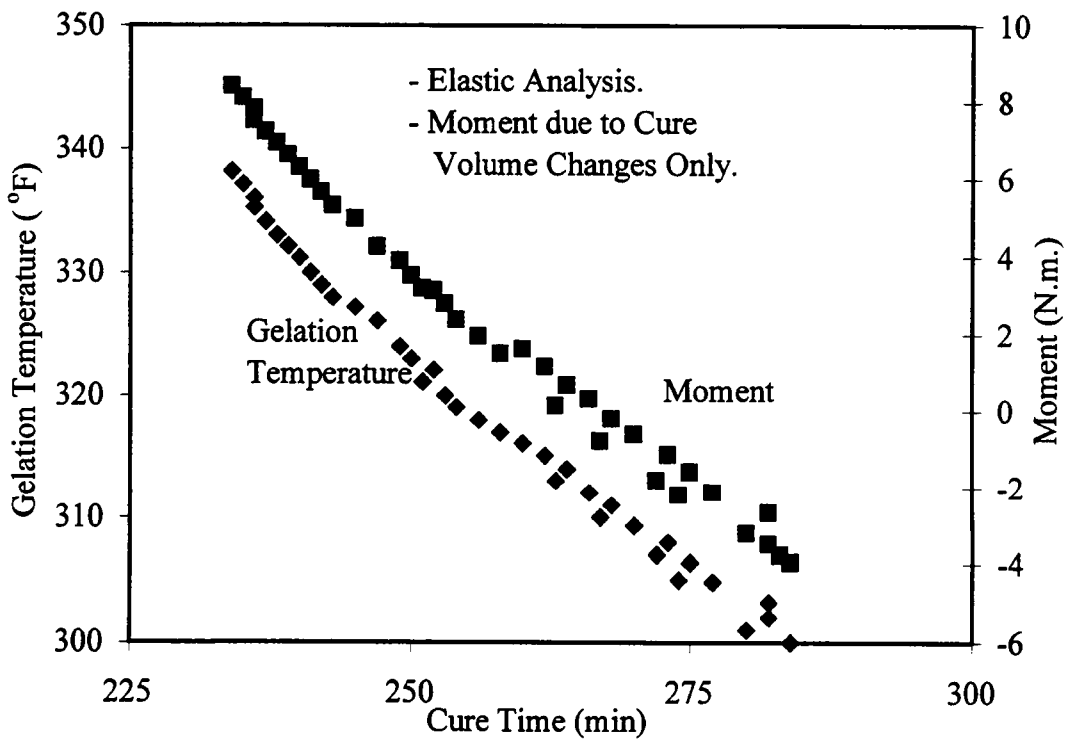

(b) Elastic analysis.

Figure 4.11 Moment due to cure volume changes at different gelation temperatures.

Moments due to cool down were also calculated for each cure cycle. Figure 4.12 (a) shows total moments (due to cure volume changes and cooldown thermal shrinkage) when different gelation temperatures are used. Cure cycles with lower gelation temperatures produce lower moments. Clearly, final moments are not zero for any cure cycle. It should be noted that the given values of the moments are due to both cure volume changes and cool down shrinkage based on continuous loading history from gel point until cool down is complete. This means that moments due to cure volume changes are allowed to relax even during cool down. For comparison purpose, stress relaxation was not considered and moments were recalculated assuming elastic behavior. Results of the elastic solution are shown in Figure 4.12 (b). Elastic solution predicts residual moments that are about 15% higher than the viscoelastic results.

Case Study

Experimental data shown in Section 3-3-5 for $[90°_4/0°_4]$ unsymmetric laminates made of AS4/3501-6 graphite/epoxy and cured with two different cycles was used to test the validity of the model. The time-temperature sequence of the two cycles can be found in Figures 2.6 and 2.22. Using OPTICURE, the first cycle (standard cure cycle) was found to result in gelation temperature of 343°F and the second cycle (modified cure cycle obtained from the feedback control system) results in 314°F. Test data, shown in Figure 3.30, indicate that the modified cure cycle reduces curvature of unsymmetric laminates with about 14%.

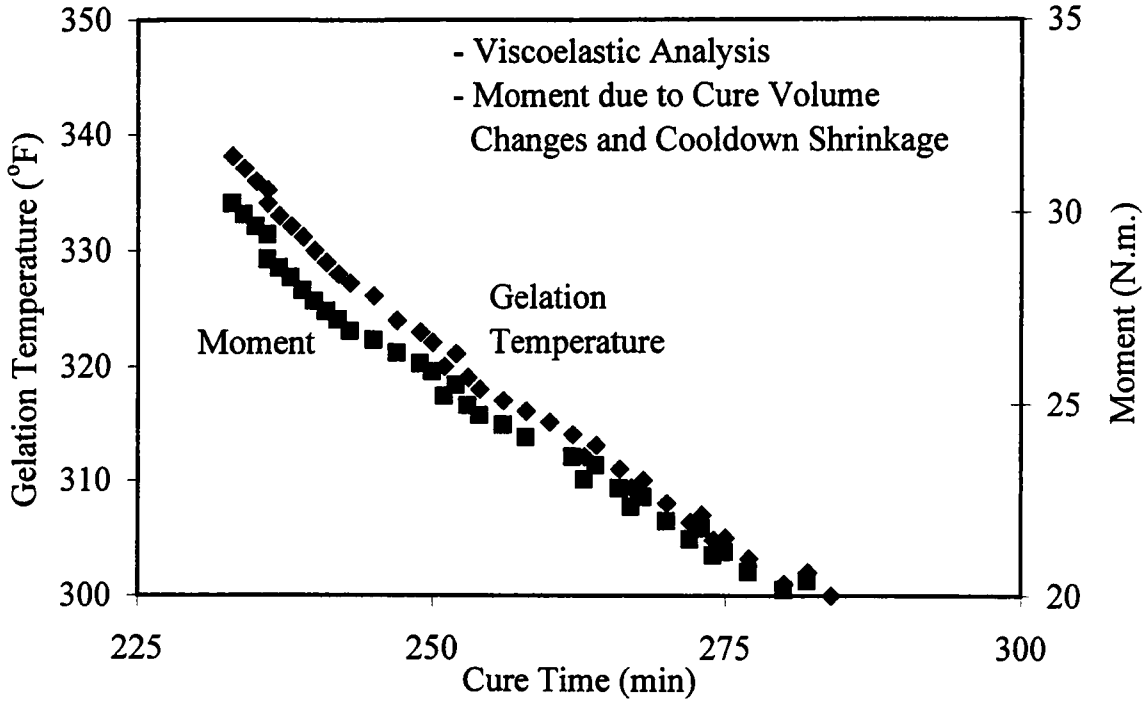

(a) Viscoelastic analysis.

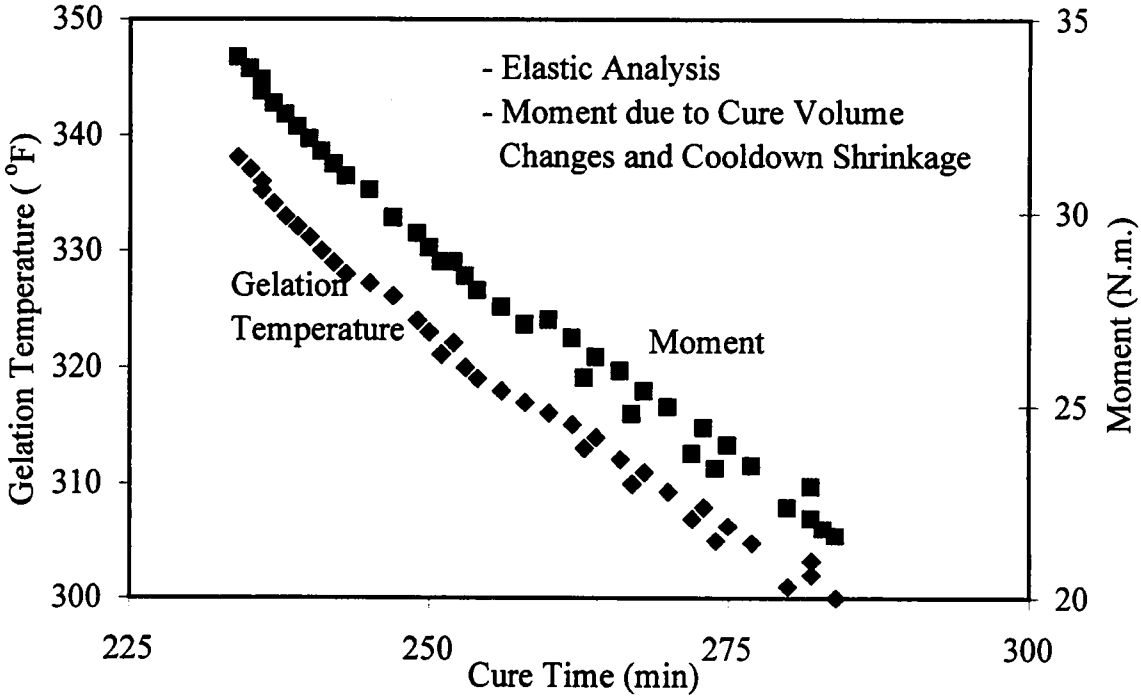

(b) Elastic analysis.

Figure 4.12 Moment due to cure volume changes and cooldown shrinkage at different gelation temperatures.

Using OPTICURE to compare moments for both of the cure cycles, the results indicate that the moments due cure volume changes and the total moments at the end of the first cycle are 2.07 N.m. and 7.71 N.m. respectively. The same moments due to the modified cycle are 0.24 N.m. and 6.22 N.m. respectively. The percentage reduction in total moment when using modified cure cycle is about 19% which is 5% higher than those values obtained experimentally for curvature. The difference between predicted and measured values is due to the difference between model assumptions and actual processing conditions. For example, the laminates were cured in a Vacuum Hot Press with two half-inch steel plates one at the top of the layup assembly and the other is at the bottom which was not considered in the model. This affects the boundary conditions of the heat transfer problem and hence may shift the gel point away from that predicted by the model.

4-4-2 Effect of Heating Rate beyond Gelation

In this section, the effects of changing heating rate beyond gelation on cure induced stresses are studied. Heating rate beyond gelation affects the pattern of volume changes and stress relaxation. Figure 4.13 shows typical effects of the heating rate on polymer volume changes beyond gelation (i.e. *effective* volume changes) as obtained from OPTICURE. There is a sharp change in the slope of the total volume change at the point at which temperature reaches its limit (at 350°F). Figure 4.14 shows the same relationship at different heating rates. The sharp change in the slop is also seen. Note that the distribution of *effective* volume changes varies with time at each heating rate.

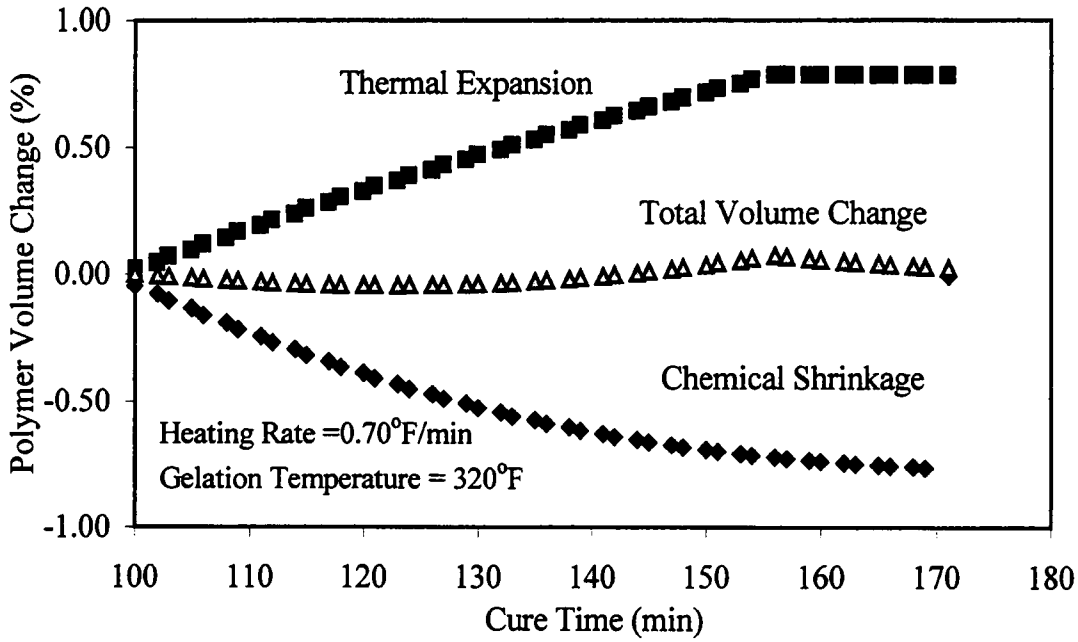

Figure 4.13 Typical cure volume changes beyond gelation.

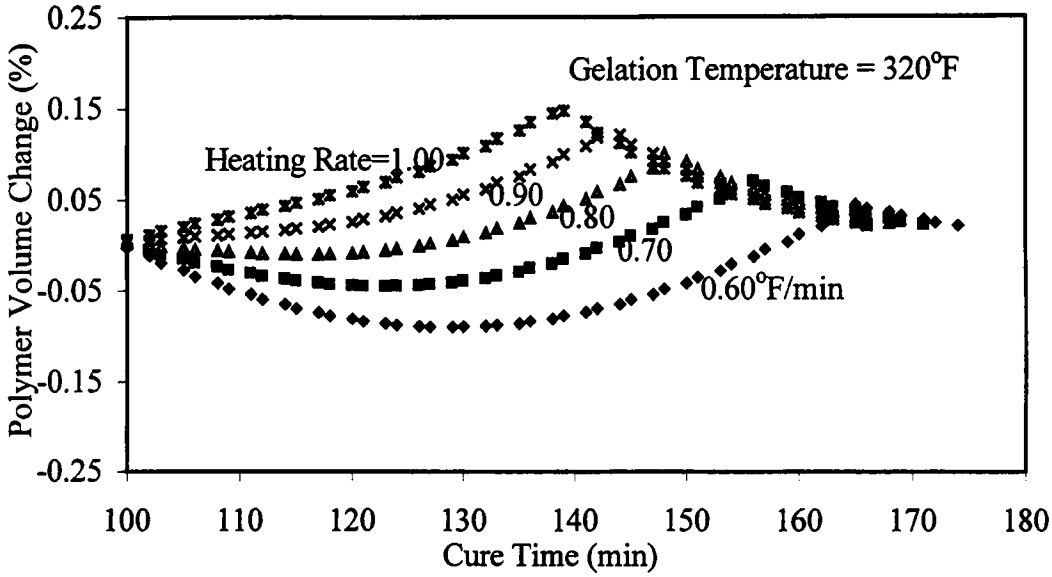

Figure 4.14 Effect of heating rate beyond gelation on polymer volume changes.

Figure 4.15 Moment due to cure volume changes at different heating rates.

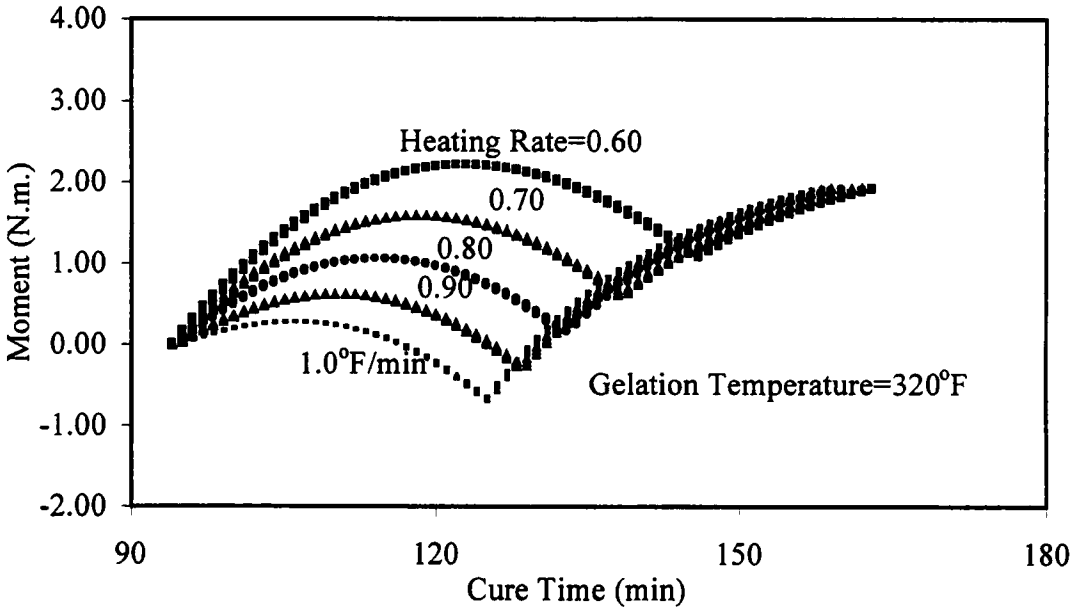

However, all heating rates produce the same end value of *effective* volume at the completion of cure although the total time for different cycles is different.

Interestingly, the slow and fast heating rates have similar effects on stress relaxation. For example, OPTICURE results show that for gelation temperature of 320°F, the moment due to cure volume changes in 16-ply laminate is 2.584 N.m. based on elastic analysis. Elastic analysis is not path dependant and all heating rates produce the same moment. Using viscoelastic analysis, the same moment was found to be 1.975 N.m. and 1.956 N.m. for heating rates 0.7°F and 1.0°F respectively. Compared with the elastic analysis, stress relaxation has almost the same effect for both heating rates. It seems that on one hand, slow heating rate means longer cure time and hence more stress relaxation. On the other hand, fast heating rate results in curing at higher temperatures, which means faster relaxation of stresses. Intermediate heating rates will partially contain both effects. This means that for a given gelation and cure temperature, changing heating rate beyond gelation may not change the extent of stress relaxation significantly.

Figure 4.15 shows moments produced by cure volume changes when different heating rates are applied beyond gelation to complete the cure. In all cases, the moment distribution with time changes but the values at the completion of cure vary only slightly. This can be explained considering that all those five cycles have the same amounts of *effective* shrinkage and *effective* thermal expansion (starting from the same gel point), so that the net values of the strains at the end are the same. Considering that changing heating rate may not change the extent of stress relaxation significantly as discussed above, it is expected that the values of the moments when the cure is complete

may not vary significantly with heating rate. Different gelation temperatures (310°F, 330°F, and 340°F) were considered and similar findings were obtained regarding the effect of changing heating rate on residual stresses.

4-5 SUMMARY AND CONCLUSION

A procedure to evaluate and minimize cure induced stresses was developed. This includes the development of a mechanical optimization model and a computer program, OPTICURE, to study the effect of changing the cure cycle on the development of residual stresses in composite laminates. The model and the program can be used to generate cure cycles that reduce residual stresses in thermoset polymer composites and thus enhance the dimensional stability and mechanical properties.

Gelation temperature was found to have a prominent effect on the contribution of cure volume changes to the residual stresses in thermoset polymer composites. Lowering gelation temperature will reduce residual stresses with appreciable value (19% reduction in moment in unsymmetric laminate in AS4/3501-6 graphite/epoxy composites as predicted by the model and 14% reduction in curvature as measured experimentally). On the other hand, smaller effect was found for the heating rate beyond gelation, which means that once gelation is reached at low temperature, temperature can be increased rapidly to complete the cure in short time without increasing residual stresses significantly.

It was shown that using elastic analysis results in over-prediction of the residual stresses by about 15% or more in AS4/3501-6 graphite/epoxy composites. It should be noted that

this number is based on the assumption that only volume changes beyond gelation contribute to residual stresses (20% of cure shrinkage in case of 3501-6 epoxy). If the whole cure shrinkage is considered and elastic solution is applied significant over-prediction is expected.

Similar to the findings of the single fiber stress test and feedback control system, cure cycles can be classified into three different types according to the contribution of cure volume changes to residual stresses

1- Type I: in which cure shrinkage is the dominant and stresses due to cure shrinkage will be added to cool down shrinkage producing high residual stresses.

2- Type II: in which *effective* thermal expansion and stress relaxation balance out *effective* cure shrinkage. Only cool down stresses will develop in the composite.

3- Type III: in which *effective* thermal expansion and stress relaxation have more effect than *effective* cure shrinkage and will cancel part of the stresses due to cool down shrinkage producing less residual stresses.

While type III cycle produces the lowest residual stresses, it may be significantly longer than economical cure time. Uses of the model and computer program were demonstrated with typical examples.

BIBLIOGRAPHY

1- Hahn, H. T. 1984. "Effects of Residual Stresses in Polymer Matrix Composites," J. of Astronautical Science, 32(3), 253-267.

2- Doner, D. R. and R. C. Novak. 1969. "Structural Behavior of Laminated Graphite Filament Composites," 24th Annual Tech. Conf., SPI, Inc., Paper 2-D.

3- Novak, R. C. 1970. "Fabrication Stresses in Graphite Resin Composites," J. of Engineering for Power, 92, 377.

4- Dannenberg, H. 1965. "Determination of Stresses in Cured Epoxy Resins," SPE Journal, 669-675.

5- Wang, H. B. and T. Y. Yu. 1995. "Effects of Cure History on Residual Stresses in Epoxy Resins," Polymer and Polymer Composites, 3(5), 369-374.

6- Feger, C. and H. M. Tong. 1991. "Dimensional Changes of Polyimide Films During Curing," ANTEC-91, 1742-1745.

7- Pawlak, A. and A. Galeski. 1996. "Residual Stresses in Epoxy Systems by 3-D Photoelasticity method," Polymer Engineering and Science, 36(22), 2727-2735.

8- Theocaris, P. S. and S. A. Paipetis. 1973. "Shrinkage Stresses in 3-Dimensional Two-Phase Systems," J. of Strain Analysis, 8(4), 286-293.

9- Asamoah, N. K. and W. G. Wood. 1970. "Thermal Self-Straining of Fiber-Reinforced Materials," J. of Strain Analysis, 5, 88-97.

10- Cunningham, B., J. P. Sargent, and K. H. Ashbee. 1981. "Measurement of The Stress Field Created Within The Resin Between Fibers in a Composite Material During Cooling From The Cure Temperature," J. of Materials Science, 16, 620-626.

11- Shimbo, M., M. Ochi, T. Inamura, and M. Inoue. 1985. "Internal Stress of Epoxide Resin Modified with Spiro Ortho-Ester Type Resin," J. of Materials Science, 20, 2965-2972.

12- Ochi, M., K. Yamazaki, and M. Shimbo. 1989. "Internal Stress of Epoxide Resin Modified with Spiro Ortho-Ester Type Resin," J. of Materials Science, 24, 3189-3195.

13- Ochi, M., K. Yamashita, and M. Shimbo. 1991. "The Mechanism for Occurrence of Internal Stress during Curing Epoxide Resins," J. of Applied Polymer Science, 43, 2013-2019.

14- Ming, S. M. and R. D. Schile. 1982. "An Investigation of Material Variables of Epoxy Resins Controlling Transverse Cracking in Composites," J. of Materials Science, 17, 2066-2106.

15- Plepys, A., M. S. Vratsanos, and R. J. Farris. 1994. "Determination of Residual Stresses Using Incremental Linear Elasticity," Composite Structures, 27, 51-56.

16- Plepys, A. R. "A Study of Residual Stresses Formation in Three-Dimensionally Constrained Epoxy Resins," Ph.D. Dissertation, U. of Massachusetts, 1992.

17- Korotkov, V. N., Y. N. Chekanov, and B. A. Rozenberg. 1991. "Defect Formation in Curing Epoxy in A Rigid Vessel," J. of Materials Science Letters, 10, 896-899.

18- Korotkov, V. N., Y. N. Chekanov, and B. A. Rozenberg. 1995. "Shrinkage Defect Modeling in Thermoset Composites," ICCM-10, Volume III, 165-170.

19- Lawrence, C. M., D. V. Nelson, J. R. Spingarn, and T. E. Bennett. 1996. "Measurement of Process-Induced Strains in Composite Materials Using Embedded Fiber Optic Sensors," SPIE, 2718, 60-68.

20- Crasto, A. S. and R. Y. Kim. 1994. "Using Carbon Fiber Piezoresistivity to Measure Residual Stresses in Composites," Proceedings of the 8th Technical Conference of the American Society for Composites, Cleveland, 162-173.

21- Crasto, A. S. and R. Y. Kim. 1993. "On the Determination of Residual Stresses in Fiber-Reinforced Thermoset Composites," J. of Reinforced Plastics and Composites, 12(5), 545-558.

22- White, S. R. and H. T. Hahn. 1993. "Cure Cycle Optimization for the Prediction of Processing-Induced Residual Stresses in Composite Materials," J. of Composite Materials, 27(14), 1352-1378.

23- Sarrazin, H., B. Kim, S-H. Ahn, and G. S. Springer. 1995. "Effect of Processing Temperature and Layup on Springback," J. of Composite Materials, 29(10), 1278-1294.

24- Madhukar, M. S., R. P. Kosuri, and K .J. Bowles. 1995. "Reduction of Curing Induced Fiber Stresses by Cure Cycle Optimization in Polymer Matrix Composites," ICCM-10, Volume III, 157-164.

25- Rennick, T.S. and D. W. Radford. 1996. "Components of manufacturing distortion in carbon fiber/epoxy angle brackets," SAMPE Technical Conference, 28, 189-197.

26- Hahn, H. T. and N. J. Pagano. 1975. "Curing Stresses in Composite Materials," J. of Composite Materials, 9(1), 91-106.

27- Hahn, H. T. 1976. "Residual Stresses in Polymer Matrix Composite Laminates," J. of Composite Materials, 10(11), 266-278.

28- White, S. R. and H. T. Hahn. 1990. "Mechanical Property and Residual Stress Development During Cure of a Graphite/BMI Composite," Polymer Engineering and Science, 30(22), 1465-1472.

29- White, S. R. and H. T. Hahn. 1992. "Process Modeling of Composite Materials: Residual Stress Development during Cure. Part I. Model Formulation," J. of Composite Materials, 26(16), 2402-2422.

30- White, S. R. and H. T. Hahn. 1992. "Process Modeling of Composite Materials: Residual Stress Development during Cure. Part II. Experimental Validation," J. of Composite Materials, 26(16), 2423.

31- Bogetti, T. A. "Process-Induced stress and deformation in Thick-Section Thermoset Composite Laminates," Ph.D. Dissertation, University of Delaware, 1989.

32- Bogetti, T. A. and J. W. Gillespie, Jr. 1992. "Process-Induced Stress and Deformation in Thick Thermoset Composite Laminate," J. Composite Materials, 26(5), 626-660.

33- Bogetti, T. A. and J. W. Gillespie, Jr. 1991. "Two Dimensional Cure Simulation of Thick Thermosetting composites," J. Composite Materials, 25(3), 239-273.

34- Bogetti, T. A. and J. W. Gillespie, Jr. 1989. "Process-Induced Stress and Deformation in Thick-Section Thermosetting Composite Laminates," SAMPE Technical Conference, 21, 947-959.

35- Bogetti, T. A. and J. W. Gillespie, Jr. 1994. "Influence of Processing on the development of Residual Stresses in Thick Section Thermoset Composites," Int. J. of Materials and Product Technology, 9 (1/2/3), 170-182.

36- Weitsman, Y. 1979. "Residual Thermal Stresses Due to Cool-Down of Epoxy-Resin Composites," J. of Applied Mechanics, 46, 563-568.

37- Weitsman, Y. 1980. "Optimal Cool-Down in Linear Viscoelasticity," J. of Applied Mechanics, 47, 35-39.

38- Harper, B. D. and Y. Weitsman. 1981. "Residual Stresses in an unsymmetric Cross-Ply Graphite/Epoxy Laminate," American Institute of Aeronautics and Astronautics, Paper 91-0580.

39- Harper, B. D. and Y. Weitsman. 1985. "On the Effects of Environmental Conditioning on Residual Stresses in Composite Materials," Int. J. of Solids and Structures, 21, 907-919.

40- Harper, B. D., D. Peret, and Y. Weitsman. 1983. "Assessment of Chemical Cure-Shrinkage Stresses in Two Technical Resins," AIAA/ASME/ASCE/AHS 24th Meeting, Paper 83-0799.

41- Harper, B. D. "On the Effects of Post Cure Cool Down and Environmental Conditioning on Residual Stresses in Composite Laminates," Ph.D. thesis, Texas A&M University, College Station, TX, 1983.

42- Levitsky, M. and B. W. Shaffer. 1975 "Residual Stresses in a Solid Sphere Cast From a Thermosetting Materials," J. of Applied Mechanics, 8, 651-657.

43- Levitsky, M. and B. W. Shaffer. 1974 "Residual Stresses in a Solid Sphere Cast From a Thermosetting Materials," J. of Applied Mechanics, 7, 652-657.

44- Lange, J., S. Toll, and J.-A. E. Manson. 1997. "Residual Stresses Build-up in Thermoset Films Cured Below Their Ultimate Glass Transition Temperature," Polymer, 38(4), 809-815.

45- Lange, J., J.-A. E. Manson, and A. Hult. 1996. "Build-up of Structure and Viscoelastic Properties in Epoxy and Acrylate Resins Cured Below Their Ultimate Glass Transition Temperature," Polymer, 37(26), 5859-5868.

46- Mallick, K. and D. Krajcinovic. 1992. "Cure Induced Inelastic Deformation in Thermosetting Polymers," ASME, Applied Mechanics Division, 132, 159-172.

47- Adolf, D. and J. E. Martin. 1996. "Calculation of Stresses in Crosslinking Polymer," J. of Composite Materials, 30(1), 13-34.

48- Adolf, D. and J. E. Martin. 1990. "Time-Cure Superposition During Crosslinking," Macromolecules, 23, 3700-3704.

49- Adolf, D., J. E. Martin, and J. P. Wilcoxon. 1990. "Evolution of Structure and Viscoelasticity in an Epoxy Near The Sol-Gel Transition," Macromolecules, 23, 527-531.

50- Monk, D. J., H. Youngxiange, and D. S. Soane. 1991. "Stresses in Polyimide Films During Cure and Thermal Cycling," ASME, Applied Mechanics Division, 131, 87-93.

51- Jain, L. K. and Y.-W. Mai. 1997. "Stress and Deformations Induced during Manufacturing. Part I: Theoretical Analysis of Composite Cylinders and Shells," 31(7), 672-695.

52- Jain, L. K. and Y.-W. Mai. 1997. "Stress and Deformations Induced during Manufacturing. Part II: Study of Spring-In Phenomenon," 31(7), 696-719.

53- Landro, L. Di, A. Palonca, and G. Sala. 1995. "Residual Thermal Stresses in Bismaleimide/Carbon Fiber Composite Laminates," Polymer Composites, 16(4), 276-283.

54- Sala, G. and L. Di Landro. 1997. "Viscoelastic Effects Related to Residual Stresses in Bismaleimide/Carbon Fiber Composite Laminates," Polymer Composites, 18(1), 28-39.

55- Wang, T.-M. and I. M. Daniel. 1992. "Thermoviscoelastic Analysis of Residual Stresses and Warpage in Composite Laminates," J. of Composite Materials, 26(6), 883-899.

56- Mohan, R. and T. H. Grenizer. 1995. "Process Simulation in Thermoset Composites for Cure Response and Stress Prediction," J. of Reinforced Plastics and Composites, 14, 72-84.

57- Russell, J. D. "Analysis of Viscoelastic Properties of High-Temperature Polymer Using a Thermodynamic Equation of State," M.Sc. Thesis, University of Dayton, 1991.

58- Long, E. R., S.A. Long, W.D. Collins, S.L. Gray, and J.G. Funk. 1989. "Effect of Postcuring on Mechanical Properties of Pultruded Fiber-Reinforced Epoxy Composites and the Neat Resin," SAMPE Quarterly, 21(2), 9-16

59- Springer, G. S. and S. W. Tsai. 1967. "Thermal Conductivities of Unidirectional Materials," J. of Composite Materials, 1, 166-173.

60- Lee, W. I., A. C. Loos, and G. S. Springer. 1982. "Heat of Reaction, Degree of Cure, and Viscosity of Hercules 3501-6 Resin," J. of Composite materials, 16(11), 510-520.

61- Loos, A. C. and G. S. Springer. 1993. "Curing of Epoxy Matrix Composites," J. of Composite Materials, 17(3), 135-169.

62- Russell, J. D., M. S. Genidy, M.S. Madhukar, and Andree Y. Lee. "A New Method to Reduce Cure-Induced Stresses in Thermoset Composites, Part III: Correlating Stress History to Viscosity, Degree of Cure, and Cure Shrinkage," J. of Composite Materials, Submitted.

63- Williams, R. J., M. A. Benavente, and R. A. Ruseckaite. 1990. "Criteria for Selecting Cure Cycles in Autoclave Processing of Graphite/Epoxy Composites," Polymer Engineering and Science, 30(18), 1140-1145.

64- Chiou, P.-L. "Modeling the reaction Kinetics and Chemoviscosity of an Epoxy Resin System Exhibiting Complex Curing Behavior," Ph.D. Dissertation, Texas A&M University, 1991.

65- Schapery, R. A. 1965. "A Methods of Viscoelastic Stress Analysis Using Elastic Solutions," J. of Franklin Institute, 279-290.

66- Schapery, R. A. 1967. "Viscoelastic Behavior and Analysis of Composite Materials," J. of Composite Materials, 1, 228-267.

67- Hercules Advanced Materials and Systems Company, Graphite Fibers and Prepreg Product Data, August 1991.

68- Kibler, K. G. "Time-Dependent Environmental Behavior of Graphite/Epoxy Composites," Final Report, General Dynamics Corporation, Fort Worth, Texas, Contract No. F33615-77-C-5109, Report No. AFWAL-TR-80-4052, February 1980.

69- Ho, W. J. and R. A. Schapery. "The effect of Environment on the Mechanical Behavior of AS4/3501-6 Graphite/Epoxy Material," Phase III, Vought Corporation, Final Report to the Dept. of Navy, NASC, January 1981.

70- Renton, W. J. and T. Ho. "The effect of Environment on the Mechanical Response of AS4/3501-6 Graphite/Epoxy Materials," Final Report to the Dept. of Navy, NASC, For Period June 1977-June 1978, August 1978.

71- Kim, Y. K. and S. R. White. 1997. "Process-Induced Stress Relaxation Analysis of AS4/3501-6 Laminate," J. of Composite Materials, 16(1), 2-15.

72- Tsai, S. W. and H. T. Hahn. Introduction to Composite Materials, Technomic, 1980.

VITA

Mohamed Sayed Genidy was born in Giza, Egypt on May 14, 1969. He obtained his high school diploma in 1987 at which he attended the Faculty of Engineering, Cairo University. After 5 years of study, he obtained his B.Sc. in Civil Engineering in 1992 (Distinction with Honor). Upon graduation, Mohamed started working as a structural engineer. During the same year, he started studying for a M.Sc. degree in Structural Engineering at Cairo University which he completed in 1996. During that period he met Taga and got married in 1995. In May 1996 he attended the graduate program at University of Tennessee, Knoxville. He obtained a M.Sc. in engineering science and mechanics in 1998. Mohamed worked towards his Ph.D. in engineering science and mechanics with Dr. Madhu S. Madhukar as his major advisor. The doctoral degree was granted in August 1999. Currently, Mohamed is working for a consultant engineering company and applying to become a professional structural engineer.

VITA

Mohamed Sayed Genidy was born in Giza, Egypt on May 14, 1969. He obtained his high school diploma in 1987 at which he attended the Faculty of Engineering, Cairo University. After 5 years of study, he obtained his B.Sc. in Civil Engineering in 1992 (Distinction with Honor). Upon graduation, Mohamed started working as a structural engineer. During the same year, he started studying for a M.Sc. degree in Structural Engineering at Cairo University which he completed in 1996. During that period he met Taga and got married in 1995. In May 1996 he attended the graduate program at University of Tennessee, Knoxville. He obtained a M.Sc. in engineering science and mechanics in 1998. Mohamed worked towards his Ph.D. in engineering science and mechanics with Dr. Madhu S. Madhukar as his major advisor. The doctoral degree was granted in August 1999. Currently, Mohamed is working for a consultant engineering company and applying to become a professional structural engineer.